FOUNDED 1925
INCORPORATED BY
ROYAL CHARTER 1961

"To promote the advancement of radio, electronics and kindred subjects by the exchange of information in these branches of engineering."

THE RADIO AND ELECTRONIC ENGINEER

The Journal of the Institution of Electronic and Radio Engineers

VOLUME 35 No. 3 MARCH 1968

The Technology of Thick Films

IN 1966 this Institution and the Institution of Electrical Engineers held a successful joint conference on the engineering applications of thin films, which marked the fact that the technology of thin-film circuits and elements had been mastered sufficiently for engineers to be applying them over a wide field. At that conference the words 'thick films' were heard by many of those present for the first time. Such has been the rate of growth of thick-film technology that, not quite two years later, the time has seemed ripe for a conference on the subject.

In a sense the term 'thick' film is misleading, as the emphasis is not so much on its dimensions as on the manner of its preparation. This includes the techniques of screen printing, spraying or painting through a mask on to a substrate, using inks which, after firing in a suitable furnace, will leave a pattern of conductors, resistors or capacitors, depending upon the materials used. The essence of the system is that it is rapid, cheap and reliable, and offers considerable technical advantages in many areas of application. The technology has advanced to the stage where some manufacturers are making and selling systems incorporating thick-film circuits, but application of them has not yet become widespread. Due to stringent patents on many of the inks, not much has been published about them and this has contributed to a reluctance in research and development departments to commit themselves to the technology. It is hoped that this conference will help to lift the veil a little and, by exposing both the advantages and limitations of the technology, promote its further exploitation.

The full programme of the conference, which will be held at Imperial College, London on Monday 8th and Tuesday 9th April, is given on pages 118–124 of this issue, together with synopses of most of the papers. A volume of 'conference Proceedings' containing all the papers and reprints of the discussions will be published and in accordance with usual practice a representative selection from the papers will be reprinted in *The Radio and Electronic Engineer* for the information of members unable to attend the conference.

The conference papers are being grouped under the headings: Substrates; Materials, Inks and Deposition Techniques; Assembly Techniques and Packaging; Applications. There will be twenty technical papers and two opening review papers: one will cover the British and the other the American scene. A group of papers from the U.S.A. has been obtained through the newly formed International Society for Hybrid Microelectronics who are associated with the conference. In addition, and essential to any conference, discussion groups will meet to air—and, it is hoped, answer—many of the questions.

It is encouraging to see the Institutions again taking the lead by drawing attention to a technology of great importance to the future of the electronics industry.

J. C. ANDERSON

Joint I.E.R.E.–I.E.E. Conference on

'Thick Film Technology'

with the association of the I.S.H.M.

Imperial College, Prince Consort Road, London, S.W.7

Monday 8th and Tuesday 9th April 1968

PROGRAMME AND SYNOPSES OF PAPERS

Monday, 8th April

9.00–10.00 a.m. REGISTRATION.

10.00 a.m. **Formal opening of the Conference by Major-General Sir Leonard Atkinson, K.B.E.,** *President of the I.E.R.E.*
Address by Dr. G. G. Macfarlane, *Director of Research, Ministry of Technology.*

10.15–11.15 a.m. **SURVEY PAPERS**

'Thick Film Technology in the United States'—Speaker to be announced.

'Thick Film Technology in Europe'—D. BOSWELL.

11.15 a.m.–12.30 p.m. **Session on SUBSTRATES**

Chairman: D. BOSWELL

'Processing Ceramics to give Suitable Substrate Characteristics'—B. C. WATERFIELD.

'Some Ceramic Considerations which Control and Limit the Quality of Alumina Substrates'—G. RICHARDS.

'Glazed Ceramic Substrates of High Thermal Conduction'—R. G. LOASBY and D. G. HOUGHTON.

2.00–3.30 p.m. **Sessions on MATERIALS, INKS AND DEPOSITION TECHNIQUES**

Chairmen: J. C. ANDERSON AND J. H. RICHARDS

'Ruthenium Resistor Glazes for Thick Film Circuits'—G. S. ILES.

'Thallium Oxide Resistive Glazes'—F. M. COLLINS, C. F. PARKS and M. B. REDMOUNT.

'Thick Film High-value Tin Oxide Glaze Resistors'—J. DEARDEN.

4.00–5.30 p.m.

'Reliability Characteristics of Palladium–Silver Film Resistors'—R. C. HEADLEY.

'Capacitors Compatible with Thick Film Circuit Technology'—W. L. CLOUGH.

'Glaze Capacitors for Use in Thick Film Circuits'—J. P. HOLDEN.

6.30–8.00 p.m. Conference Reception in South Side Halls of Residence

Tuesday, 9th April

9.00–10.45 a.m. **Sessions on ASSEMBLY AND PACKAGING**

Chairmen: G. W. A. DUMMER AND E. M. BRADLEY

'Packaging Thick Film Circuits and Large Scale Hybrid Integration'—J. M. WOULBRON.

'Active and Passive Components for Attachment to Thick Film Circuits'—A. F. DYSON and D. GROSVENOR.

'High Density Interconnections'—A. G. COZENS and J. E. TOMLIN.

'A Multilayer Thick Film Interconnection System'—Y. GURLER and K. C. BINGHAM.

11.15 a.m.–12.45 p.m.

'The Development of a Thick Film Interconnection Pattern for the Assembly of Silicon Integrated Circuits'—R. F. RUSSELL.

'Performance Data on Thick Film Crossovers'—T. NAKAYAMA and L. C. HOFFMAN.

'Effects of Process Conditions on the Reliability of Solder Connections to Thick Film'—I. D. SALISBURY.

'Ultrasonic Chip Bonding Techniques'—K. C. BINGHAM and Y. GURLER.

2.15–3.45 p.m. **Discussion on 'Thick Films versus Thin Films'**

Chairman: J. C. ANDERSON

Opening speakers: P. L. KIRBY AND J. C. MADDISON

4.15–5.45 p.m. **Session on APPLICATIONS**

Chairman: A. E. STEBBENS

'The Design, Construction and Performance of Thick Film Cermet Potentiometers'—B. S. METHVEN.

'Thick Film Transistors'—R. J. MYTTON, G. A. WILKIN and G. H. OLSEN.

'Thick Films in Automotive Equipment'—R. W. NOLAN.

Discussion may be taken after individual papers or after groups of associated papers.

Synopses of Papers to be presented at the Conference

Processing Ceramics to give Suitable Substrate Characteristics

B. C. WATERFIELD. (*Andermann & Ryder Limited, West Molesey, Surrey.*)

The selection of the substrate material is dependent on the application for which the deposited circuit is intended. Aluminium oxide is widely used in large production quantities giving ceramists the opportunity to develop materials and processes especially for this application. This has resulted in two basic lines of study, namely, the chemical structure of the material and its effect on the ceramic/metal junction, and the quality and the condition of the surface. The background of the work done has naturally been the applications for which the substrate itself is destined. Here there are two main divisions—thick or thin films—and also other uses or processing techniques that require special surfaces or dimensional tolerances. The normal production specifications for substrates are discussed and a brief description given of the production methods available. The reasons for the impurity ratio in the ceramic must be considered relevant to the type of deposition that will be applied and the degree of adherence that is required; there is also a connection between impurity level and surface finish which will effect the choice of metallizing media. In terms of both cost and surface texture, 'as fired' ceramics are favoured. Any subsequent machining operations will tend to expose voids which can be clearly seen on roughness traces, though a general 'flattening' of crystal peaks will take place. If a higher degree of surface finish is obligatory, then great care is needed in the selection of ceramic with particular reference to the size of grain and alumina content. Finally, the factors affecting the costs of production substrates are considered in light of the aspects discussed.

Reliability Characteristics of Palladium–Silver Thick Film Resistors

R. C. HEADLEY, B.S., M.S. (*E. I. Du Pont de Nemours & Company, Wilmington, Del., U.S.A.*)

Loaded and unloaded drift properties of palladium–silver glaze resistors as determined by various firing temperatures and times for belt furnace firing in air are described. Data are presented depicting drift behaviour for several thousand hours of exposure time to 150°C storage and electrical loadings of 40 to 60 W/in² of resistor area. While firing time exerts a negligible effect on resistor stability, firing temperature exercises a noticeable influence. Resistors under electrical load exhibit very low drift rates in most cases. No-load exposure at 150°C appears to accelerate the drift.

Some Ceramic Considerations which Control and Limit the Quality of Alumina Substrates

G. RICHARDS, B.Sc., A.I.Ceram. (*Royal Worcester Industrial Ceramics Limited, Tonyrefail, Glamorgan.*)

A brief introduction traces the growth in the use of alumina ceramics during the past 20 years, mostly resulting from the desirable properties of this chemical. These properties are compared with competitive materials illustrating that whereas a single characteristic may be surpassed by other materials, the combination of characteristics possessed by aluminium oxide is unique. The fabrication of suitable shapes from this compound is described emphasizing those which are used for manufacturing flat substrates. These include dry pressing, tape casting and ribbon extrusion.

Whereas pure (99·7%) alumina bodies are commercially available, the bulk of the market is satisfied by lower percentage alumina bodies. These are generally composed of alumina crystals embedded in a matrix of alkaline earth glasses. The effect of alumina content and the composition of this glass matrix on the fired properties is discussed.

The influence of production variables, resulting from fabrication methods, firing shrinkage, and firing history, on properties such as mechanical strength, surface finish and dimensional tolerances is also discussed. A practical specification for the economic production of flat substrates is derived by attention to these ceramic considerations.

Glazed Ceramic Substrates of High Thermal Conduction

R. G. LOASBY, B.Sc., Ph.D., and D. G. HOUGHTON. (*United Kingdom Atomic Energy Authority, Aldermaston, Berkshire.*)

A technique is described for the manufacture of glazed ceramic substrates which have a surface finish approaching that of glass without appreciable degradation of the thermal conductivity of the ceramic base.

The development of a centrifugal technique for the deposition of glass frits on ceramic substrates is described, and the influence of the important parameters, such as particle size and size distribution, carrier choice, centrifugeing time and speed, on the quality of the product is assessed. The investigation indicated that most of the variables did not need accurate control but that the final surface finish was related critically to frit particle size and the film thickness.

Using frit powders in the size range to 7 μm, glass layers of thicknesses from 8 to 30 μm have been studied on surfaces of initial smoothness values 500 to 1000 nm c.l.a. The final surface finish, which varies as a complex inverse function of the film thickness, had values varying from 50 to 375 nm over this thickness range. A 99% yield figure in tests with evaporated capacitors was obtained on the deposited surface.

Calculated thermal resistance values for the coatings lie in the range 1×10^{-2} to 4×10^{-2} degC cm²/W; the determination of experimental values is at present in progress.

Thallium Oxide Resistive Glazes

F. M. COLLINS, Ph.D., C. F. PARKS and M. B. REDMOUNT. (*Airco Speer, Research and Development Laboratories, Niagara Falls, N.Y., U.S.A.*)

Compositions of thallium oxide and glass have been developed for the preparation of thick film glaze resistors. Formulations of these materials in the form of pastes are readily applied and processed on ceramic substrates by conventional procedures. Firing is conducted under non-critical conditions at somewhat lower temperatures than are employed for other glaze materials, in the neighbourhood of 570°C. Outstanding uniformity and reproducibility are obtained.

An exceptionally wide range of sheet resistance values, extending from about 20 ohms to one megohm per square, is attained with good control by changing the relative proportions of the ingredients. Throughout most of this resistance range the fired resistors exhibit satisfactory overall stability under varying conditions of temperature, moisture and load. The temperature coefficient of resistance, for example, is less than ± 200 parts in 10^6 per degC over a four-decade range of sheet resistance values.

By employing formulations of slightly different constituents, accommodation of these glazes to different substrate materials can be achieved. The performance characteristic of formulations recently developed for use on alumina, for instance, appear very satisfactory. These glazes may be terminated with many of the commercially-available conductive glazes. It is concluded that this system offers several significant economic and technological advantages for the preparation of a variety of thick film resistive elements.

Ruthenium Resistor Glazes for Thick Film Circuits

G. S. ILES. (*Johnson, Matthey & Co. Ltd., Wembley, Middlesex.*)

The rapid development of thick film microcircuits has created a need for preparations that will provide resistor films on a variety of substrates. Until recently the majority of the resistive preparations available required a firing profile with a peak temperature around 750°C, necessary to complete complex chemical changes within the glaze resistor. This not only imposed the need for very close control of the firing cycle and furnace atmosphere to ensure reproducible values, but limited the choice of substrate to materials, such as 95–98% alumina ceramics, capable of withstanding this temperature. A prerequisite to attaining consistent values is the surface condition of the substrate. Relatively low cost materials like mica and glass, which inherently possess flat, highly finished surfaces, are excluded, since they either exfoliate (dehydrate) or deform at temperatures exceeding 650°C.

To overcome these limitations and take advantage of the mechanism of conduction through ruthenium dioxide a series of glaze resistor preparations has been developed. The objective was an ink based on a chemically-inert system that would be far less dependent on firing conditions than those hitherto available. To be viable the system has to be capable of producing a wide range of resistivities; possess acceptably low temperature coefficients; contain the spread of resistance values within narrow limits and be economically competitive. The use of valency control and the techniques adopted to achieve these requirements are described.

Thick Film High-value Tin Oxide Glaze Resistors

J. DEARDEN, B.Sc., F.R.I.C. (*Welwyn Electric Ltd., Bedlington, Northumberland.*)

Very stable high-value resistors were required for use in such devices as current monitoring units and for spasmodic use in flat thick film circuits. The high-value system obtainable by diluting a conductor with an organic resin binder did not meet the stability requirements and the more stable conducting glaze systems were expensive and did not extend to sufficiently high values.

The requirements have been met by the development of a resistive glaze based on semiconducting tin oxide powder and glass. The repeatable properties of this combination are dependent on the method which has been developed for the preparation of the semiconducting tin oxide powder which is produced by burning a tin–antimony alloy powder in an oxygen atmosphere. This gives an extremely fine powder with a particle size of about 0·1 μm. Because of the chemical inertness and fine particle size of the tin oxide it has been found possible to dilute it over a very wide range of glass contents to provide surface resistivities from 10^4 to 10^{11} ohms per square with only a very small change in temperature coefficient of resistance.

Finished resistors are available up to a value of 10^{12} ohm.

Capacitors Compatible with Thick Film Circuit Technology

W. L. CLOUGH, A.R.I.C. (*Welwyn Electric Ltd., Bedlington, Northumberland.*)

The recent upsurge of interest in the screen-and-fire process has led to a considerable amount of progress in resistor technology, and many new materials and techniques have been developed. By comparison, relatively little has been written about capacitor elements which are compatible with this process.

Three approaches can be considered. In the first, the capacitor is regarded entirely as a discrete component and is manufactured or purchased independently. The problems of integration become those of surface bonding and of the protection of devices with irregular outlines. These can be accentuated when transfer moulding is the desired final encapsulation process.

The second approach is to produce the resistor network on a high permittivity ceramic substrate, and manufacture capacitors *in situ* by the printing of appropriate electrode regions. This technique has the advantage of simple processing and produces co-planar components, but it necessitates a compromise on thermal and mechanical properties of the substrate material. Empirical design allowance for stray capacitance introduced by other components must also be made.

The third and probably the best approach is to produce the capacitor by printing and firing of a suitable dielectric glaze. This introduces no compromise on substrate, no design allowances for strays, the component is co-planar and is produced by identical processes to the resistors. Multilayer techniques offer the prospect of significantly wider range of values, and adjustable capacitors may eventually permit close tolerances to be achieved. Undue optimism about this approach must, however, be tempered by consideration of the complexity of the process sequence when active R–C networks, possibly with multi-layer capacitors, are being proposed.

Glaze Capacitors for Use in Thick Film Circuits

J. P. HOLDEN. (*Morganite Research and Development Limited, Wandsworth, London, S.W.18.*)

This paper describes development work on a number of thick film systems. For low value capacitors (tens of picofarads) glass dielectrics have been chosen, whereas for higher values it has been necessary to use a mixture of a high permittivity ceramic and a binder material. Existing thick film conductor compositions have been used for electrodes. In the work on the low-value systems, a large number of combinations of different dielectric and electrode materials and their processing conditions have been assessed, and several usable systems have been determined. The reasons for the poor performance of other systems have been studied and are described.

The need to use multiphase dielectrics for higher values, and the behaviour to be expected from such systems are discussed. Dielectrics have been made from mixtures of high permittivity ceramics based on barium titanate and various glasses or bismuth oxide, and again the various materials and processing parameters have been varied to attain the optimum performance. Data on the performance of high and low value capacitor systems are included.

Packaging Thick Film Circuits and Large Scale Hybrid Integration

J. M. WOULBROUN, Ph.D. (*Microtek Electronics, Inc., Cambridge, Mass., U.S.A.*)

Thick films are widely used for packaging electronic circuits. The technology allows high packaging density and provides high systems reliability at the lowest volume production cost. The thick films deposited on ceramic substrates are particularly effective at high frequencies, high power dissipation, for tight component tolerances and for the interconnection of silicon integrated circuits. The scope of applications is therefore unlimited. Typical examples for thick film circuits include commercial or spacecraft computers, communication systems and instruments. This paper describes thick film circuits as well as various packaging concepts used by systems designers which are typical of the present 'state of the art'. The examples chosen include single modules, sub-systems and complete data processing systems.

High Density Soldered Interconnections

A. G. COZENS and J. E. TOMLIN. (*IBM United Kingdom Laboratories Ltd., Hursley Park, Winchester, Hampshire.*)

This paper describes work carried out during development of various interconnection techniques for use in conjunction with thin film planar devices. The special character of the substrate imposed a number of limitations on processing and assembly; the most restrictive was that all interconnections should be made at the lowest possible temperature, at the same time being capable of repair.

The first section of the paper covers the method of mounting integrated circuit chips directly on the 2 μm thick copper circuitry using soldering techniques for both chip mounting and the connections from chip to copper circuitry.

The second section describes the connection system used to make ground and signal connections between adjacent planes. The pitch of the signal connections is 0·010 in (0·254 mm), whilst the earth connection was continuous or semi-continuous. Both types of connection were made by soldering techniques. The special handling and soldering equipment produced for this work is illustrated, and the processes used to manufacture connection straps and overlays described.

The metallurgical aspects of soldered interconnections are discussed, particularly with regard to the effects of short range diffusion which greatly influences both the metallurgical structure and the resultant mechanical integrity of joints in the size range covered in this paper. Diffusion control may be achieved by matching the thermal inputs with the aid of diffusion barriers. The method and quality of deposition of solder in the joint area assumes an importance not arising in interconnections currently in use.

Ultrasonic Chip Bonding Techniques

K. C. BINGHAM and Y. GURLER. (*International Computers & Tabulators Ltd., Stevenage, Hertfordshire.*)

The papers describes a method of attaching silicon integrated circuit chips to planar conductor patterns on alumina substrates. An ultrasonic bonding technique is shown to be capable of achieving acceptable insertion yields for chips with 10 connections when mounted on ductile electro-deposited pillars. Chip replacement is possible when repairs or repeat insertions are necessary.

Preliminary results of reliability testing are given both for storage at 75°C and 125°C and thermal cycling over a temperature range of 140 degC.

Active and Passive Components for Attachment to Thick Film Circuits

A. F. DYSON, Dipl.E. and D. GROSVENOR, B.Sc. (*Erie Electronics Ltd., Great Yarmouth, Norfolk.*)

This paper discusses the development of suitable passive components (resistors and capacitors) for use with thick film circuits. The techniques of attachment of these components to the circuits are also discussed. Experience with the attachment of certain types of semiconductors to thick film circuits is also related.

A Multilayer Thick Film Interconnection System

Y. GURLER and K. C. BINGHAM. (*International Computers & Tabulators Ltd., Stevenage, Hertfordshire.*)

The availability of silicon integrated circuits containing most of the active and passive components of an electronic circuit demands new interconnection techniques. Present-day methods using packaged circuits mounted by soldering or welding on copper clad printed circuit boards are wasteful of space, circuit speed and tend to reduce the overall reliability of the completed system.

Substitution of ceramic for the printed circuit board carrying screen printed conductors and dielectric layers gives a multilayer interconnection system mechanically and dimensionally compatible with the uncased semiconductor circuit chips. Multilayer systems containing at least four superimposed planes having controlled electrical characteristics can be produced if the dielectric materials are carefully chosen. A range of materials complying with this specification will be described.

The paper then describes a multilayer interconnection system suitable for 50–100 unencapsulated integrated circuit elements of the type used in high-speed computers. The power and earth planes with their associate dielectrics are made using the thick film technique. Methods of producing the conductor and dielectric films are discussed. Two additional conductor planes, forming the signal matrix in which the logic connections are made, are deposited by the thin film technique.

The Development of a Thick Film Interconnection Pattern for the Assembly of Silicon Integrated Circuits

R. F. RUSSELL. (*The Plessey Company Ltd., West Leigh, Havant, Hampshire.*)

The high utilization of s.i.c.s for digital circuitry indicates the importance of developing a technique for the assembly of a number of s.i.c.s in one package. Such a system could offer reduced module size, improved reliability and reduced cost.

A thick film pattern is deposited on a high alumina substrate, providing the interconnection pattern and the areas on which the chips are mounted by conventional techniques. The successive layers of the interconnection pattern are generated by screen printing: conductor—glass insulation—conductor, and sequentially firing the layers on to the ceramic surface. The layers offer high adhesion for external contacts, crossover areas and low resistivity interconnections.

The chips are eutectically back-bonded to the substrate, the eutectic being formed at the interface of the chip and printed film under controlled conditions of temperature and pressure. The electrical connection to the circuit is made using ultrasonic wire bonds with 0·001 in diameter aluminium wire. The interconnection of the chips is thus made with an appreciable reduction in the number of 'man made' joints, associated with flat pack or TO–5 assemblies.

The encapsulation of the assembled module is accomplished by sealing a ceramic lid of the same material as the substrate, to the base substrates, by reflowing a glass film between the lid and the substrate. The external connections are made to areas of the thick film pattern which extend outside the sealed region, removing the problems associated with additional metal ceramic seals.

Performance Data on Thick Film Crossovers

T. NAKAYAMA, Ph.D. and L. C. HOFFMAN, Ph.D. (*E. I. Du Pont de Nemours & Company, Wilmington, Del., U.S.A.*)

The availability of a good printable "crossover composition", for insulating two or more levels of printed wiring from each other, is important for making thick film technology broadly acceptable. Capacitance, dissipation factor and insulation resistance as functions of atmospheric humidity and of time under voltage load were measured on crossovers isolated with a dielectric composition which has been recently developed for this purpose. The results obtained indicate that this composition will meet all essential performance criteria. Typically, when the dielectric is used to isolate two 0·5 mm wide conductors crossing at right angles, the crossover will show a capacitance of 2·0 pF, an insulation resistance of 2×10^{13} ohms, and a breakdown voltage well in excess of 250 V.

Effects of Process Conditions on the Reliability of Solder Connections to Thick Films

I. D. SALISBURY. (*Standard Telephones and Cables Limited, Paignton, Devon.*)

For reliable soldering to thick film circuits, it is necessary to have control over the conductor firing and soldering process in such a manner that the important parameters, which will ultimately affect reliability of the solder connection, are closely controlled. This is best achieved by mechanization of the processes, thus reducing dependence on operator skill and in-line inspection time and effort.

The soldering process has been split into various sections so that main problem areas can be localized and the effect of each process in obtaining a reliable solder joint seen. These are as follows:

1. Conductor firing, its effect on solderability and adhesion.
2. The effects of soldering conditions on the deposited film.
3. Methods of soldering for a production process.
4. Requirement for added components for reflow soldering.
5. Reflow soldering of added components to the thick film circuit.

The Design, Construction and Performance of Thick Film Cermet Trimming Potentiometers

B. S. METHVEN, B.Eng. (*Morganite Resistors Ltd., Jarrow, Co. Durham.*)

The cermet trimming potentiometer is a miniature lightweight control having an extremely rugged construction. The nature of the resistive element provides an inherent freedom from catastrophic failure and offers a wide range of possible ohmic values.

The design and its influence on some of the more fundamental properties of this control is discussed. The effects of both electrical and environmental stresses liable to be imposed in practice are given in some detail. This form of control is shown to have a number of advantages over the more conventional wirewound device some of which can play an important role in present-day high speed, high reliability electronic circuits.

Thick Film Transistors

R. J. MYTTON, B.Sc., G. A. WILKIN, B.Sc. (*International Research and Development Company Ltd., Newcastle-upon-Tyne*) and G. H. OLSEN, B.Sc., C.Eng., M.I.E.R.E. (*Rutherford College of Technology, Newcastle-upon-Tyne.*)

The paper reviews the problems associated with the development of an insulated-gate field effect transistor compatible with conventional thick film screening techniques. Experimental results are given of a preliminary investigation of these problems. Particular emphasis is placed on the methods of forming the semiconductor and insulator layers. Several possible configurations are evaluated in terms of device stability and performance.

Instability associated with the gate insulator layer has received much attention, and mechanisms of degradation are discussed, together with suggested improvements. Problems of making low impedance contacts to the semiconductor layer, using screened and fired layers, are considered, and a satisfactory technique is reported. The semiconductor ink includes a fluxing agent to encourage grain growth at relatively low temperatures, and details of this, together with the semiconductor doping level, are presented.

Laboratory devices are evaluated, and the frequency dependence of their transconductance is interpreted in terms of gate insulator capacitance variations. The effect of temperature on performance is discussed, and consideration is given to suitable device encapsulants for longer term stability. The ultimate performance of the device is related to the fundamental practical limitations, such as source, drain and gate registration, insulator dielectric properties and thickness, and semiconductor resistivity and mobility. Comparisons are made with performance obtainable using hybrid techniques, and the general feasibility of the device assessed.

Thick Films in Automotive Equipment

R. W. NOLAN. (*Joseph Lucas (Electrical) Ltd., Sutton Coldfield, Warwickshire.*)

The problems facing the manufacture of microelectronic equipment for motor vehicles are outlined. They arise from the physical and electrical environment, the power levels to be controlled which result in high currents, a need for very low saturation voltages, low thermal resistances and efficient heat sinks. These items are then considered with reference to a hybrid integrated circuit alternator voltage regulator, and the design employed to develop an economic unit is discussed. The methods include the use of a printed and fired thick film circuit, with dice mounted directly to the circuit. The assembly is encapsulated into a combined heat sink and cover. Manufacturing costs present another major problem and these are discussed in relationship to those of equivalent electromechanical and discrete component assemblies.

Other areas where microelectronics may be employed include the ignition system, the control of petrol injection system, windscreen wiper control systems, automatic speed controllers.

U.D.C. 621.391.82:629.19

Satellite-borne Equipment for a Global Survey of Terrestrial Radio Noise

By

B. N. HARDEN,
M.Sc., C.Eng., M.I.E.E.†

AND

V. A. W. HARRISON
(*Associate*)†

Presented at a Symposium on 'The Ariel III Satellite' held in London on 13th October 1967.

Summary: A description is given of the design and development of the equipment which has been flown in the satellite *Ariel III* to study the radio noise generated by lightning discharges in thunderstorms. Receivers measure the average voltage of the envelope of the noise in six narrow-band channels near 5, 10 and 15 MHz and count, up to a specified maximum rate, the number of atmospherics received in these channels. The frequencies of operation were selected so that the transmission properties of high-frequency radio waves in the ionosphere may be used to define the area near the Earth's surface from which reception is possible at any one time. The observations will be used to deduce the distribution of the noise sources and their variations in intensity.

1. Introduction

Over a period of years, measurements of the characteristics of high-frequency atmospheric radio noise have been made at a limited number of points on the Earth's surface. The advent of satellite techniques has, however, made it possible to carry out a global survey of the distribution of noise sources (lightning discharges) and to record their variations in intensity and frequency of occurrence.

In the noise experiment on *Ariel III*, the directional properties of high-frequency waves propagating through the ionosphere are used to define the storm areas from which atmospherics are observed. For a receiver at an altitude above that of the peak electron density of the ionosphere, the radius, r, of the area near the ground from which reception is possible is given approximately by

$$r = h\sqrt{\left(\frac{f}{f_0}\right)^2 - 1}$$

where h = altitude of satellite,
f = signal frequency,
f_0 = vertical incidence critical frequency of the ionosphere.

When f exceeds f_0 by a small amount, only atmospherics from storms near the sub-satellite point are received. In a full analysis, other factors such as refraction, ionospheric tilts, multihop propagation and absorption must be considered.

Because the critical frequency varies with geographical location, time of day and season, it would be desirable to make measurements over a range of frequencies from 3–20 MHz but the restrictions on an experiment in a satellite and the need to minimize interference from transmitters on the ground has limited operation to frequencies in the bands allocated for the 5, 10 and 15 MHz standard frequency services.

Pairs of receivers tuned to frequencies just above and below the centre frequency of each band are used, so that sporadic narrow-band signals may be recognized against a background of broadband atmospheric noise. The average voltages of the envelopes of the noise waveforms in the six receiving channels and the numbers of atmospherics with amplitudes exceeding pre-determined thresholds are recorded at regular intervals in the satellite and later telemetered to ground stations. The two sets of measurements ensure coverage of the wide range of noise levels expected from the intense thunderstorm areas over the tropical land masses and the quieter regions at higher latitudes.

The maps of noise sources and other information so obtained will, in addition to their scientific value, be of use in the design of radio communication circuits and will allow assessment of the possible interference effects of noise with satellite-borne receivers.

The experiment follows previous work at the Radio and Space Research Station (R.S.R.S.) which has included the location of thunderstorms with a network of twin-channel cathode-ray tube direction finders,[1] the development and operation of lightning flash counters[2,3] and radio-frequency noise measurements over a wide band of frequencies.[4]

The scope of this paper is limited to a description of the systems engineering design of the equipment, including mention of the effect of design constraints

† Science Research Council, Radio and Space Research Station, Slough, Buckinghamshire.

on the measurements that could be made. The results of the experiment, following an analysis of the data obtained, will be the subject of a later paper by other authors.

2. Development of the Measurement System

A suitable system had to be selected as a compromise between the idealized requirements of the experiment and the practical limitations imposed by operation in a small satellite. Some of the more important factors are considered here.

The planned orbit was circular at a height of 550 km and an inclination of 80°. This covers the thunderstorm areas of the world and was expected to be suitable for measurements at frequencies up to about 15 MHz at the solar epoch of the experiment, with only a small proportion of observations lost due to ionospheric cut-off at about local noon above the tropics.

The spacecraft carries five experiments and weighs about 90 kg with power supplied by solar cells in conjunction with a storage battery. The consequent limits on weight, power and telecommand facilities for the noise experiment implied the use of a simple receiving system operating at pre-set frequencies and gains. The available d.c. power for the experiment was 500 mW which made the direct measurement of noise power with a fixed gain impractical because of the wide dynamic range required in the receivers. At these frequencies, measurements on the ground[5] showed short-term peak values of the noise waveform about 20 dB above the r.m.s. value and calculations indicated that long-term variations of the r.m.s. value of 30 dB could be expected. Any distortion in amplification and square-law detection of the peaks would prevent accurate noise power measurements.

The alternative possibility of measuring average voltage of the noise envelope is satisfactory where storm activity is high since good linearity of amplifiers and clipping of peaks of noise over about 20 dB above the average level are unimportant. However, a complementary measurement is needed where activity is low and a method of counting the number of atmospherics under these conditions was therefore introduced.

The satellite has a p.f.m. telemetry system in which analogue outputs in the range 0 to +5 volts from the experiments are sampled by low- and high-speed encoders; low-speed data are stored by a continuous-loop tape recorder for telemetering on command to the ground, and the high-speed data are transmitted in real-time. The low-speed system has two modes of operation and, in both, the format consists of two frames each of sixteen channels lasting a total of 27·92 seconds. The single mode high-speed system has six frames each of sixteen channels sampled in

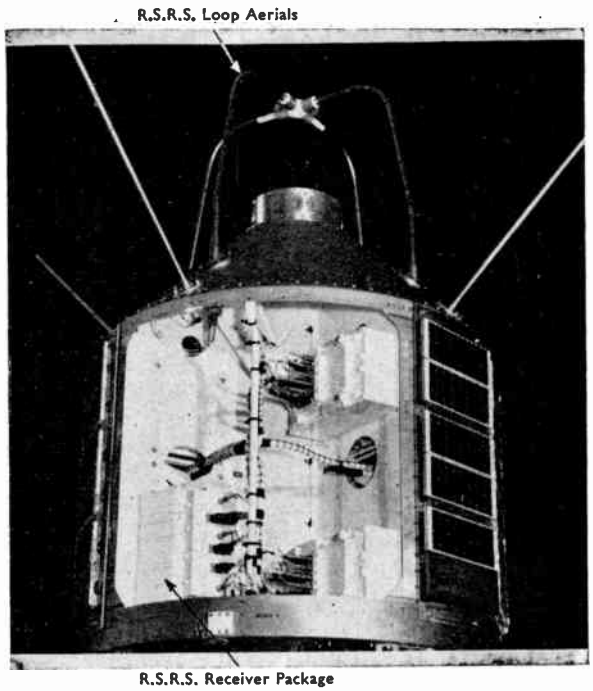

Fig. 1. The R.S.R.S. equipment in the satellite.

1·75 seconds. The R.S.R.S. experiment was allocated ten outputs in one of the modes of low-speed operation and seven high-speed outputs.

Complete orbital coverage is thus available and the sampling rate of each output gives a reasonable integration period (25·3 seconds) for measurements with an acceptable spatial resolution (about 200 km). The loss of data for about one orbit in five during the second mode of low-speed operation when the R.S.R.S. experiment is inoperative, is not important. Six of the high-speed outputs are convenient for observing the counts of atmospherics over much shorter time intervals.

A major constraint in the system was the siting of aerials. Extendible dipole aerials are not satisfactory because of detuning in the ionosphere[6] and loop aerials wound with copper tape on nickel-zinc ferrite tubes, 38 cm long and 2·5 cm in diameter, were initially considered. These gave adequate performance but involved severe mounting and thermal problems in the proposed positions on the satellite booms. The final solution was a pair of screened loops mounted orthogonally on the conical section of the satellite as shown in Fig. 1. In this position, the plane of each loop passes through the satellite spin-axis so that a continuous null in the reception of atmospherics from near the ground is avoided. The use of more than two loops was unacceptable because of inter-

action with the turnstile telemetry aerial and because of obstruction of the field of view of the Meteorological Office experiment. The size of the loops was controlled by the space available under the heat-shield of the launch vehicle. The loop areas and receiver noise figures give an overall sensitivity just above the desired level, that of galactic noise, which at these frequencies has an average value of the envelope in a 1 kHz bandwidth of about 16 dB below 1 μV/m.

The remaining problem was the selection of the fixed frequencies of operation so that interference from man-made transmissions might be minimized and its presence recognized. The grouping of three pairs of receivers in the standard-frequency bands at 5, 10 and 15 MHz seemed to be a reasonable answer since there are few transmitters in these bands and sporadic narrow-band interference would give different outputs from a pair of receivers, in contrast to the equal responses to the broad-band atmospherics.

A block diagram of the system is shown in Fig. 2.

3. Details of Design

3.1 *Aerials*

Two balanced screened single-turn loop aerials are used, each with an area of about 0·12 m^2. One aerial is tuned to 10 MHz and the other provides separate outputs at 5 and 15 MHz. The tuning elements are enclosed in small containers which are attached to the aerials within the cone of the satellite for protection against wide temperature variations.

The aerials are constructed from aluminium alloy and are gold-plated to provide a stable surface of good electrical conductivity. A cruciform of p.t.f.e. encloses the gaps of the loops and gives mechanical strength. Each of the four bases has an adjuster to take up small irregularities in the surface of the cone. The total weight of the aerials is 0·93 kg.

Radiation patterns were measured on an outdoor site using a developmental model of the satellite; no significant departure from the ideal patterns for a

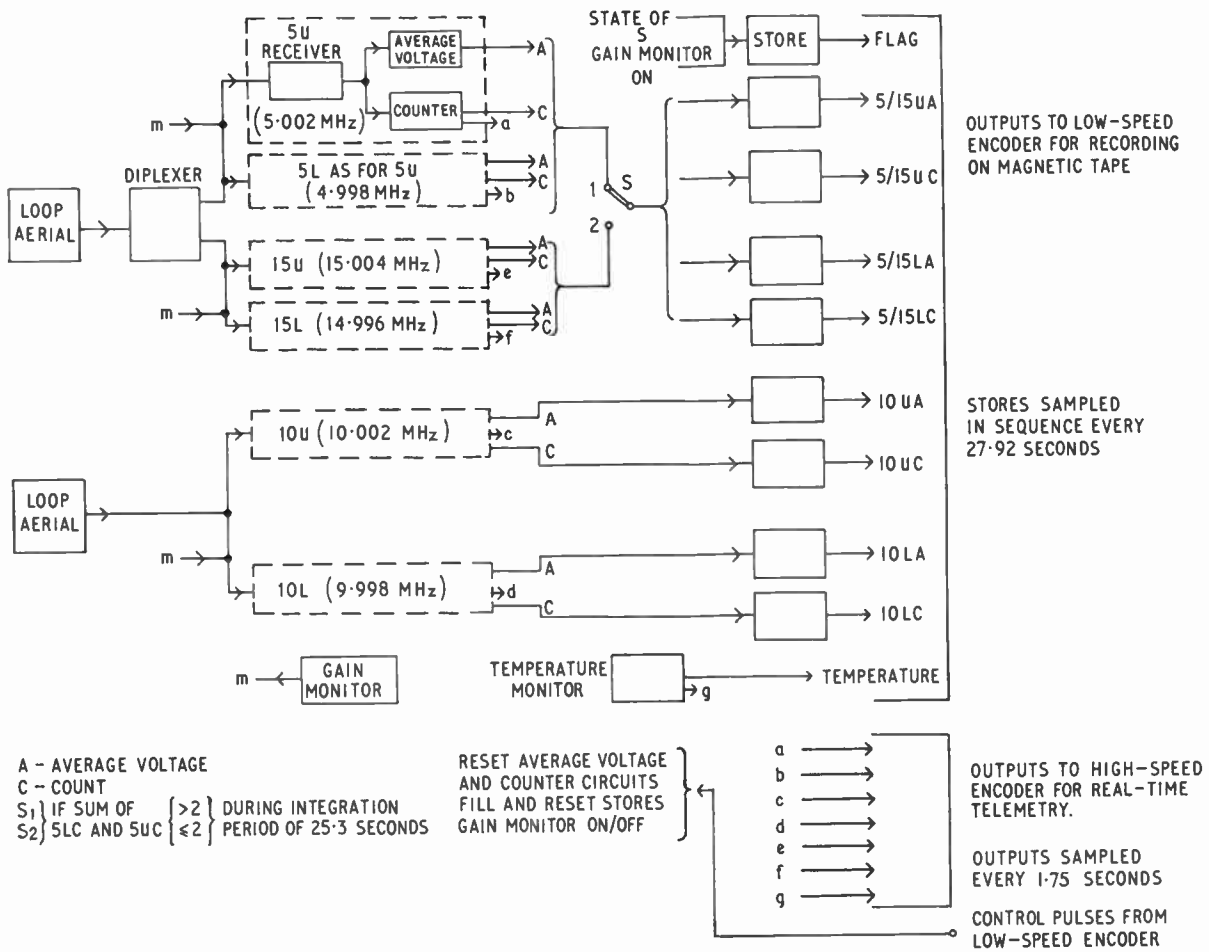

Fig. 2. Block diagram of the system.

loop was observed. The effective lengths were also measured to assess the influence of the satellite structure on performance. Aerial parameters (for free space) are given in Table 1.

Table 1

Aerial parameters

Frequency (MHz)	5	10	15
Effective length (m)	0·013	0·026	0·039
Loaded Q-factor	77	73	121

3.2 *Receivers*

The three pairs of receivers, which are crystal-controlled, operate at 4·998 and 5·002 MHz, 9·998 and 10·002 MHz and 14·996 and 15·004 MHz, each pair being fed from its appropriate aerial output through a cascode r.f. amplifier.

Each receiver is a homodyne, i.e. with the local oscillator set in the centre of the pass band. Both side bands are accepted and passed to an intermediate-frequency amplifier with the low centre-frequency of about 300 Hz. The r.f. spectrum of each band of noise being examined thus consists of two sections, each of the i.f. bandwidth, disposed symmetrically about the nominal signal frequency. The response curves for the pair of 10 MHz receivers are given in Fig. 3, the power bandwidth being 1580 Hz.

The main gain of the receivers and the required bandwidth are obtained by three stages of feedback-stabilized i.f. amplification and by RC filter networks. The amplifiers give a gain of about 60 dB and are temperature compensated for the range $-15°$ to 60°C.

By adopting a homodyne system, second-channel interference is avoided, problems with stability of frequency, bandwidth and gain are eased and the i.f. filter components are small and light and do not need adjustment. The attendant disadvantages of the presence of $1/f$ noise and spurious signals resulting from the small separation between the local oscillator and signal frequencies of each pair of receivers, were overcome by the use of adequate pre-amplifier gain, balanced mixer circuits and low-frequency cut-off of the i.f. response.

Following the i.f. amplifier, separate channels are used for measurement of average voltage and for counting atmospherics. For average voltage, a linear detector and integrator are followed by a logarithmic amplifier. A complete receiver has a dynamic range of greater than 30 dB. The counting circuit consists of a detector, discriminator and counter. The threshold level of the discriminator is set 9 dB above that of the average voltage of the envelope of internal noise of the system and peaks which exceed this level are recorded as counts. Since high-frequency noise from a lightning discharge may be received with varying amplitude for an appreciable fraction of a second, multiple counts from a single atmospheric are reduced by introducing a delay of 200 ms between the initiation of successive counts; the maximum count is then about 125 for each low-speed measurement.

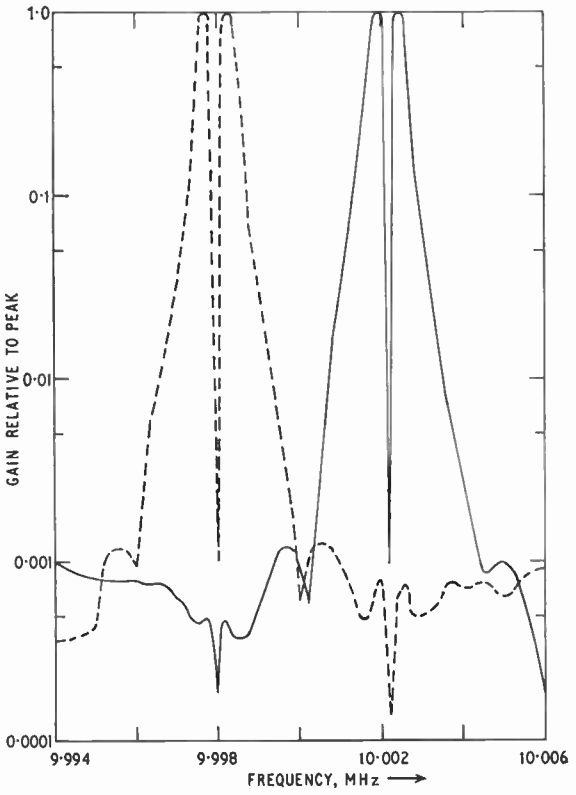

Fig. 3. Measured signal frequency responses of the 10 MHz receivers.

3.3 *Outputs and In-flight Gain Monitor*

Measurements of average voltage and count are made by all receivers during each low-speed sampling sequence which lasts 27·92 seconds. The observing periods of 25·3 seconds are synchronized to the timing of the telemetry encoder and the remaining 2·62 seconds are used to process the data and re-set the circuits.

Ideally, all the observing periods at the different frequencies should be coincident. However, since outputs are sampled sequentially by the encoder, 'sample and hold' stores must be included. To reduce the periods of data storage prior to sampling, it is

convenient to synchronize the 10 MHz measurement cycle so that it is delayed with respect to the 5 and 15 MHz cycles by the duration of three telemetry channel widths (2·62 seconds). The 'sample and hold' stores also ensure that the output levels do not vary by more than 1% during sampling; levels varying by more than this are not decoded correctly in the data-processing equipment on the ground.

The outputs of the 10 MHz receivers are continually sampled by the low-speed encoder but the outputs of either the 5 MHz or the 15 MHz receivers are selected for sampling at the end of each observing period by an internal logic switch. The selection is based on the presence or absence of counts in the 5 MHz receivers. If at least two counts are obtained, indicating 5 MHz reception, only the 5 MHz outputs are sampled since under these conditions the area on the ground from which noise is received at 15 MHz is unsuitably large. If fewer than two counts are registered in the 5 MHz receivers, either ionospheric cut-off is occurring at 5 MHz or there is effectively no storm activity; in this case the 15 MHz outputs are sampled to resolve the two possibilities.

Voltage-regulating diodes operated in the avalanche mode form wide-band r.f. noise generators which are switched on every sixteenth low-speed sequence to give in-flight monitoring from which any long-term variation in the gain of each receiver can be detected. A further check on performance is provided by the recorded values of the receiver noise levels under quiet conditions, i.e. when no storms are present or when the receiver frequency is below the critical frequency of the ionosphere.

A separate low-speed telemetry channel is used to identify the selection of 5 or 15 MHz outputs and the presence of gain monitor data. A tenth telemetry channel measures the temperature of the receiver package.

The allocation of six high-speed telemetry outputs is used to observe the levels in each counter channel. The build-up of counts during an integration period may thus be examined.

4. Effects of Environment on Design

Electrical, mechanical and thermal properties, compatibility and the possibility of radiation damage were factors involved in the design of the equipment for operation in the environment of space and in close proximity to other systems in the satellite.

4.1 *Environmental Specification*

The specified environmental conditions for prototype design qualification of the receiver package were: temperatures ranging from −15°C to +60°C; pressures down to 10^{-5} torr; linear acceleration of 38*g*; sinusoidal swept-frequency vibration from 5 to 2000 Hz with a maximum acceleration of 40 *g* (zero to peak); random motion vibration, 20 to 2000 Hz with an acceleration of 11·5 *g* r.m.s.

4.2 *Components and Parts*

Only components of known high reliability were included and all were tested and identified prior to use so that case histories could be followed. The numbers of components in the equipment are given in Table 2.

Miniature quartz crystals, designed to withstand vibration levels of 10 *g*, were mounted in small cans packed with polyester fibre to meet the more stringent vibration specification.

Table 2

Components per equipment

Component	Quantity
Capacitors:	
Ceramic	216
Polyester	66
Silver mica	24
Solid tantalum	134
Wet tantalum	12
Connectors:	
Coaxial	6
Multiway	3
Crystals (quartz)	6
Diodes	130
Resistors:	
Metal oxide	827
Carbon composition	43
Thermistor	1
Transistors	315
Transformers (r.f.)	18

In the construction of the aerials a copper-to-aluminium weld capable of withstanding a wide range of temperature and high vibration levels was required. The welds were made in argon after pre-plating the copper with silver. Sample welds were tested for several weeks for electrolytic damage and one weld was subjected to thermal stress by cycling one hundred and thirty times from −80°C to +80°C while under a tension of 0·9 kg. No sign of damage was noted.

To ensure satisfactory performance of the nickel-zinc ferrite pot cores used in the r.f. circuits, special

precautions were taken in mounting, ageing and avoidance of magnetic fields. The last factor was of particular importance, especially in the neighbourhood of electromagnetic vibrators, since it was found that fields greater than about 30 oersteds can cause long-term detuning effects.

4.3 *Radiation Damage*

To provide information on radiation damage, planar transistors, operated under conditions likely to be experienced in the equipment, were subjected to gamma and electron irradiation. One type under test was rejected.

A low-loss insulating material was also required for the telemetry and R.S.R.S. aerials and information available at the time of initial design work suggested that p.t.f.e. suffered significant loss of strength after irradiation. A series of tests showed that in vacuum the tensile strength of p.t.f.e. is maintained up to radiation levels far in excess of that expected to be encountered by the satellite and therefore the material could be used for construction of the aerials.[7]

4.4 *Assembly and Mechanical Construction*

The six receivers and logic circuits were constructed in seven trapezoidal-shaped trays in which the components were mounted hairpin-wise as shown in Fig. 4. This gave a good packing density with access for assembly, soldering and inspection. The components were given a thin coating of a resilient epoxy resin for protection during tests and were finally encapsulated with a polyurethane foam.

The trays were then clamped together and all interconnections brought to a distribution card in the lid. This also carried all connectors and, in turn, was clamped along the length of the package. The lid was deep enough to accommodate any filter elements that might have been required as a result of radio-frequency interference tests on the satellite.

The complete package, weighing 2·6 kg, was finished in white acrylic paint which was specified (for thermal control) by the satellite designers. The package is shown mounted in the satellite in Fig. 1.

4.5 *Compatibility*

For compatibility with other experiments and satellite equipment, the normal precautions of adequate decoupling were employed, supplemented by a two-wire power system and separate signal and power-return lines.

Redundant connections were provided where feasible and circuits designed, within the power and weight limits, to ensure that failure of any one component would not cause a significant increase in the power required by the experiment.

5. Test Procedures and Integration

In addition to a developmental set of equipment, five models were constructed for use in the various stages of preparation of the satellite:

D1—a mechanical model for layout and vibration tests;

D2—an electrical model for systems tests and r.f. compatibility tests;

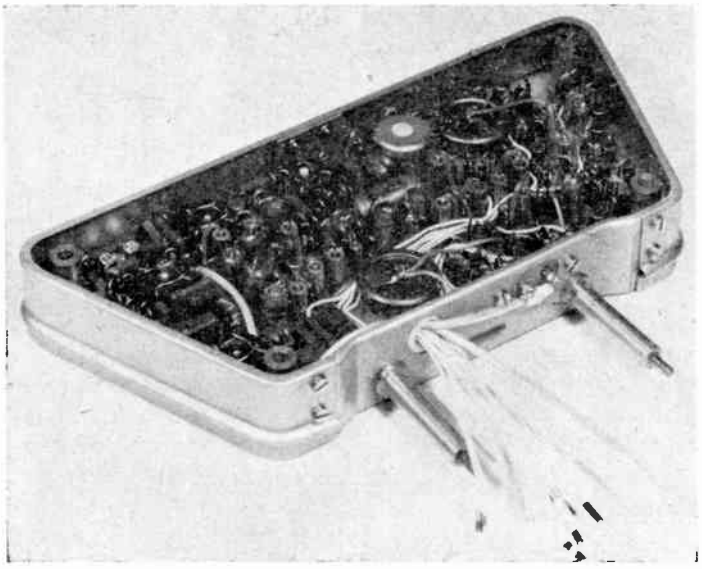

Fig. 4. A receiver before encapsulation.

P1—a prototype model for design qualification with complete electrical and environmental tests (hot and cold storage and operation, humidity, spin, acceleration, vibration, solar simulation and thermal vacuum tests);

F1—the flight model, subjected to full electrical and limited environmental tests;

F2—a flight back-up model tested as for F1;

F3—a flight spare model tested as for F1.

At all stages of preparation, facilities were provided by the satellite contractors for integration and performance tests. Long uninterrupted sequences of data were available for checking operation and controls were included in the equipment to allow the in-flight monitors to be switched on whenever required.

The major problem affecting integration of the R.S.R.S. experiment in the satellite was radio-frequency interference. The presence of three experiments involving the reception of very weak radio signals at frequencies from a few kilohertz to 15 MHz meant that general solutions had to be applied. Interference generated in units was suppressed at source by filters and additional screening. Interference in cable looms was minimized by separation of the looms and the use of screened cables. Grounded bulkhead connectors were used for all screened cables passing through the skin of the satellite and filter units fitted at entry points of all leads to solar cells.

Tests were arranged to prove that any small amplitude-modulation content of the frequency-modulated telemetry transmitter did not affect the experiment and that noise from d.c.-to-d.c. converters was sufficiently low.

During the launch preparations, electrical and mechanical checks were carried out satisfactorily although, as expected, in the final stages the receivers were affected by interference from converters in the guidance system of the *Scout* rocket and from radar installations.

6. Interpretation of Data Outputs

Interpretation of the outputs telemetered from the satellite to the ground, in terms of the h.f. noise radiated by the sources, needs a knowledge of propagation conditions from the sources to the vicinity of the satellite and of the characteristics of the receiving equipment. Only the latter are considered here; the other factors will be treated elsewhere.

Since the satellite is spinning, the voltages induced in the loop aerials are affected by the attitude of the satellite. A correction factor, k_1, for any observing period is determined by information from solar aspect sensors in the satellite and by solar reflections to ground stations from mirrors supplied by R.S.R.S. and mounted on the satellite body.[8]

The effective length of a loop aerial is affected by the presence of the ionosphere. At the altitude of the satellite, collisional effects in the ionosphere are negligible so that the actual effective length, l, is equal to $k_2 \times l_F$,[6]

where l_F is the effective length in free space

and $k_2 = \sqrt{1 - 8{\cdot}04 \times 10^{-11} N f^{-2}}$

where N is the electron density (electrons/m^3)

and f is the frequency of measurement in MHz.

Values of N are available from the Birmingham University experiment on the satellite.

The receivers were calibrated in terms of fluctuation noise. Input-output characteristics were obtained using random-noise generators matched to the receiver inputs; an input r.m.s. voltage V (in μV) from the generator gives a reference level on the average voltage output of a receiver. The same output is given by a fluctuation noise type field of r.m.s. amplitude E_f (in dB relative to 1 μV/m) incident on the aerial, such that

$$E_f = 20 \log_{10} \left[\left(\frac{Vn}{l_F Q} \right) \left(\frac{1}{k_1 k_2} \right) \right]$$

where Q = loaded Q-factor of aerial,

n = transformer step-down ratio

and other symbols are defined above.

The r.m.s. value of the envelope of the field $E_{f(env)}$ is 3 dB above E_f.

The receiver sensitivities in a screened room at 15°C, with $k_1 = k_2 = 1$, for a signal/noise ratio of unity, are such that

for the 5 MHz receivers,

$E_f = -7$ dB relative to 1 μV/m

for the 10 MHz receivers,

$E_f = -8$ dB relative to 1 μV/m

for the 15 MHz receivers,

$E_f = -11$ dB relative to 1 μV/m

To obtain the response to atmospheric noise which has a different waveform, it is convenient to use, in conjunction with the receiver characteristics for fluctuation noise, a level-probability curve for a 'standard atmospheric' derived from observations on the ground from a large number of typical discharges. The curve used for receiver design is given in Fig. 5 and is based on observations made at R.S.R.S.

Since the receiver characteristics are reasonably linear over most of the dynamic range, an approximate

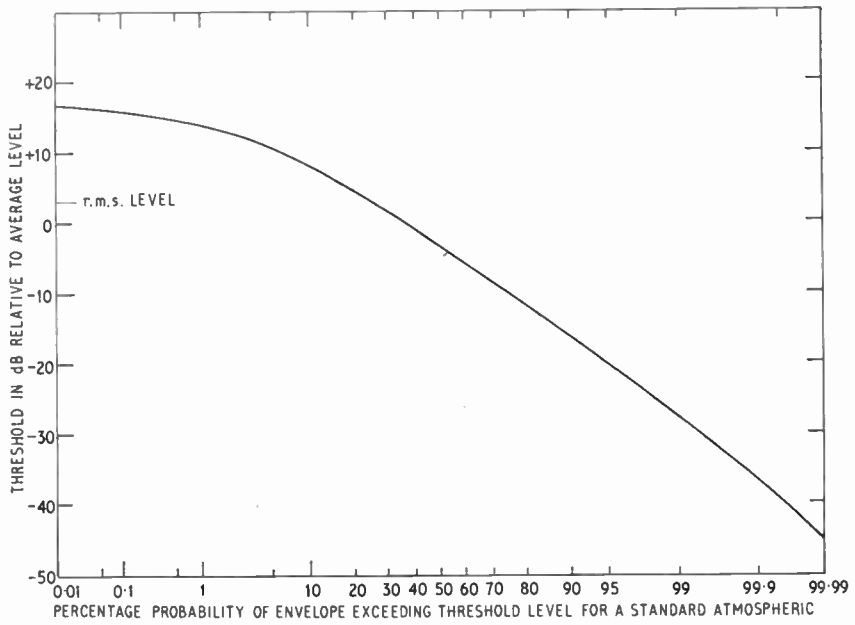

Fig. 5. Level probability curve for a 'standard atmospheric'.

value for the r.m.s. of the envelope of the incident atmospheric noise field $E_{a(env)}$ (in dB relative to 1 μV) which gives the reference level on the output, may be obtained using the relationships (expressed in dB):

(*a*) for fluctuation noise,

the average of the amplitude of the envelope = the r.m.s. of the envelope − 1

(*b*) for noise from a 'standard atmospheric', (see Fig. 5),

the average of the amplitude of the envelope = the r.m.s. of the envelope − 3

Therefore $E_{a(env)} \simeq E_f + 5$

$$= 20 \log_{10} \frac{Vn}{l_F Q} \frac{1}{k_1 k_2} + 5$$

This value of $E_{a(env)}$ applies for the specific power bandwidth of the receivers (1580 Hz) and may be converted for other bandwidths since at the frequencies used in the experiment, the r.m.s. value of the envelope of the field is proportional to the square root of the power bandwidth.

7. Performance in Orbit

The satellite was launched on 5th May 1967 into an orbit of apogee 598 km, perigee 494 km and inclination 80° and both recorded and real-time data received on the ground showed that all sections of the R.S.R.S. equipment were functioning as intended. The receivers continue to function at the date of completion of this paper.

At times, the outputs from pairs of receivers are closely correlated while at others, the effects of interference are shown by differences in the recorded values. As expected, saturation of the counting channels has been observed over the main thunderstorm areas. The selection of 5 or 15 MHz outputs for sampling is in general accord with ionospheric conditions and storm distributions below the satellite. The lowest noise levels that have been recorded are slightly below those observed in a screened room before launch.

A full analysis of the results is being carried out at R.S.R.S. and will be reported by different authors.

8. Acknowledgments

The equipment was developed and manufactured by Pye Laboratories Ltd., Cambridge, to a specification prepared at R.S.R.S. The contributions of Mr. D. Weighton, Mr. J. Blades and Mr. B. Cox are gratefully acknowledged.

The copper-aluminium welds were made by the British Welding Research Association.

Every assistance in testing was provided to R.S.R.S. by representatives in the Trials Team from the Royal Aircraft Establishment, Farnborough, the British Aircraft Corporation and the General Electric Company.

Many members of R.S.R.S. contributed to the project, in particular, Mr. F. Horner who proposed the survey and provided data on atmospheric noise

characteristics, Mr. R. Dalziel who supervised the work and Mr. G. Douglas who assisted in the testing of the equipment.

The work described was carried out at the Radio and Space Research Station of the Science Research Council and is published with the permission of the Director.

9. References

1. C. Clarke and V. A. W. Harrison, 'Low-frequency direction finder', *Wireless Engineer*, **32**, pp. 109–14, April 1955.
2. F. Horner, 'The design and use of instruments for counting local lightning flashes', *Proc. Instn Elect. Engrs*, **107B**, pp. 321–30, July 1960.
3. F. Horner, 'Analysis of data from lightning flash counters', *Proc. Instn Elect. Engrs*, **114**, pp. 916–23, July 1967.
4. 'Advances in Radio Research', Vol. 2, pp. 122–204 (Academic Press, London, 1964).
5. F. Horner, 'Narrow-band atmospherics from two local thunderstorms', *J. Atmos. Terrestr. Phys.*, **21**, pp. 13–25, 1961.
6. W. C. Bain, 'Aerials in an ionosphere of zero conductivity', *Proc. Instn Elect. Engrs*, **110**, pp. 897–8, May 1963.
7. V. A. W. Harrison, 'The comparative strengths of polytetrafluoroethylene and polychlorotrifluoroethylene under nuclear radiation', *The Radio and Electronic Engineer*, **35**, No. 1, p. 54, January 1968 (Letter).
8. R. B. Bent, 'Attitude determination of the *Ariel III* satellite', *The Radio and Electronic Engineer*, **35**, No. 3, p. 183, March 1968.

Manuscript first received by the Institution on 20th October 1967 and in final form on 4th January 1968.
(Paper No. 1173/AMMS9.)

Research on Soldering Techniques

One of the major technological advances in the electronics industry over the past decade has been the use of printed circuit boards on which the individual components are assembled. An important prerequisite of circuit boards is that they should be quickly and perfectly wetted by the solder during the wave- or dip-soldering operation. According to the Annual Report of the International Tin Research Council for 1967, a number of firms in the electronics industry had found that the solder dewetted or retracted into ridges and globules on circuit boards which apparently had been adequately prepared for soldering. Laboratory investigations at the Tin Research Institute in Greenford, Middlesex, showed that solderability was satisfactory for short times, but progressive dewetting occurred as the time of contact with the solder increased. Detailed electron-microscope study revealed the cause of poor solderability to be numerous inclusions in the copper surface, probably resulting from abrasive cleaning of the copper. It is therefore recommended by the Tin Research Institute that the copper on printed circuits should be cleaned only by chemical means. A limited study is now in progress on the effects of some metallic impurities in the solder bath on the minimum wetting-time of printed circuit material.

Bright tin plating has aroused much interest because of its superior appearance over the matt coating. Investigations have confirmed that it also has excellent solderability, and it is suggested as an alternative to tin-lead plating on printed circuits.

The wetting-time solderability test unit at the T.R.I. Laboratories, which provides a controlled time of immersion in the solder, has been in constant use, especially in answering industrial problems, and a prototype 'commercial' instrument has been designed and built. A manufacturing firm is now producing a similar industrial unit for sale to the electronics industry. Besides its principal use for testing printed circuit-board samples, the test machine may also be employed for carrying out solderability tests on solder tags, terminala posts and, with special accessories, on plated-through holes in circuit boards or eyelets. It may also be used for area-of-spread type solderability tests. This rotary arm method of testing for solderability is being considered, along with other tests, by the Electronic Engineering Association and the International Electrotechnical Commission for use as a national or international standard.

All these methods of testing for solderability are subjective and require an operator who is familiar with the appearance of defectively and fully wetted soldered surfaces. To assist inspection a number of photographic 'standards' have been prepared at the Institute's Laboratories, showing printed circuit boards exhibiting various degrees of wetting, dewetting and non-wetting.

INSTITUTION NOTICES

Dinner of Council and Committees

The Twelfth Dinner of the Institution's Council and Committees will be held on Thursday, 16th May 1968, at the Savoy Hotel, London. The guests of honour will be the Immediate Past President, Professor Emrys Williams, Ph.D., B.Eng., and Mrs. Williams.

Further details may be obtained on application to the Secretary, at 9 Bedford Square, London, W.C.1.

Elections and Transfers to Membership of the Institution

It has been the custom of the Institution to send to Corporate Members of the Institution in the United Kingdom a list showing the names of applicants for election and transfer. Following the required lapse of 28 days, and in the absence of any objection being raised by a Corporate Member to any proposal, the Council has confirmed the elections and transfers in question and the lists then have been published in the *Proceedings*.

In the interests of speed and economy a change in this procedure is to take place. With effect from the beginning of the next Institution year (April 1968) lists of applicants for membership will be included in the end section of each issue of *The Radio and Electronic Engineer*. Two issues later and provided that no objections have been lodged and sustained by the Council, an announcement will be given in *The Radio and Electronic Engineer* that the members previously listed have been duly elected.

The last of the separate lists of applicants for membership (List No. 80) is being enclosed in copies of this issue sent to Corporate Members of the United Kingdom.

Notice is hereby given that the elections and transfers given in Lists No. 77 and 78 have now been confirmed by the Council.

The President Entertains Engineers from Overseas

On 29th February the President of the Institution, Major-General Sir Leonard Atkinson, K.B.E., gave a luncheon party in the Royal Over-Seas League's House in London, in honour of two distinguished engineers from overseas. He was supported by senior members of the Council in entertaining Mr. Elhanan Pelles, C.E., Director General of the Association of Engineers and Architects in Israel, and Mr. Leopold M. Nadeau, Director General of the Council of Canadian Professional Engineers.

Both Israel and Canada have compulsory registration for engineers, and discussions in the past have centred on the position of Corporate Members of the Institution in relation to registration.

The President and his colleagues were able to continue the exchanges of views which took place during the visit to Israel last year by the Immediate Past President, Professor Emrys Williams, and the Director of the Institution, Mr. Graham D. Clifford. Mr. Clifford has met Mr. Nadeau and other officers of the various Associations of Professional Engineers in Canada on his visits to Ottawa and Montreal, and several matters of mutual interest could therefore be reviewed.

The Paris Component Show

The Institution will again have a stand at the Salon Composants Electroniques, to be held at Porte de Versailles, Paris, from Monday, 1st April to Saturday, 6th April (inclusive). Institution publications, in particular *The Radio and Electronic Engineer*, will be exhibited. Committee Members of the French Section will be present at the stand during the week.

European Physical Society

Further progress has been made in the formation of a European Physical Society. At a meeting of the Steering Committee in Geneva on 30th January representatives from several Eastern European countries attended for the first time.

Substantial agreement was reached on the constitution, aims and activities. Certain details, particularly financial, remain to be decided, but the Society should become a legal and operating organization within the next three months.

Further information on the Society may be obtained from Dr. L. Cohen, Secretary of The Institute of Physics and The Physical Society, 47 Belgrave Square, London, S.W.1

Control of Artificial Limbs

A Symposium on 'The Basic Problems of Artificial Prehension, Movement and Control of Artificial Limbs' is to be held in London from 31st October to 1st November 1968. The Symposium will take place at the Institution of Mechanical Engineers and is co-sponsored by the Institution of Electrical Engineers.

The programme, consisting of invited and contributed papers, will cover the following subjects:

fundamental nature of handling—prehension and movement; physiology of muscular control; control and adaption; communication and instrumentation in prosthetics; problems of power operation and control; acceptability by the patient.

Further information is available from Mr. E. P. Davies, Institution of Mechanical Engineers, 1 Birdcage Walk, London, S.W.1.

U.D.C. 621.311.61:629.17

The *Ariel III* Power System

By
F. C. TREBLE, B.Sc., C.Eng., M.I.E.E.,†
R. C. COOK, B.Sc.†
AND
P. G. GARRATT, B.Sc.†

Presented at a Symposium on 'The Ariel III Satellite' held in London on 13th October 1967.

Summary: The solar cell/battery system, which provides power for the experiments, data handling equipment, tape recorder, telemetry transmitter and command receiver on the *Ariel III* satellite, is described, with particular reference to novel features and the techniques employed to ensure adequate performance with the utmost reliability.

1. Introduction

Power for the experiments, data handling equipment, tape recorder, telemetry transmitter and command receiver on board *Ariel III* is obtained from two arrays of silicon solar cells. One array supplies power to the loads through converters and regulators, while the other charges a battery for operation in the Earth's shadow. The average continuous total load is 6·7 W and the peak load is 12·7 W.

The prime design requirement was that the system should work reliably in the space environment throughout the planned life of one year, under all orbital conditions from 'full Sun' to maximum darkness. It was required to withstand pre-launch handling, testing, storage and transportation and also the severe vibration and acceleration imposed on it during launch. As with all satellite systems, weight had to be kept to a minimum.

Since only the Meteorological Office experiment imposed any attitude constraint on the satellite, it was a design requirement that the solar cells be capable of providing adequate power in any attitude with respect to the Sun. The other experiments would not then be affected by a failure to achieve the design attitude at injection nor by subsequent perturbations.

Underlying the design concept was the assumption that the storage battery, consisting as it did of hermetically-sealed cells with a restricted temperature range, was the most vulnerable part of the power system. Therefore special care was taken to study its operational requirements for long life and ensure as far as possible that these requirements were met. Also, it was arranged that, in the event of battery failure, the satellite could continue to function fully during the periods of daylight.

2. General Arrangement and Mode of Operation

The power system is shown in block form in Fig. 1. As most of the power is required at +12 V, this line is fed direct from the load array; the other voltages are obtained by using a d.c. to d.c. converter.

The battery is charged through a regulator whose constant-current/constant-voltage characteristic is automatically modified to suit the temperature of the battery. At 40°C the battery temperature sensor limits the charge to 100 mA, a level sufficient to maintain full charge without overheating the battery or adversely affecting subsequent cycling performance.

If, for any reason, the battery voltage falls below 14 V, the voltage sensor disconnects the battery from the load (relay A2) and puts it on constant-current charge at 300 mA via the auxiliary charging regulator. At the same time, the main charging regulator is short-circuited (relay A1) thus connecting the two arrays in parallel via the discharge regulator. This ensures adequate power to maintain the satellite in full 'daylight only' operation.

If the battery recovers, a re-set circuit in the voltage sensor unit returns it to service. But if it fails to respond, the charge is discontinued when the voltage falls to 9 V and 'daylight only' operation continues.

The discharge regulator allows current to be drawn from the battery when the load array voltage falls below 13 V and prevents discharge when it is above 13 V, which is normally the case in sunlight. Overstressing of this unit at times when the array voltage is high and the battery voltage low, a situation which may occur when the satellite first emerges from a long period in the Earth's shadow, is avoided by a protective circuit.

Isolating converters are inserted in the load and battery circuits to permit the positive terminals of both arrays to be earthed. This was necessary to meet a requirement (imposed by the Birmingham University experiment) that no exposed metal should be positive with respect to the satellite frame.

3. The Solar Cells

The solar cells are mounted on the four curved doors and the four booms of the satellite (Fig. 2). Each of the small rectangles represents a module of 48 cells,

† Ministry of Technology, Royal Aircraft Establishment, Farnborough, Hants.

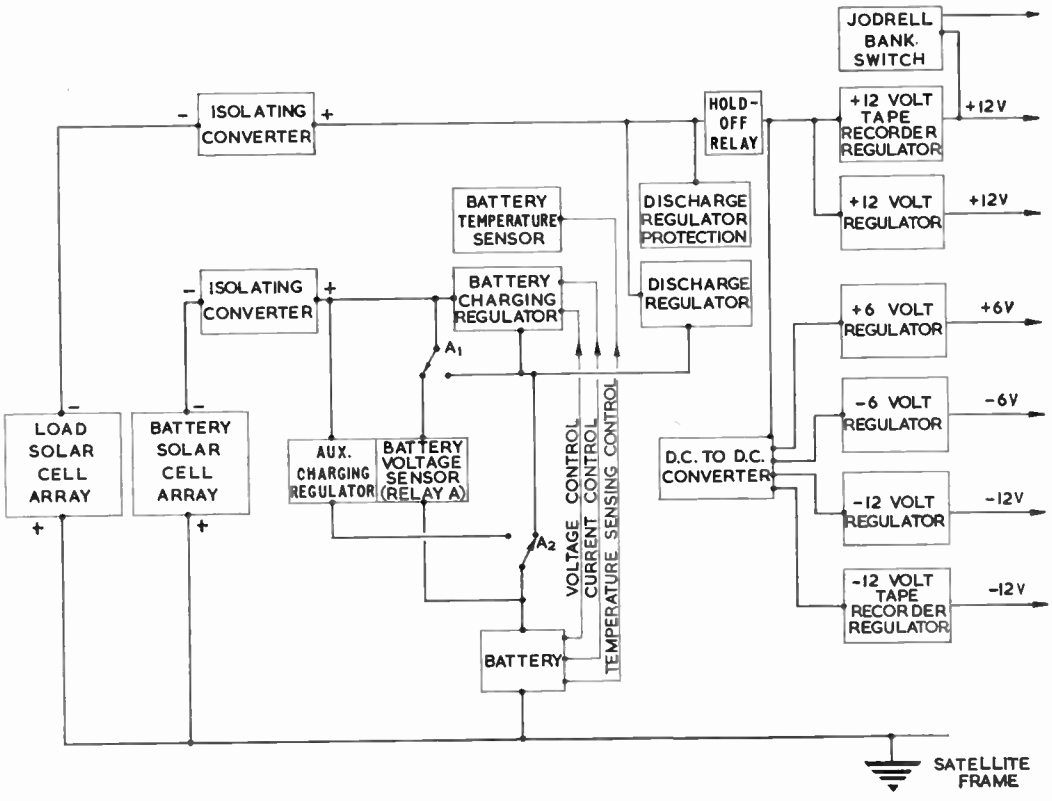

Fig. 1.
The *Ariel III* power system.

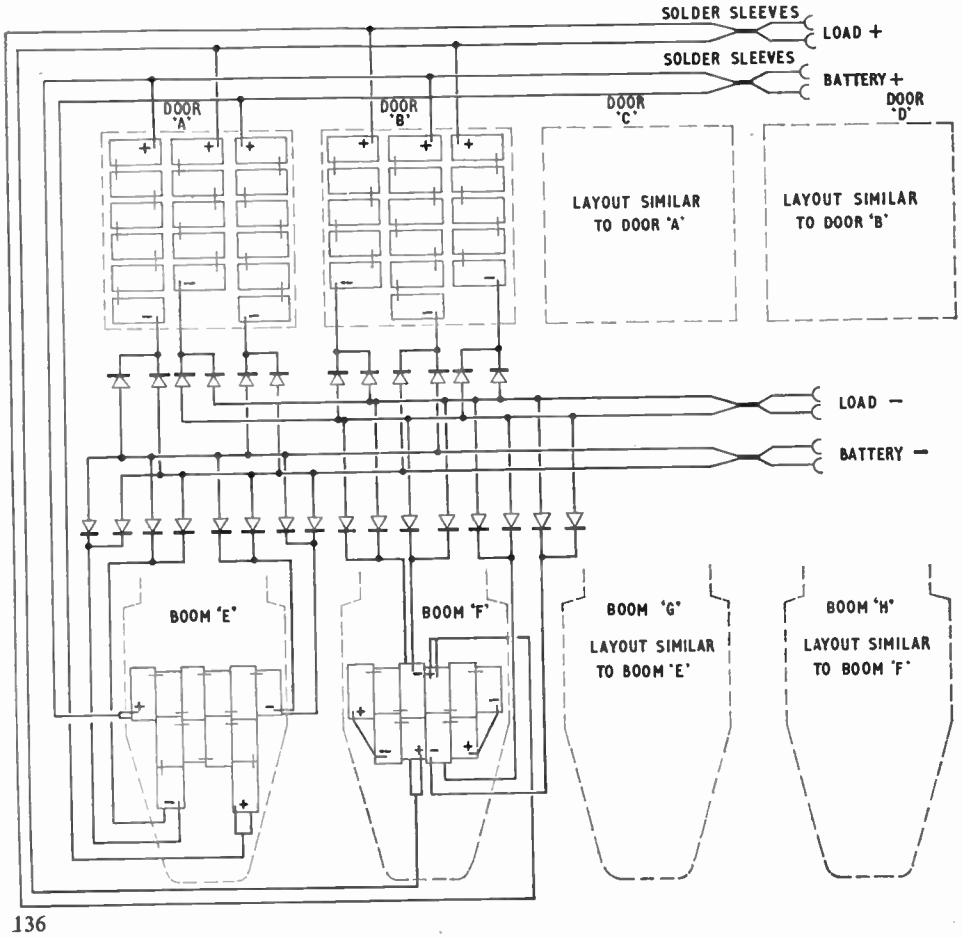

Fig. 2.
The solar cell system.

each 1 cm × 2 cm, eight in series × six in parallel. Five modules in series form a panel in the load array and six form a panel in the battery array. Six load and six battery panels are alternated around the body. Booms E and G each carry four battery panels of double-sided modules, while booms F and H each carry four load panels. Thus, each array comprises fourteen panels in parallel, making a total of 7392 cells on the satellite.

The modular construction was chosen in preference to large single panels in order to minimize scrap during the development phase, facilitate handling and environmental testing before satellite integration and simplify spares provisioning and rectification of faults. The paralleling of individual rows of cells in the modules minimizes loss of power in the event of multiple open-circuit failures.

A computer was used to carry out detailed assessments of the performance of the system as it was developed. These assessments took into account current cell performance, predicted temperatures, radiation damage and shadowing effects from aerials, booms and body. The final assessment showed that the system was capable of meeting continuously all load requirements for one year in orbit, irrespective of the solar orientation. An initial capability of about 15 W was necessary to achieve this.

As examples of this study, Figs. 3 and 4 show the predicted end-of-life performances of the load and battery arrays with the satellite axis normal to the Sun vector. Two curves are shown in each case, one representing the hottest and the other representing the coldest conditions likely to occur. The load and critical battery requirements are also indicated. The critical battery requirement occurs at the change-over from the constant current to the constant voltage charging mode. As already mentioned, the charging current is automatically reduced at a battery temperature of 40°C. Hence, the locus of the curve contains two points at this temperature. Both load and battery requirements are seen to lie wholly within the output curves.

The silicon solar cells, developed and manufactured by Ferranti, are of the radiation resistant 'n on p' configuration, with a nominal base resistivity of 10 Ω cm and a conversion efficiency of about 10% in sunlight above the atmosphere. They measure 1 cm × 2 cm, are 0·3 mm to 0·4 mm (0·014 in to 0·016 in) thick and have a junction depth of 0·25 to 0·5 μm.

A special feature of these cells is the untinned nickel-copper-gold contacts, which are extremely adherent and easily soldered. The positive contact covers the whole of the back surface, while the negative contact is in the form of a three-fingered grid on the active surface.

Another unusual feature is that the cells are processed in disk form, the last operation being to scribe and break the disk to form two cells. The edges thus formed are not perfectly straight or normal to the surface but give a high shunt resistance.

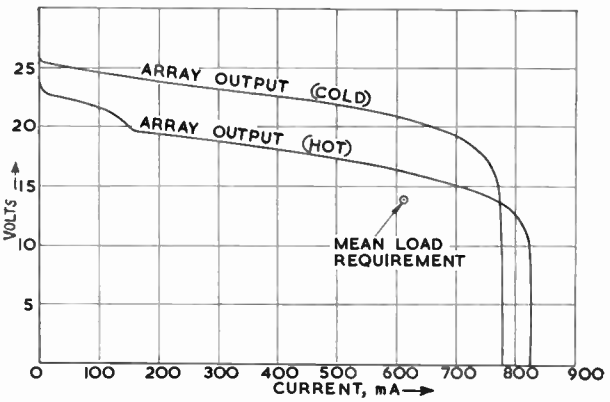

Fig. 3. Predicted performance of load array in design attitude.

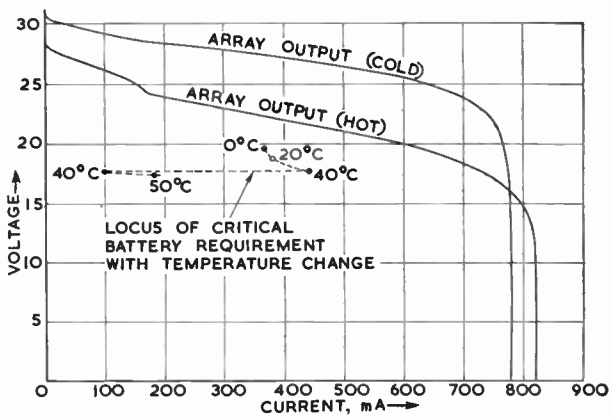

Fig. 4. Predicted performance of battery array in design attitude.

Measures taken to ensure the reliability of the cells included an adhesive tape pull-off test on every contact and visual inspection under a microscope. Independent quality assurance tests were carried out on a 1% sample of each week's production.

Figure 5 shows the construction of the 48-cell body module. It weighs just under 40 gm (1·4 oz) and delivers just over 1 W into a matched load in normal incidence sunlight above the atmosphere.

Each row of six cells, called a 'sub-module', is connected in parallel by soldering the back contacts to 0·152 mm (0·006 in) printed circuit board and the front contacts to a narrow copper strip. Eight matched sub-modules are connected in series by small tags and the matrix is then cemented to a honeycomb panel and connected to three Teflon insulated terminals at each end. Finally, a 0·152 mm thick glass cover slip is cemented to each cell to provide a highly emissive surface and give protection against micrometeorites and low-energy radiation.

The boom modules are similarly constructed, except that the honeycomb is 2·5 cm (1 in) thick and cells are mounted on both faces.

The module assembly process was designed to facilitate rapid production and maintain a consistently high standard of quality and reliability. Special jigs were used for every assembly stage and only the series connections were hand-soldered, the other soldered joints being made in heated jigs under a closely-

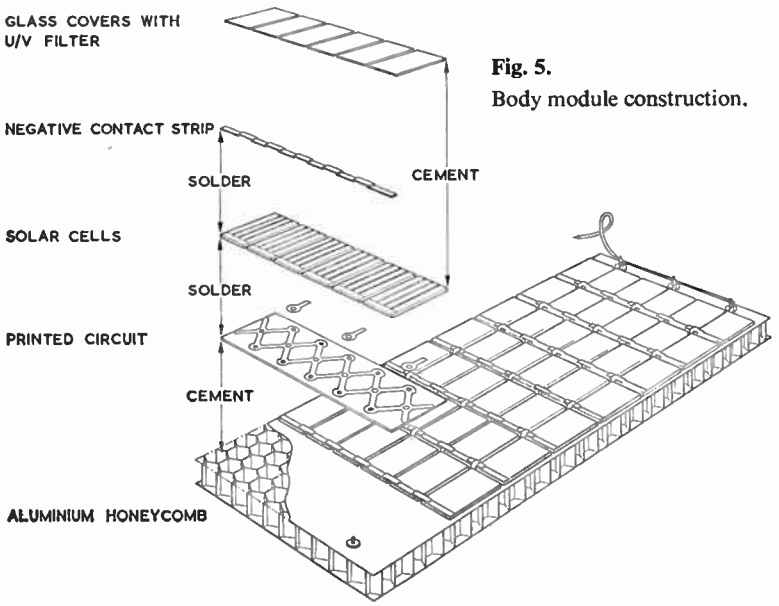

Fig. 5. Body module construction.

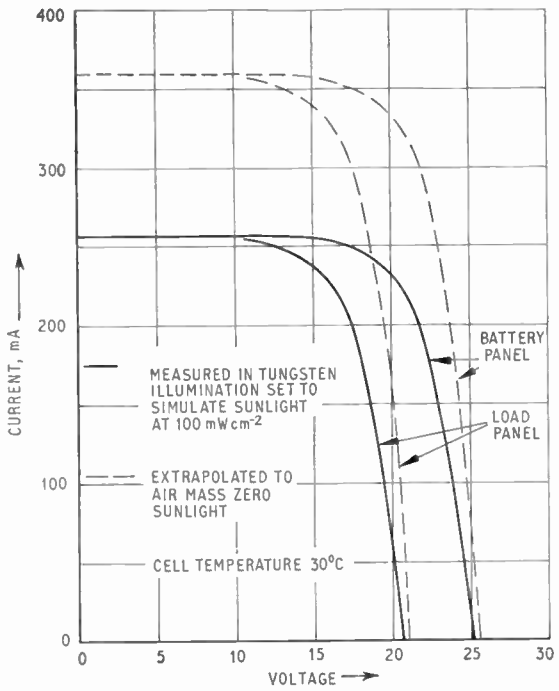

Fig. 6. Typical solar cell panel performance characteristics.

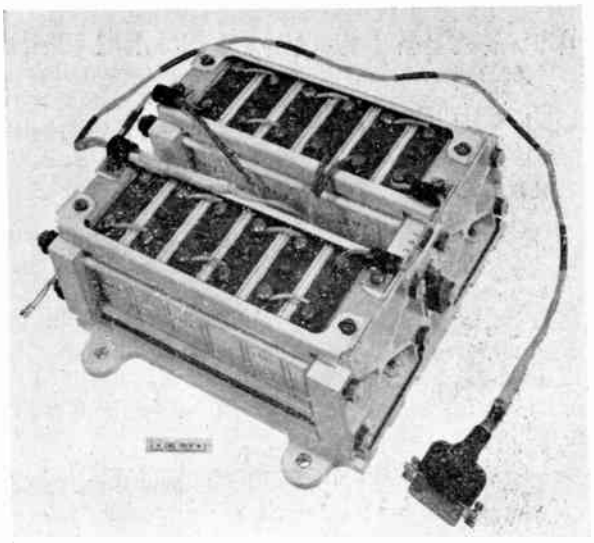

Fig. 7. The storage battery.

controlled time/temperature cycle. Before acceptance, every module was thermally cycled in vacuum twenty times between −80°C and −50°C.

After assembling the modules on the doors and booms of the satellite, the voltage-current characteristic of each panel was measured in filtered 3000°K tungsten light. Figure 6 shows typical characteristics of the load and battery panels as measured at 100 mW/cm^2 and extrapolated to 140 mW/cm^2, the solar constant. The conversion efficiencies calculated from these curves, which agreed well with similar measurements made on the constituent modules, averaged 8·9%.

The solar arrays on the flight satellites were fully tested in natural sunlight at the launching site. Each body panel and boom side was illuminated in turn (the others being covered) and its voltage current characteristic was traced on an X-Y plotter in a test circuit plugged into the turn-on connection. The intensity of the sunlight was monitored by a calibrated module mounted in the same plane as the panel being tested. The measured curve was then extrapolated to sunlight above the atmosphere.

4. The Battery

The battery (Fig. 7) consists of twelve Gulton 3 A-h, hermetically-sealed nickel-cadmium cells connected in series, giving a nominal voltage of 16 V. The cells are arranged in two stacks of six, with an insulated separator between adjacent cells, and are compressed between stiff end-plates to limit deformation due to the internal pressures generated on over-charge. An alumina-loaded epoxy resin is set between the cells and the base-plate to facilitate cooling and the cell tops are individually potted with a filled epoxy-polyamide resin for extra insurance against electrolyte leakage.

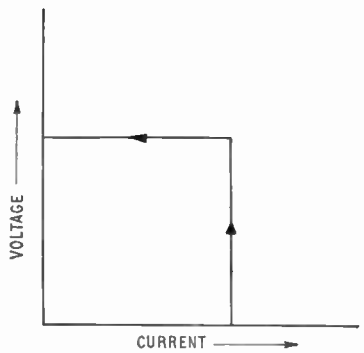

Fig. 8. Output characteristic of the battery charging regulator.

The flight cells were selected on the basis of uniform capacity and end-of-charge voltage, after eliminating all those exhibiting abnormal electrical or mechanical features.

Aspects of battery performance, such as charging characteristics, over-charge behaviour, thermal effects and charge-discharge cycling effects were fully investigated before the parameters of the charging characteristic were fixed. The basic constant-current/constant-voltage charging characteristic is shown in Fig. 8. Since the charging efficiency decreases and the maximum permissible over-charge current increases with increasing temperature, it is necessary to vary the initial current and the transition voltage with temperature to ensure that at all operating temperatures, the battery receives a full charge without excessive over-charge. Figure 9 shows the variations which were specified as a result of the operational study.

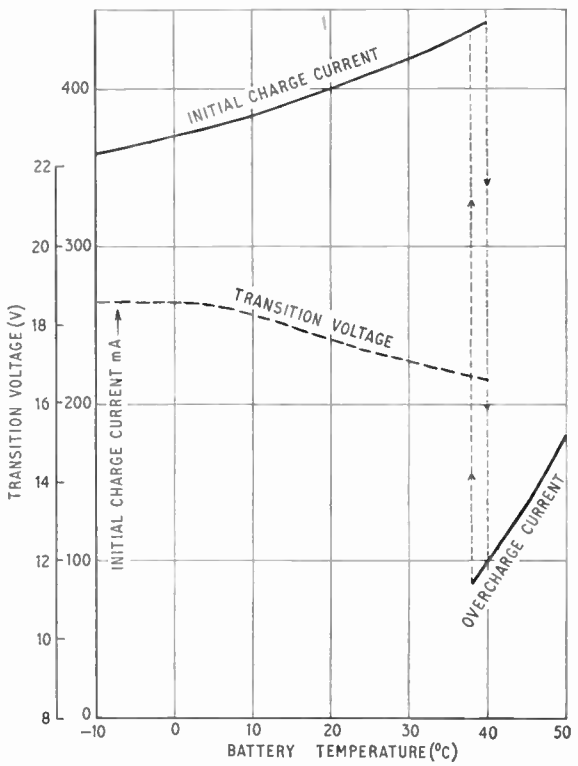

Fig. 9. Variation of transition voltage and initial charge current with battery temperature.

The depth of discharge during orbits of maximum darkness is about 10%. Under these conditions and subject to the temperature remaining within the design range of −10°C to +40°C, as it has done so far, the battery is expected to function satisfactorily during the planned life of the satellite.

5. The Power Conditioning Equipment

The power conditioning equipment, which comprises all the units shown in Fig. 1, except the solar cell arrays and the battery, is grouped in three boxes of similar mechanical design. Figure 10 shows the power storage control box, which contains the main and auxiliary charging regulators, the battery temperature and voltage sensors, the discharge regulator with its protective circuit, the hold-off relay and the solar cell array current monitor amplifiers. Another box houses the voltage regulators and main converter, and a third the isolating converters.

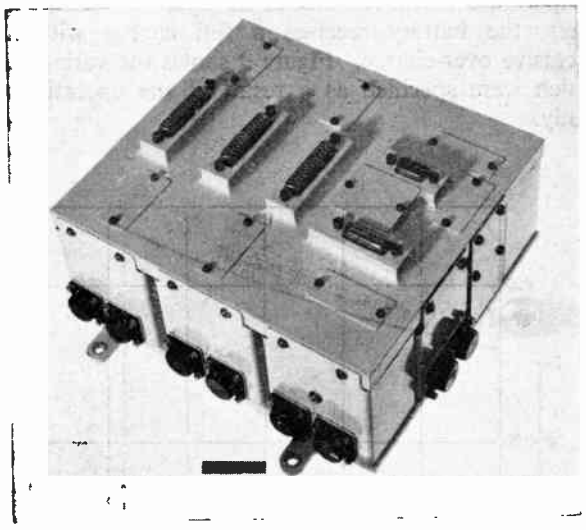

Fig. 10. Power storage control box.

The individual units are mounted on a machined aluminium alloy base-plate. A top plate carries the inter-unit connecting matrix, the input and output connectors and components for monitoring performance parameters.

Each individual circuit is constructed as a pre-tested self-contained potted unit. The components are stacked between parallel interconnecting matrices of the type used in the data handling system. Welded connections are used wherever possible, in the interests of reliability and high packing density, and there is full joint and lead redundancy. In the case of high-risk components such as solid tantalum capacitors, full redundancy is provided against predominant failure modes. For other components, redundancy is provided only to the extent necessary to ensure 'daylight only' operation.

During initial satellite integration, considerable interference was found to exist between the d.c.-to-d.c. converters and the highly sensitive radio receivers of three of the experiments (Sheffield University, Jodrell Bank, and R.S.R.S.). This necessitated the extensive use of screening and input power line filters. Each transformer is screened with multiple layers of copper foil and each complete converter assembly enclosed in a 0·5 mm (0·020 in) thick mu-metal box. At every point where power enters the satellite body, whether from the solar cell arrays or from external test-circuits, screened a.f./r.f. filters are used. These filters are so designed that current loops cannot flow through the satellite structure and r.f. earthing occurs at the satellite skin.

Components were selected on the basis of experience gained by the Americans and were subjected to ageing and functional tests in an endeavour to eliminate potential sources of failure. In addition to the formal type-approval tests, a 3½-month thermal vacuum test was carried out on two integrated systems, complete with storage battery, to assess the effects of long-term operation in a space environment. During these tests, the systems were operated under simulated orbital conditions, including a 20-day period of continuous battery over-charge. Results were completely satisfactory in both cases.

6. Orbital Performance

Table 1 shows the performance and temperatures of the *Ariel III* power system in orbit. The figures have been obtained from an analysis of 'quick-look' telemetered housekeeping data received from the STADAN station at Winkfield in Berkshire.

Table 1

Performance of the *Ariel III* power system

Regulated Line Voltages:	
Nominal value	Maximum deviation from set value
+ 12 V	0
+ 6 V	± 10 mV
− 6 V	+ 0 − 10 mV
− 12 V	+ 0 − 10 mV
Temperatures	
Power regulator box	+ 15°C to + 39°C
Power storage control box	+ 15°C to + 37°C
Battery	+ 8°C to + 38°C
Body array	− 27°C to + 30°C
Boom array	− 53°C to + 7°C

The solar cell arrays are performing as predicted and have met all power demands to date.

Variations of battery charge current with temperature have been in accordance with the designed characteristic, except that, after six days of overcharge during the first continuous sunlight period between orbits 97 and 359, the current increased slowly until the satellite entered eclipse and cycling re-commenced, after which the correct conditions were re-established. A possible explanation for this behaviour is that the terminal voltage of nickel-cadmium batteries tends to fall slightly after prolonged charging at a constant rate. This would cause the charging regulator to increase the charge current until such time as the battery temperature reached 40°C, when the current would be automatically reduced to 100 mA.

To sum up, the performance of the power system to date has been completely satisfactory, and there is nothing in the results that is symptomatic of incipient failure.

7. Acknowledgments

The authors thank their colleagues Messrs. A. A. Dollery, S. E. A. Pomroy, J. F. China and C. J. West for their help in the preparation of this paper. They also acknowledge the work of other members of Space and Materials Departments, R.A.E. and the contractors in the development, manufacture and testing of the *Ariel III* power system. The paper is reproduced by permission of the Controller, H.M. Stationery Office. Crown Copyright reserved.

Manuscript first received by the Institution on 6th September 1967 and in final form on 1st January 1968.
(Paper No. 1174/AMMS 10.)

I.E.R.E. Graduateship Examination, November 1967—Pass Lists

The following candidates who sat the November 1967 examination at centres outside Great Britain and Ireland succeeded in the sections indicated. The examination, which was conducted at 57 centres throughout the world, attracted entries from 403 candidates. Of these, 185 sat the examination at centres in Great Britain and Ireland and 218 sat the examination at centres overseas. The names of successful candidates resident in Great Britain and Ireland are published in the January–February issue of the *Proceedings* of the I.E.R.E.

	Candidates appearing	*Pass*	*Fail*	*Refer*
Section A: Great Britain	105	46	51	8
Overseas	120	31	85	4
Section B: Great Britain	80	27	47	6
Overseas	98	12	74	12

OVERSEAS

The following candidates have now completed the Graduateship Examination requirements and thus qualify for election or transfer to Graduate or Corporate Membership of the Institution.

BAILLIE-SEARLE, C. G. *Durban, South Africa.*
BHATIA, R. N. *India.*
CULVER, R. A. *New Zealand.*
EASAW, G. J. *Malaysia.*
GLENDENNING, J. S. I. *Singapore.*
LAU HON SHIANG *Singapore.*
LOCHORE, M. *New Zealand.*
MANNION, M. H. *New Zealand.*
NORMAN, A. R. *New Zealand.*
PANDEY, A. K. *India.*
RICHARDS, I. R. *New Zealand.*
SMALL, B. C. *New Zealand.*

The following candidates have now satisfied the requirements of Section A of the Graduateship Examination.

ASHMEAD, P. J. *Rhodesia.*
AUFRECHT, T. *Israel.*
AYRES, M. J. *Indiana, U.S.A.*
CALLAGHAN, V. D. *Singapore.*
CARMEL-LENT, G. *Israel.*
CORNER, K. D. *New Zealand.*
DANIEL, W. H. *Ceylon.*
GILL, B. S. *India.*
GLUR, C. R. *Johannesburg, South Africa.*
GOH WEE LENG *Singapore.*
GOH YAM PIN *Singapore.*
GUPTA, R. C. *Agra, India.*
HARRISON, J. M. *Cyprus.*
KONG SHI WEI *Hong Kong.*
LAU CHO WING *Hong Kong.*
LAU PEY KEE *Singapore.*
LIM GIOK LIAN *Singapore.*
MAN SHU WAI *Hong Kong.*
NG TECK SENG *Singapore.*
NISSAM, R. *Israel.*
OGUNSANWO, Z. O. *Nigeria.*
RAIBENBACH, I. *Israel.*
RAJESWARAN, T. N. *Ceylon.*
SARVAGUNANATHAN, B. *Ceylon.*
SHEN CHUNG WAH *Hong Kong.*
SMITH, W. A. M. *Hong Kong.*
SOMASUNDARAM, S. *Ceylon.*
VARSANO, H. *Israel.*
VARTAK, V. B. *Bombay, India.*
WITHANAGE, W. *Ceylon.*
WONG CHI CHUNG *Hong Kong.*

Changes in Maritime Radio

The 1967 Maritime World Administrative Radio Conference, convened by the International Telecommunication Union, was held in Geneva from 18th September to 3rd November. Mr. R. M. Billington, Head of the United Kingdom Delegation, was elected Chairman of the Conference and Mr. Ashot Badalov (U.S.S.R.), Mr. R. T. Bartley (U.S.A.) and Mr. Yves Place (France) were elected Vice-Chairmen. The work was divided among three Committees dealing with radio telegraphy, radio telephony and operational regulations. Seventy countries were represented by over 300 delegates. The advisers to the U.K. Delegation included Captain F. J. Wylie, R.N. (Retd.) (Fellow) (formerly Director of the Chamber of Shipping Radio Advisory Service and a founder member of the Institution's Radar and Navigational Aids Group Committee).

Since the last revision in 1959 of the Radio Regulations applying to the maritime mobile service, there has been considerable expansion in the service with increased demand for radio telephone and radio telegraph channels. This trend meant that the conference was required to make substantial amendments to those parts of the 1959 Radio Regulations and the Additional Radio Regulations which apply to the maritime mobile service. Time-tables have been drawn up for the progressive introduction of the new provisions which will affect the type of radio equipment installed on ships and coast stations in the maritime mobile service.

The main decisions of the Conference were as follows:

(*a*) The gradual introduction up to 1st January 1982 of single-sideband radio telephony in the medium frequency bands allocated to the maritime mobile service between 1605 and 4000 kHz, so that twice as many radio telephone channels as at present will be accommodated.

(*b*) The gradual introduction up to 1st January 1978 of single-sideband radio telephone technique in the high-frequency bands between 4·0 and 23 MHz allocated to the maritime mobile service. The Conference also recommended that a world administrative radio conference should be convened in 1973 to establish a new frequency allotment plan for sharing out the new single-sideband channels to the coast stations.

(*c*) A rearrangement of the frequencies assignable to ship radio telegraph stations using the high-frequency maritime mobile service bands between 4 and 27·5 MHz; this rearrangement, of course, takes account of the evolution of maritime radio communication, namely:

(i) the reduced channel-spacing now possible, thanks to the stability and other improvements of present-day transmitters and receivers (which means that the number of available channels is increased);

(ii) the assignment of frequencies for the transmission of oceanographic data;

(iii) the allocation of frequencies for narrow-band direct-printing telegraph systems (teleprinters) and data transmission systems.

(*d*) The reduction from 50 kHz to 25 kHz of the separation between channels used by the radio telephone maritime mobile service in the 156–174 MHz band; this provision, which will make additional channels available, will be introduced in stages and will become fully operative on 1st January 1983.

(*e*) The conditions governing the use of selective calling (selective calling means that each ship is allocated its own code signal, which is similar to a telephone number, and is equipped with an automatic receiver which responds to the transmission of the code signal by a coast station).

(*f*) The introduction of a 'radio communication operator's general certificates for the maritime mobile service', which administrations may issue instead of the existing radio telegraph operator's certificates (1st and 2nd class), if they wish.

(*g*) The conditions governing the use of emergency position-indicating radio beacons (the purpose of such radio beacons is to facilitate the finding and rescuing of the crews of ships or aircraft lost at sea who have been unable to transmit alarm and distress signals).

(*h*) In general, measures to increase safety at sea (signal codes, watch-keeping and use of distress frequencies).

The Conference also adopted a number of resolutions designed mainly to cover the transition periods preceding the entry into force of the decisions adopted.

U.D.C. 621.396.946

Some Design Aspects of the *Ariel III* V.H.F. Communications System

By

R. S. HILDERSLEY†

Presented at a Symposium on 'The Ariel III Satellite' held in London on 13th October 1967.

Summary: Some design aspects of the *Ariel III* v.h.f. communications system are described with particular emphasis on the measures taken to enhance reliability. Throughout the design and development of the satellite common-user electronics equipment, component and circuit redundancy techniques have been employed wherever practicable in order to achieve the maximum degree of reliability. These redundancy techniques can be applied to low-frequency circuits without serious degradation of performance; at v.h.f., however, the techniques create intolerable difficulties. The command receiver, transmitter, and other units comprising the v.h.f. system were designed for maximum reliability, using redundancy techniques wherever possible. In addition to these measures, a stand-by transmitter was incorporated. The implications of this major modification in terms of its improvement to overall reliability, and its effect upon the command system is discussed.

As a common aerial system was used for the command receiver, and the telemetry transmitter, sufficient isolation of the transmitter was required to maintain the command receiver sensitivity. A solution adopted for this purpose is mentioned and this is followed by a general description of the command system, telemetry link and constructional techniques. Operational results since launch are included.

1. Introduction

Operational reliability is of paramount importance in space electronics equipment, and this has been the overriding objective throughout the *Ariel III* programme. This paper discusses the v.h.f. system both in terms of measures taken to achieve reliability, and also the overall management of the satellite. The system itself is very simple (Fig. 1), comprising a telemetry transmitter, a command receiver and decoder, and the r.f. interconnections between these units and the aerials. Work began in August 1964 and was based on information obtained from the R.A.E., and from N.A.S.A. at the Goddard Space Flight Center.

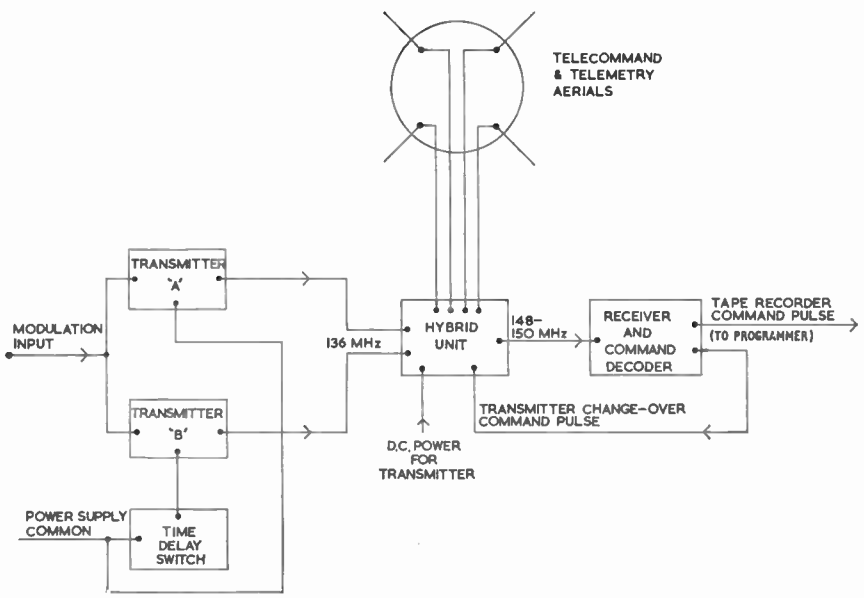

Fig. 1.
Block diagram of the *Ariel III* v.h.f. system.

† The General Electric Co. Ltd., Applied Electronics Laboratories, Portsmouth, Hampshire.

In several respects the r.f. system of *Ariel III*, as finally constituted, differed from that of *Ariel I* and *Ariel II*. A stand-by transmitter was installed against the possibility of telemetry failure, and the command receiver was of an entirely new design. The transmitter also differed in many respects from the American design, although to a less radical extent.

2. Redundancy Techniques

Good design practice dictates that all components in a circuit are operated within their specified ratings, and this is the normal 'reliability' approach for any electronic equipment. However, in spite of such precautions, catastrophic failures are possible and their effects can be minimized by introducing redundant components or circuits into a system. As an example, smoothing capacitors connected across power supply lines can be arranged in a 'hammock' network (Fig. 2). This arrangement deals both with short-circuit and open-circuit failures, and has been used extensively where tantalum capacitors are necessary. In other cases amplifiers have been duplicated or complete unit redundancy has been employed, as in the data handling system (e.g. high-speed and low-speed encoders). Decoupling the power supply in a v.h.f. amplifier at 150 MHz normally requires capacitors having the lowest effective series impedance. The self-resonant frequency of a 100 pF glass-dielectric capacitor, for example, is about 150 MHz and typical high-k ceramic capacitors of 330 pF resonate at about 80 MHz. This effect must be taken into account, as the impedance of a decoupling capacitor increases at frequencies above self-resonance. A hammock network at v.h.f. has an appreciably lower self-resonant frequency for a given value of capacitance, and leads to intolerable feedback problems. Ceramic, porcelain and glass dielectric capacitors have a lower failure rate than tantalum capacitors (see Table 1). In addition, these capacitors have a rated working voltage of between 200 V and 350 V d.c. but are normally operated from a supply of only 12 V. This further reduces their failure rate and therefore they can be connected across the supply without significantly reducing the overall reliability of a unit.

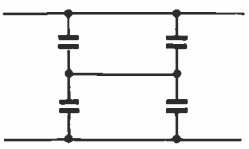

Fig. 2. Hammock network of capacitors.

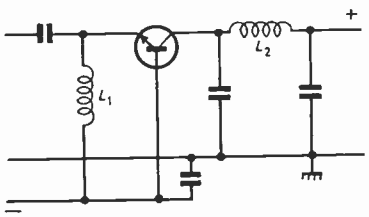

Fig. 3. Transmitter power amplifier stage decoupling.

(The total series resistance of L_1 and L_2 must not exceed 0·5 ohm to maintain circuit efficiency. A transistor short-circuit failure could therefore increase the current catastrophically.)

Table 1

Failure rate for different items in v.h.f. unit

Component type	Failure rate per 1000 hours (%)
Planar transistor, low power	0·001
Planar transistor, v.h.f. power	0·005
Diode	0·005
Quartz crystal	0·01
Resistor, carbon composition	0·0001
Resistor, metal oxide	0·00008
Capacitor, tantalum-solid	0·01
ceramic	0·0005
glass and porcelain	0·0005
trimmer	0·005
silver mica	0·0005
Transformers, toroidal	0·005
V.h.f. chokes and coils	0·001
Soldered joints	0·0001
I.f. filter, crystal	0·02

In designing the telemetry transmitter it was found that the d.c. resistance of series decoupling elements must be minimized in order to obtain the best power conversion efficiency (see Fig. 3). This represents another reliability embarrassment because a transistor short-circuit failure could therefore cause an increase in supply current of two orders-of-magnitude. The hazard is minimized by operating transistors conservatively, and also by arranging to conduct away dissipated heat where necessary. In the case of the command receiver, the power dissipation of transistors is so low that higher values of series decoupling resistance can be tolerated. This has enabled a design aim to be satisfied, namely, that a catastrophic failure of any one component shall not increase the supply current to the unit by more than 50%.

Although a full discussion of v.h.f. unit reliability calculations will not be entered into, it is appropriate

to give the estimated failure rates of typical components (see Table 1). The estimated mean time between failure (m.t.b.f.) for each unit was calculated by taking into account the total number of components of each type. The resulting m.t.b.f. for the telemetry transmitter was about 56 years, and 29 years for the telecommand unit. The relatively low figure given for the latter unit is accounted for by its more complex circuit and larger number of components; the unit actually comprises two items, namely, the receiver itself and the command decoder.

3. Introduction of the Stand-by Transmitter

As a result of the estimated failure rates quoted, it might have been argued that the probability of a failure during one year in orbit was sufficiently low. However, the possibility that a single component failure in the transmitter could result in a total loss of satellite information, resulted in urgent consideration being given to duplicating this unit. The study was extended to the possibility of duplicating the command receiver, and although this was found to be feasible, the proposal was not adopted because of the additional weight involved.

It was necessary that installation of the new unit should be accomplished with the minimum disruption to the satellite electronics system in general. Furthermore, it was essential that both units should never operate simultaneously; not only would the r.f. interference have been intolerable but the additional load would have disrupted the power system. These requirements could have been satisfied in a number of ways, but the simplest available solution was adopted. This was to use a relay to switch the aerial system between the outputs of the two transmitters; several types of miniature relays were found to have contact systems with sufficiently low capacitive and inductive losses. The use of a magnetic latching relay identical with the type already specified for use in the data handling system offered the following two important advantages: (a) the relay was a component qualified for use in the satellite and with a known reliability record; and (b), by using a latching relay, the power supply requirements would be minimized, only a short current pulse being necessary to effect the change-over.

The magnetic latching relay was incorporated in the hybrid coupler unit and therefore it was possible to duplicate the coaxial cable connecting the transmitter to the aerial system. Contact reactances were tuned out, thus reducing the insertion loss, due to the relay, to an insignificant level, certainly less than 0·1 dB By modifying the transmitter output circuits it was possible to feed the d.c. power supply down the coaxial cable, enabling the relay contact to switch both the d.c. input and r.f. output simultaneously. It was thus impossible for the transmitters to operate simultaneously.

The transmitters were identical and interchangeable units, with a simple parallel connection for their modulation inputs, thus avoiding the necessity for additional switching.

Installation of a redundant transmitter into the satellite introduced additional demands upon the command system. The obvious requirement that the command system must be modified to cater for an additional execute channel to effect transmitter change-over. Also, the overall reliability of the command system now assumed greater importance; some modifications were consequently introduced as follows:

(a) The address circuits in the command decoder were completely duplicated.

(b) The command system, which had previously been operated from common power supply lines with the transmitter, would now use a completely independent supply. If a transmitter should fail in a short-circuit mode, the ability of the command system to remove the faulty unit from the disrupted supply would thus be unaffected.

It was estimated that the reliability of the telemetry link had been improved by about 30% as a result of the changes described; this is a somewhat pessimistic figure, which takes the entire command system failure rate into account.

4. The Aerial System and R.F. Link

A four-pole turnstile aerial array was used both for telemetry transmission and command reception. The two channels have a frequency separation of about 12 MHz with telemetry at 136·56 MHz and telecommand between 148 MHz and 149 MHz. The system was designed to have an adequate bandwidth, but with optimum efficiency at the telemetry frequency. American experience with *Ariel I* had indicated great difficulty in avoiding desensitization of the command receiver by the telemetry transmitter. This effect was due to two causes:

(a) direct input to the receiver at the telemetry frequency, and

(b) wide-band noise components from the transmitter extending across the telecommand frequency band.

The problem had not been solved completely in the case of *Ariel I* nor in *Ariel II* and desensitization figures of 10 to 15 dB had been encountered in American satellites.

Both the above causes of receiver desensitization were reduced by means of a hybrid coupler providing

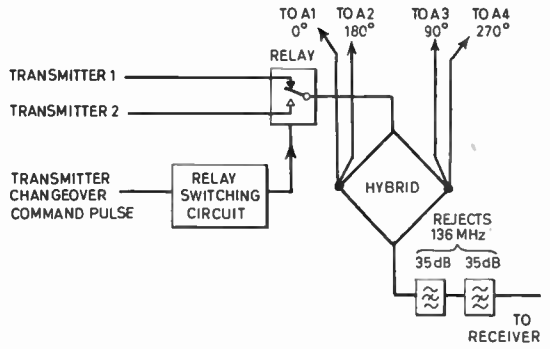

Fig. 4. Hybrid coupler.

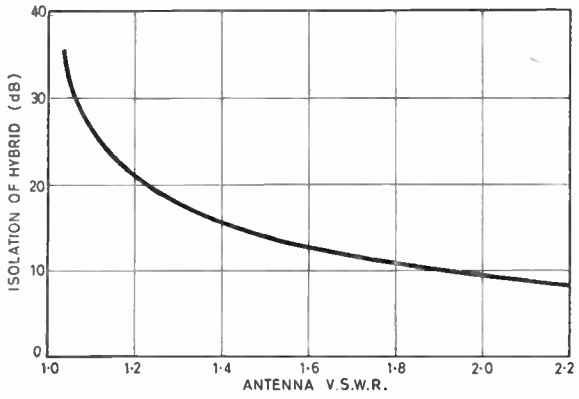

Fig. 5. Isolation of hybrid ring versus v.s.w.r. of antenna.

Table 2(a)

Ariel III telemetry link: Tracking safety margin

Parameter	'Worst case' value
Transmitter power output (250 mW)	24 dBm
Power in residual carrier (±1 radian modulation)	19 dBm
R.f. cable loss between transmitter and aerials	−1 dB
Satellite radiation pattern loss (with respect to isotropic)†	−7 dB
Transmission path loss (at 3000 km maximum slant range)‡	−145 dB
Ground receiving aerial gain§	22 dB
Polarization loss‖	−3 dB
Carrier power level into ground receiver (*A*)	−115 dBm
Ground receiver phase lock threshold (*B*)	−143 dBm
Tracking safety margin (*A*)−(*B*)	28 dB

† This was the deepest fade measured simultaneously on two orthogonal linearly polarized receiving aerials during satellite radiation pattern trials at R.A.E., Lasham.

‡ Ionospheric loss is omitted as it is unlikely to occur except at high latitude stations where it tends to vary widely.

§ This figure holds for either linearly or circularly polarized configurations of the auto-follow SATAN aerial array used at Winkfield. The circularly polarized arrangement is used for *Aerial III*.

‖ This figure is variable but −3 dB is appropriate for a linearly polarized transmitting aerial operating in conjunction with a circularly polarized receiving aerial (or vice versa). The canted turnstile aerial system of *Ariel III* radiates circular polarization on the satellite spin axis and linear polarization around the equatorial plane of the satellite (broad-side aspect). During a pass over Winkfield, *Ariel III* normally presents a broad-side aspect with respect to the receiving aerial.

a nominal isolation of at least 15 dB; this was augmented by a filter. In the case of *Ariel III*, the following further measures were taken:

(a) A new receiver was designed, with r.f. and mixer circuits capable of handling a strong interfering signal at the telemetry frequency.

(b) The transmitter was designed to have a low content of wide-band noise in its output.

(c) The filter incorporated in the hybrid coupler increased the isolation at 136 MHz to more than 80 dB. The *Ariel III* command receiver could withstand an input of 0 dBm at the telemetry frequency for only 1 dB desensitization at the correct telecommand frequency. Since the transmitter had an output of +24 dBm, and isolation across the hybrid coupler was at least 80 dB, there was a safety factor of more than 56 dB. In practice no command desensitization, due to the telemetry system, was detected during any of the *Ariel III* trials.

The hybrid coupler (see Fig. 4) was made from 50 Ω miniature coaxial cable, and a phase reversal of 180° at one arm was obtained by reversing the inner and outer conductors. This increased the bandwidth over which good isolation was obtainable and extended it in practice to at least ±50 MHz relative to 136 MHz. The isolation across the hybrid ring depended upon the voltage standing wave ratio (v.s.w.r.) of the aerials (Fig. 5) and the figure of 15 dB corresponded to a v.s.w.r. of about 1·4; this was a 'worst case' estimate. Since a v.s.w.r. of better than 1·15 at the aerials was actually achieved, the resulting isolation was about 22 dB. The 136 MHz rejection filter was a two-section *m*-derived network having an insertion loss at the telecommand frequency of less than 1 dB.

A progressive phase shift of 90° was required at each aerial rod; this was obtained by cutting each feeder to a critical length. To prevent phase errors from adversely affecting the aerial system radiation pattern, the phase shift at each aerial rod was established to within ±2° of the nominal figure in each case. The satellite radiation pattern was, ideally, completely

Table 2(b)

Telemetry link Data safety margin

Parameter	'Worst case' value
Transmitter power in data sidebands (±1 radian modulation)	22·4 dBm
Cable loss between transmitter and aerials at r.f.	−1 dB
Satellite polarization loss (with respect to isotropic)	−7 dB
Transmission path loss (at 3000 km maximum slant-range)	−145 dB
Polarization loss	−3 dB
Ground receiving aerial gain	22 dB
Diversity reception improvement†	3 dB
Video signal level (after combination) (C)	−109 dBm
Noise:	
Ground receiver noise factor $N = 2{\cdot}8$ (or 4·5 dB)	
With ambient temperature $T_A = 290°K$, the effective receiver noise temperature $T_R = (N-1)T_A = 520°K$.	
With galactic noise temperature, $T_G = 1400°K$.	
System noise temperature $T_S = T_R + T_G = 1920°K$.	
Total system noise power (D) $= kT_SB$ watts or −119 dBm where k = Boltzmann's constant $= 1{\cdot}38 \times 10^{-23}$ J/deg K and B = system bandwidth in Hz (Winkfield video bandwidth = 50 kHz).	
Effective data signal/noise in 50 kHz video bandwidth (C)−(D)	10 dB
Margin covering operation, data demodulation, tape record and replay	−3 dB
4:1 bandwidth improvement on entering 12·7 kHz input of R.S.R.S. comb filter	6 dB
Therefore, S/N in comb filter (E)	13 dB
Required S/N for 95% data accuracy from comb filter when on a.g.c. operation (F)	−6 dB
Therefore, data safety margin (E)−(F)	19 dB

† This figure holds only when equal power is picked up by each aerial array. In general, however, diversity reception will always cancel the polarization loss.

omni-directional. In practice the physical shape of the satellite, the positions and angles of solar cell paddles, and the experimenters' aerials and probes all tended to modify the pattern. It was necessary to know the extent to which the resultant radiation departed from a true isotropic level. Since the problem was not amenable to calculation, an extensive programme of tests was initiated by the R.A.E., mainly using one-third scale model satellites at Lasham. A full account of the results of this research is beyond the scope of this paper, but it was predicted that satisfactory communication with the satellite would be maintained provided polarization diversity techniques were employed by the ground stations; these techniques are standard practice at the Space Tracking and Data Acquisition Network (STADAN) stations.

As a result of operational experience with *Ariel I* and *Ariel II* it was known that a transmitter power output of 250 mW was adequate to maintain reliable data acquisition via STADAN. This information was supported by calculations made to determine the safety factor for both the data and telecommand links. It is difficult to give precise figures, partly because the STADAN stations use several types of aerial having a gain-spread of about 9 dB. Table 2 assumes the use of a system having a gain of 22 dB. Ideally, the calculations should be presented under three headings: 'worst case', 'probable case' and 'best case', allowing each parameter to be presented with appropriate values under these headings. For simplicity, however, only the 'worst case' figures are given.

From the above, it will be seen that the safety margin under worst case conditions and at maximum slant range, was adequate for maintaining phase lock and a receiver video output signal/noise ratio of 10 dB. The safety margin would have been reduced considerably if a telemetry aerial had failed to erect after launch. Furthermore, it was necessary to allow for some deterioration in the system performance during an orbital lifetime of up to two years. For these reasons it was concluded that the telemetry transmitter power should be not less than 250 mW.

Similar calculations for the telecommand link were made and are given in Table 3.

Table 3

Ariel III Telecommand Link

Parameter	'Worst case' value
Ground transmitter power (1·2 kW)†	60·8 dBm
Transmitting aerial gain (circularly polarized)†	16 dB
Path loss (at 3000 km maximum slant range)	−145 dB
Satellite radiation pattern loss‡ (with respect to isotropic)	−10 dB
Polarization loss‡ (satellite broad-side on)	−3 dB
Coupling loss of r.f. cables, etc., in satellite at command frequency	−2 dB
Signal level into satellite command receiver	−83 dBm (G)
Lower limit set for satellite command unit sensitivity	−106 dBm (H)
Command link safety margin (G)−(H)	23 dB

† Values given are for the Winkfield station.

‡ See corresponding footnote to Table 2(a).

A smaller safety margin could be tolerated for the command link as compared with telemetry because commands are not normally sent under maximum slant range conditions. Furthermore, the STADAN stations employ a variety of transmitter and aerial combinations giving an effective gain spread of up to 27 dB.

5. The Command System

Ariel III, in common with *Ariel I* and *Ariel II*, is a scientific satellite in which the minimum number of commands are required for satisfactory management. Operation of the power conditioning and data handling systems, for example, is completely automatic with sufficient redundancy incorporated to ensure reliable operation during the orbital life-time. The experiments also operate automatically according to the satellite program, and only the tape recorder needs to be commanded into the replay mode as a regular part of the operations plan. It was logical, therefore, that the N.A.S.A. Tone Command Standard was selected (see Aerospace Data Systems Standards, N.A.S.A.). This uses a timed sequence of audio tone bursts for each command, the command transmitter being amplitude modulated to 80% during bursts. A single address tone is allocated by N.A.S.A. for all commands in a satellite, and execute tones are chosen by the project according to the commands required. The tone frequencies lie in the a.f. range of 1 kHz to about 6 kHz, and the system is intended for satellites requiring only a small number of 'on/off' commands. The choice of a.m. for the transmission is convenient, as it enables the satellite receiver to be of simple design.

As implied in Section 3, a second command was incorporated when the stand-by transmitter was introduced; no commands other than these were considered to be either desirable or necessary. At this point, reference must be made to the international agreement whereby a satellite must cease r.f. transmission at the end of its intended life-time, in order to relieve waveband congestion. This requirement was satisfied in *Ariel III* by connecting a Bulova timer switch in the power supply to the stand-by transmitter (see Fig. 1). The timer will break the supply about one and a half years after launch, and thereafter the transmitter change-over command will enable the satellite to be silenced. This arrangement was adopted in the interest of overall operational reliability, in preference to the alternative of having a completely separate on/off command available at any time after launch. This would have involved a total of three execute command channels in the decoder. Reliability estimates indicated that the on/off command would reduce the reliability of the telemetry link, since resumption of transmission after a period of silence would depend upon the continued operation of the telecommand system. The Tone Command System uses comparatively simple circuits in the interest of reliability, but security of command against interference is thereby inherently less than with more complex digital systems. Although the receiver is designed to have the minimum r.f. bandwidth, this gives little benefit to security owing to the large number of satellites in operation. A study of possible r.f. interference reveals at least four satellites using the same carrier frequency, and a further seventeen on an adjacent channel (10 kHz separation). Command security with *Ariel III*, therefore, depends mainly upon narrow bandwidth audio filters in the decoder followed by 'arming' circuits to recognize the trailing edge of the address tone.

The r.f. bandwidth required for the command receiver was assessed on the following basis:

Highest modulation tone	±6·3 kHz
Doppler shift (assuming a 600 km circular orbit)	±3·6 kHz
Stability of receiver local oscillator (±0·002%)	±2·75 kHz
	±12·65 kHz

In addition to this bandwidth a further allowance was made for the frequency tolerance of the command transmitters; this was stated by N.A.S.A. to be 0·002% although it was known that in practice, frequencies are held to within about ±100 Hz. The receiver was therefore designed to have a 30 kHz bandwidth.

After a preliminary study of the American *Ariel II* receiver circuit, which was a double superheterodyne using a ceramic i.f. filter at 455 kHz, it was decided that a completely new approach would be appropriate for *Ariel III*. This new receiver was designed with reliability and low power consumption as primary objectives. All the performance requirements in the original design aims were satisfied for a power consumption of about 50 mW with no input signal, rising to 120 mW at the maximum permissible input level. A block diagram of the command receiver and decoder is shown in Fig. 6. From this it will be seen that the receiver is a single conversion superheterodyne with a local oscillator operating 10·7 MHz below the carrier frequency. The r.f. amplifier is preceded by two pairs of coupled tuned circuits (Fig. 7) with adjustable capacitive coupling. This enabled a flat pass-band characteristic to be secured, and a rejection of 60 dB at ±21·4 MHz relative to the centre frequency. The r.f. selectivity provided by these tuned circuits was sufficient to ensure that second channel and other spurious responses were at least 60 dB below the fundamental response. A balanced mixer using two

transistors gave several performance advantages to the receiver compared with more conventional circuits. These characteristics may be enumerated as follows:

(a) redundancy of operation, whereby failure of one transistor would not be catastrophic,

(b) high converter efficiency,

(c) low level of converter noise,

amplifier uses two transistors in a series 'cascode' circuit. Owing to the action of the a.g.c. damping diodes, the effective impedance across the balanced mixer output tuned circuit can vary by a factor of about 50 : 1, whereas the resistive input impedance of the crystal filter must be kept within $\pm 10\%$. This has been one of the major problems in designing the i.f. amplifier. The 'cascode' circuit provides the

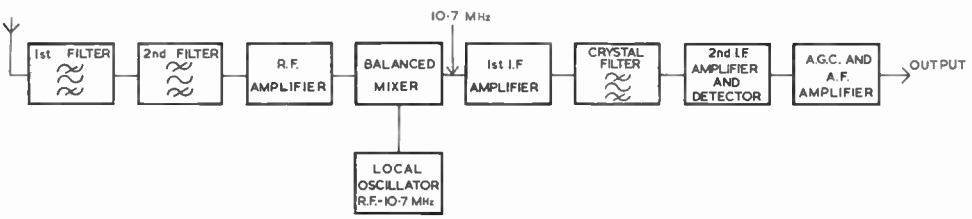

RECEIVER

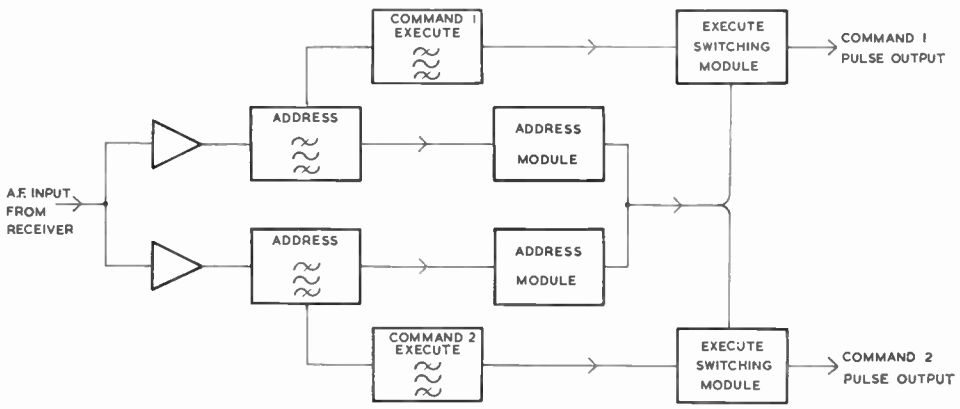

DECODER

Fig. 6. Block diagram of command receiver/decoder.

(d) attenuation of signals generated at i.f. in the r.f. stage,

(e) attenuation of local oscillator component fed back into the r.f. input.

The mixer stage i.f. output circuit consists of a balanced centre-tapped transformer. Two diodes are arranged back-to-back across the primary, and are used for a.g.c. purposes by damping the tuned circuit. The push-pull connection reduces distortion of the r.f. envelope which would otherwise occur. The first i.f. necessary isolation, and in consequence the pass-band characteristics of the receiver are independent of input signal level. The crystal filter is followed by a second i.f. amplifier and a low level a.m. detector diode. An amplified a.g.c. system is used, with the delay point set to correspond with an r.f. input level of approximately 0·7 μV. The a.g.c. current is applied to the diodes following the mixer stage, providing a range of 50 dB gain reduction without envelope distortion. This range is increased by a single diode following the r.f. stage.

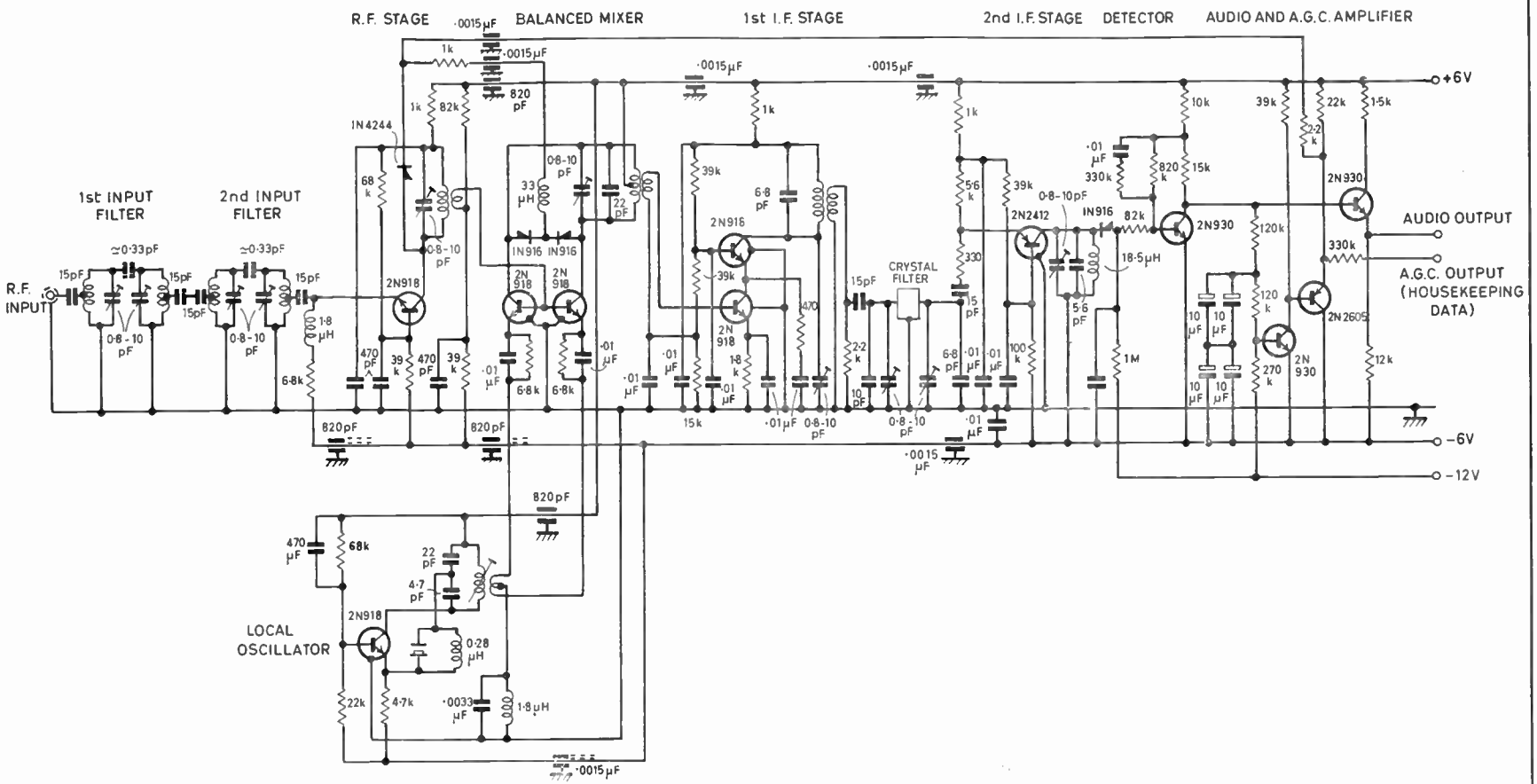

Fig. 7. Circuit diagram of the command receiver.

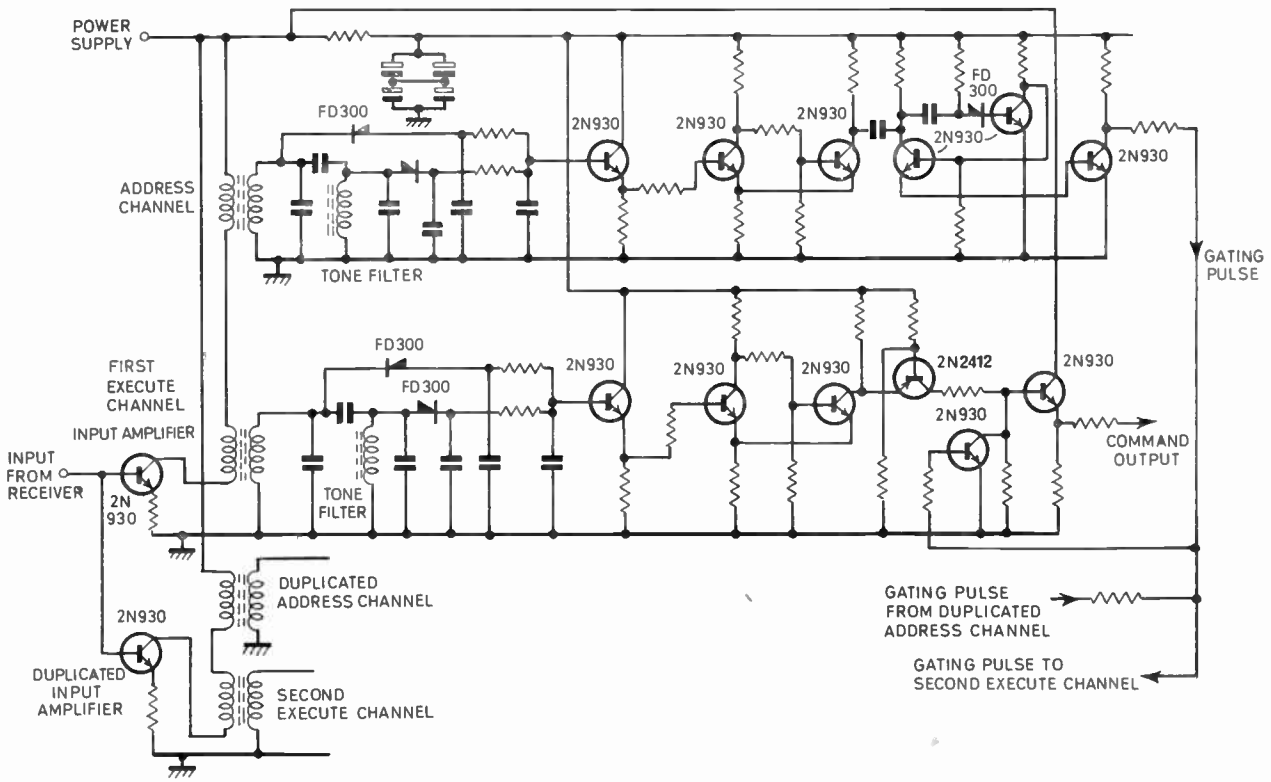

Fig. 8. Circuit diagram of the decoder.

A diode with low capacitance was selected in order to prevent loss of gain when no a.g.c. is applied, and a supplementary delay to the applied a.g.c. current prevented the receiver noise factor from being impaired at low signal levels above a.g.c. threshold. The a.g.c. system provides an output held constant to within 0·2 dB for input variations of 80 dB above a threshold level of 0·7 μV.

The crystal filter used in the *Ariel III* receiver was the subject of a considerable number of tests, and was developed from a standard design operating at a centre frequency of 10·7 MHz, and with a bandwidth of 30 kHz. Although these components are normally intended for mobile communications equipment, they were not designed to withstand the severe vibration imposed by the *Ariel III* launch vehicle. However, as a result of close collaboration with the manufacturers, Standard Telephones and Cables Limited, a foam encapsulated filter was developed. The encapsulation eliminated mechanical weaknesses inherent in the original design without having any adverse effect upon its electrical performance. A failure mode analysis indicated that the filter would not fail catastrophically as a result of open or short circuit component failures. Vibration tests on the unmodified filters confirmed however, that three toroidal transformers incorporated in the design were the weakest items. The encapsulation of these coils, wound with 44 s.w.g. wire, resulted in no subsequent failures.

The command decoder was designed and tested as a separate unit from the receiver itself, although the two were assembled together for final overall tests and use in the satellite. The a.f. output from the receiver has a d.c. component corresponding to detected signal level. This is used to turn on the input amplifier in the decoder, and the muting thus obtained prevents random noise from operating the system.

The address circuits, including the input amplifier filter, and timing circuits, were duplicated in the interests of reliability. Toroidal coils in the tone filters were wound with the thickest practicable wire gauge as the coils used in the American decoders had suffered a number of failures during laboratory tests. The higher Q resulting from this thicker wire was reduced as required by means of parallel resistors.

The decoder circuit is shown in Fig. 8. Each address and execute channel comprises a filter with two coupled tuned circuits. The broad and narrow band outputs are combined in opposition by means of the diodes to

prevent spurious operation by random noise. The filters will only respond to tones having a frequency within about ± 100 Hz of the correct channels; such a narrow bandwidth implies tuned circuits of great stability. The toroid core material and tuning capacitors were chosen to have matching temperature characteristics such that the resonant frequency was within ± 10 Hz over the temperature range; S.T.C. modular silver mica capacitors were used. The gating circuits following these filters ensure that command action will only result from tones having the correct sequence and duration.

Tests on the *Ariel III* command unit, before launch, indicated that random noise, or speech and music from broadcasts on the command carrier frequency will not cause spurious commands to be initiated.

6. The Telemetry Link

The overall characteristics of the satellite p.f.m. telemetry data waveform are fully described elsewhere.† It is the function of the transmitter to accept this square-wave input signal, and to produce a modulated r.f. transmission that will be compatible with the N.A.S.A. STADAN ground stations. Amplitude modulation, frequency modulation, or phase modulation could have been used, but phase modulation was selected for the following three main reasons:

(i) it enabled full benefit to be derived from coherent detection provided by the STADAN phase lock receivers,

(ii) the stable carrier component, which is a characteristic of p.m. enabled the telemetry transmitter to be used for tracking purposes and therefore the necessity for a separate tracking beacon transmitter was avoided, and

(iii) phase modulation permitted the satellite transmitter to be of simple design using a constant amplitude variable phase filter modulator circuit originally devised by N.A.S.A.

Full details as to N.A.S.A. requirements for telemetry system compatibility have been published but the principal clauses affecting the design of a spacecraft transmitter are as follows:

(a) The phase deviation must be such that at least 10% of the total transmitted power shall remain in the carrier. This requirement is to assure both reliable data acquisition and maintenance of phase lock by the ground receivers. The central carrier is also required for spacecraft tracking purposes. With a phase-modulated system, the depth of modulation may be defined and measured in a number of ways. The most direct technique is to measure the power level at the carrier frequency both with and without square wave modulation. This power ratio (known as 'carrier drop') is calculated from:

$$\text{carrier drop (dB)} = 20 \log \sec \theta$$

where

θ = phase deviation.

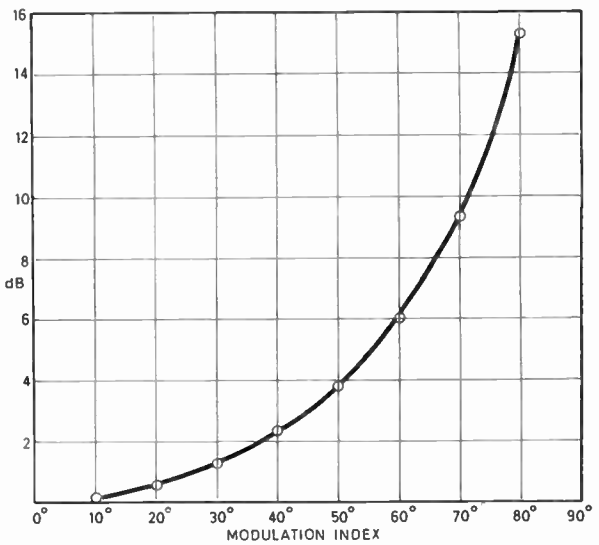

Fig. 9. Carrier drop with square-wave modulation.

This has been plotted as a graph (Fig. 9) and from the curve it will be seen that the N.A.S.A. requirement for 10% of the total transmitted power remaining in the carrier corresponds to a deviation of 72°. The modulation index chosen for *Ariel III* was 57° (1 radian), resulting in one-third of the power remaining in the carrier. By setting the modulation to this somewhat lower level, a better compromise was reached for data acquisition by the ground receivers. Furthermore, it was known that the temperature coefficient of the transmitter modulation circuit was such that the deviation tended to increase at low temperatures. Great care was taken to set the modulation index, at 20°C, to within $\pm 10\%$ of 57°. This ensured that, under all operating conditions, the phase deviation of the telemetry would not exceed 70°.

(b) Incidental amplitude modulation of the carrier shall not exceed 5%.

(c) The carrier frequency shall not change by more than 5 Hz with the application of modulation.

† A. Laws, 'The data handling system for the *Ariel III* satellite', *The Radio and Electronic Engineer*, 35, No. 2, pp. 83–87, February 1968.

(d) The amplitude of any spurious output from the transmitter shall be at least 60 dB below the level of the fundamental.

(*Note*: Particular emphasis was placed on the third harmonic, which could have caused interference to radio astronomy.)

(e) Consideration shall be given, in the transmitter design, to limiting the power radiated outside the assigned bandwidth. This requirement is for the purpose of reducing the adjacent channel interference.

Because of power supply limitations it was necessary that the target figure of 250 mW output should be provided by a power input of not more than 1·2 W. The transmitter circuit was therefore designed to be as efficient as possible; most units produced slightly over 300 mW for about 0·95 W input. Silicon transistors were used throughout.

The circuit diagram of the transmitter is given in Fig. 10. The oscillator is crystal controlled, using a glass encapsulated fifth-overtone unit, and operates at 68·28 MHz. This crystal, as for the receiver local oscillator, is supplied to a specification calling for a frequency stability of $\pm 0{\cdot}001\,\%$ over the temperature range of $-20°C$ to $+60°C$. The oscillator circuit is designed to have a long-term stability of better than $\pm 0{\cdot}002\,\%$; this allows for the combined effects of supply voltage and temperature variations. A buffer amplifier follows the oscillator and isolates the crystal oscillator from any load variations due to the phase modulator which could affect the output frequency. The tuned circuit in this stage reduces the amplitude of harmonics present in the oscillator output and the resistive network enables the correct impedance (50 Ω) to be presented to the modulator.

The phase modulator produces a linear phase excursion and has a low value of amplitude modulation content in its output. The circuit is a bridged T-network using a voltage-variable capacitance diode in one arm and a voltage-variable inductance in the other arm. The variable inductance comprises a quarter-wave line made from semi-flexible coaxial cable, and a second variable capacitance diode. The modulator is designed to operate with a characteristic impedance of 50 Ω and this governs the capacitance of the voltage-variable diodes. To prevent the diodes from rectifying the r.f. signal, the sum of the modulating voltage plus the d.c. bias must exceed the peak value of the r.f. voltage. Diodes having an effective capacitance of about 47 pF were required to realize the operating impedance of 50 ohms, and they needed a bias of 4 V d.c. for a junction capacitance of this value. The square-wave modulating waveform had an amplitude of about 6 V, and the r.f. input voltage to

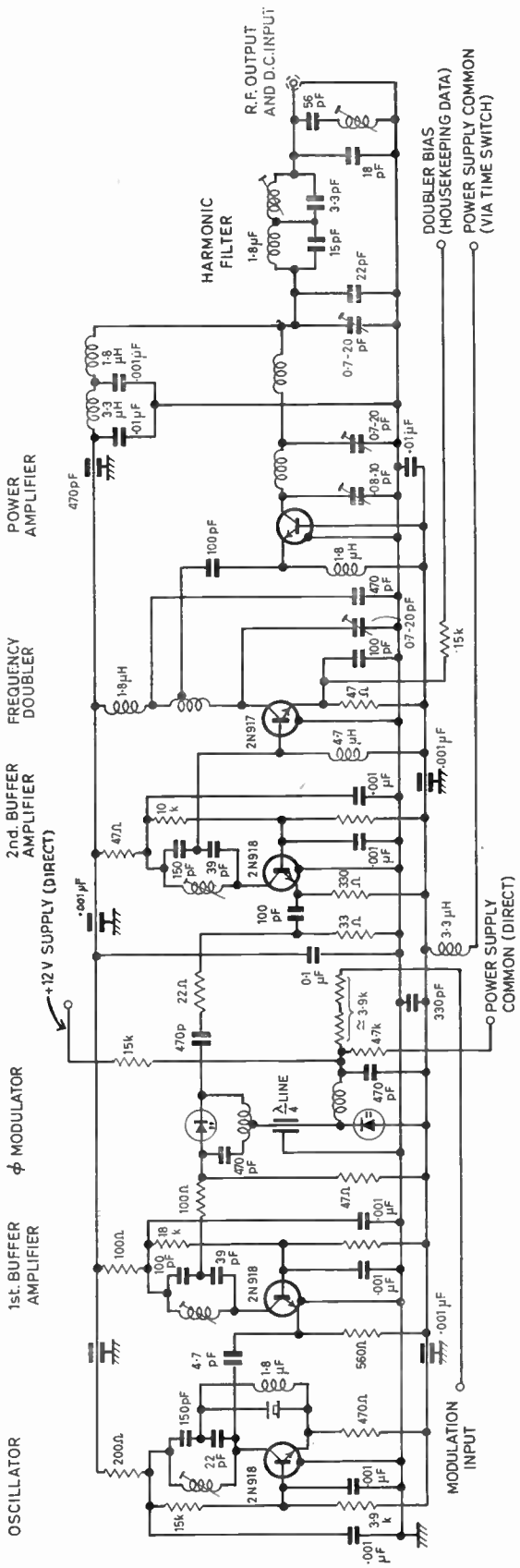

Fig. 10. Circuit diagram of the transmitter.

the modulator was only about 100 mV. Bias for the diodes was derived from the power supply, and the modulating input signal was directly coupled, in order to preserve this waveform at low frequencies.

The modulated r.f. signal (deviation $\pm 0{\cdot}5$ radian) is fed via a resistive pad to maintain the correct terminating impedance of 50 Ω into a buffer amplifier similar to the one following the oscillator. This amplifier operates linearly, and isolates the modulator from input impedance variations of the frequency doubler. The doubler stage produces an output at the final carrier frequency of 136·56 MHz and also doubles the phase deviation of its input signal to the required value. The transistor is driven into saturation to reduce residual amplitude modulation.

The power amplifier stage transistor was operated in the common-base mode; the power dissipated in this transistor was only about one-tenth of its permissible rating. Like the frequency doubler, the amplifier was driven into saturation by the input signal. The r.f. output from this final stage was obtained by matching into a 50 Ω output impedance and then into a band-pass filter designed to suppress residual components at the oscillator frequency, and all other spurious outputs up to and including the seventh harmonic. These output circuits were directly coupled, to permit power supply for the transmitter being fed via the coaxial cable.

The heat developed in the frequency doubler and final amplifier transistors was conducted away to the top cover of the transmitter by means of beryllia heat-conducting assemblies, and the maximum recorded temperature rise of the transmitter, when tested in the thermal vacuum chamber, was less than 2 degC above ambient. Extensive tests were carried out also with the transmitter operating into both open-circuit and short-circuit loads, and no failures could be induced.

Installation of the redundant transmitters made it necessary to ensure that the unit would operate immediately and normally on command, after being quiescent for an extended period of time. Thermal vacuum tests revealed that parasitic oscillations could be produced under certain conditions and at low temperatures. The low temperatures reduced the r.f. drive available at the doubler and p.a. stages, causing these circuits to operate as relaxation oscillators. The problem was solved by reducing decoupling impedances at low frequencies (between 100 kHz and about 10 MHz). Finally, the modified transmitters were tested in low temperature vacuum with the supply voltage varied from 7·5 to 13 V to ascertain the stability margin (the specified voltage range was 11·87 to 12·15 V). No spurious mode operation could thereby be induced, and no subsequent failures of any type have occurred.

7. Constructional Techniques and Testing

The v.h.f. units were assembled into light alloy boxes milled out of solid material, providing a light-weight structure of great mechanical stability. The physical design of the satellite was such that no stringent limitations were imposed on the overall size of the electronic packages. It was more important to minimize their weight, and to ensure that they were sufficiently rugged to withstand the vibration developed by the launch vehicle. Both the receiver and transmitter were constructed from a number of printed circuit sub-assemblies, using low-loss glass fibre board. Each sub-assembly was fitted into an appropriate compartment of the milled-out box. Greater consistency of performance was achieved by this construction, compared with point-to-point hand wiring. After assembly, the units were tested and encapsulated with polyurethane foam. The major steps in these procedures were as follows:

(a) Assembly.

(b) Alignment of all circuits and electrical testing according to production test specification.

(c) Foam-encapsulation.

(d) Realignment of all tuned circuits and locking of trimmers, repeating production test specification, but with additional checks over the temperature and supply voltage ranges.

(e) Environmental testing, including vibration, thermal vacuum, and constant acceleration.

(f) Repeating all relevant tests in (d) above, except alignment.

The detailed examination of all test results of this series of tests was important, as it sometimes revealed small performance changes. Any modifications or re-adjustments found to be necessary in prototype models were followed by repeated test sequences. A sufficient number of models was produced to ensure that the flight equipment would satisfy all design aims. The test procedure also gave confidence that the performance would remain stable for an extended period of time after launch.

8. Operational Results since Launch

The satellite telemetry and telecommand systems have operated without any faults since the launch on 5th May 1967. The telemetry signal, as received by the STADAN stations, has enabled phase-lock to be maintained under maximum slant range conditions with a signal/noise ratio margin substantially as predicted in Section 4. The telecommand system also has operated perfectly, all commands for tape recorder replay having been obeyed. 'Housekeeping' channels, telemetred via the high-speed data link, have provided valuable information as to the satellite itself, e.g.

temperatures, battery charge state, etc. The command receiver a.g.c. level is of particular interest in this context. First, the data provide direct information as to the telecommand signal field strength according to the orbital position of the satellite; this has confirmed the range calculations made before launch, as in the case of telemetry. Second, the a.g.c. level will provide long-term information as to the condition of the receiver itself since any deterioration would reduce the a.g.c. level. The ground station at Winkfield transmits a 30-second burst of unmodulated command carrier before initiating any command, in order to facilitate this investigation. These stations also record the telemetry receiver a.g.c. levels thus making it possible to deduce further information as to the true radiation pattern of the satellite.

9. Acknowledgments

The project has involved much co-operation, principally with the R.A.E. and also with N.A.S.A., and the author wishes to thank Mr. R. W. Hogg of the Space Department, R.A.E., for his help. The management of the G.E.C. Applied Electronics Laboratories, Portsmouth, are thanked for their permission to publish this paper.

Manuscript first received by the Institution on 4th October 1967 and in final form on 17th January 1968. (Paper No. 1175/ AMMS 11.)

N.A.T.O. CONFERENCES

Survival of Communication Networks

As part of its programme in Operational Research, the N.A.T.O. Science Committee each year supports a number of conferences in that field. A Conference on 'The Survival of Communication Networks' is being held in Ile de Bendor, near Toulon, France, from 21st to 25th June, 1968.

Communication networks and their survival under particular hazards will be considered in a broad context, covering warfare, civilian defence in war, maintenance of civilian order when endangered by insurgency or crime, natural disasters, and internal breakdown through overloading and confusion. (Their exposure to illicit obtaining of information is excluded from discussion at this conference.)

There will be about eighteen invited presentations, intended chiefly to orient the discussion, for which ample time will be provided. The proceedings of the conference will be published in the form of a book. It is the intention that neither the participants at the conference nor the papers and ensuing discussions should be limited necessarily to those with strong military links.

While the numbers who can attend the Conference will be limited by reasons of space, anyone interested in participating is invited to write to: D. B. Manwaring, Superintendent (General), Ministry of Defence, Defence Operational Analysis Establishment, Parvis Road, West Byfleet, Surrey.

AGARD Bionics Symposium

The N.A.T.O. Advisory Group for Aerospace Research and Development in Paris is sponsoring a Symposium on Bionics, to be held at Brussels from 18th to 20th September 1968. The Symposium will emphasize the practical importance and potential applications of bionics principles to aerospace research and operation.

Thirty-three invited papers will be presented at the Symposium, representing authors from seven countries belonging to N.A.T.O. Topics to be covered include auditory, visual and olfactory information processing; adaptive control and learning systems; navigation; orientation; propulsion; energetics; and advanced information processing.

Further information on the programme and details of registration may be obtained on application to: Director of Plans and Programmes, A.G.A.R.D., 64 rue de Varenne, 75 Paris VII; or from Professor P. Rylant, Institut de Physiologie Solvay, Université Libre de Bruxelles, 115 Boulevard de Waterloo, Bruxelles 1.

Space Research Experiments

British Experiments Launched in Orbiting Observatory

OGO-E, the Orbiting Geophysical Observatory satellite launched from the Eastern Test Range at Cape Kennedy on 4th March by the U.S. National Aeronautics and Space Administration (N.A.S.A.), carries two experiments for British universities. In the first, a spark chamber devised at the University of Southampton (Professor G. W. Hutchinson) will detect and measure energetic photons in the primary cosmic radiation, which consists mainly of very high energy particles coming from unknown sources in space. For the second experiment, measurements of the density and temperature of electrons in the magnetosphere will be made by the Mullard Space Science Laboratory, Department of Physics, University College London (Professor R. L. F. Boyd).† Both experiments are supported by Science Research Council grants.

The object of the Southampton University experiment is to discover and identify sources of cosmic radiation through a study of gamma-ray photons. The greater part of the cosmic radiation consists of electrically charged particles whose directions of travel through space are disturbed by the galactic and interplanetary magnetic fields and whose points of origin are therefore difficult or impossible to determine. The Southampton experiment is designed to detect the rarer uncharged gamma rays which travel undeflected in straight lines from their points of origin. A study of these gamma rays should enable their sources to be detected and their positions determined with considerable accuracy.

The University College electron temperature probe is an improved version of the probe used in the first U.S.–U.K. co-operative satellite *Ariel I* and in the N.A.S.A. Direct Measuring *Explorer* 31 (*DME-A*), but more sensitive than any similar instrument flown so far. It provides a wide dynamic range and high sensitivity to cover the extensive variation of electron temperature and density expected between the extremes of *OGO-E's* elliptical orbit. Its sensitivity to electron densities as low as 10 per cubic centimetre will enable measurements to be made in the solar wind when the spacecraft's orbit carries it through the magnetosphere into interplanetary space. Little is yet known about the complicated structure of the Earth's magnetosphere and these measurements will help scientists to learn more about it and how energy from the solar wind is transferred through this protective envelope to the lower atmosphere.

The Orbiting Geophysical Observatory (*OGO*) is a standardized spacecraft capable of carrying out a number of varied investigations. *OGO-E*, the fifth satellite in this series, was launched by an *Atlas Agena* rocket into a highly eccentric orbit ranging from 173 to 92 061 nautical miles at an inclination of 31·1°. In addition of the two British experiments it carries 20 experiments from U.S. research laboratories, one experiment from France and one from Holland.

STADAN (Satellite Tracking and Data Acquisition Network) stations providing supplementary tracking data include the station at Winkfield, Berkshire, operated by the Radio and Space Research Station of the Science Research Council.

Petrel's First Scientific Payloads

Petrel, Britain's small and low-cost space research rocket, having successfully completed its initial proving trials, has now started a new series of test flights in which scientific experiments are carried. Experiments chosen for the first payload-carrying round, launched successfully on 3rd February from the South Uist range in the Hebrides, were devised at the Science Research Council's Radio and Space Research Station at Slough, Buckinghamshire. A similar group of experiments was launched on 29th February in a second round in this series. Further rounds in the series will carry experiments for university research groups; these include an electron temperature experiment designed by the Electron Physics Department of the University of Birmingham.

The R.S.R.S. experiments will provide more information about the high-speed electrons from space which continually bombard the Earth's upper atmosphere. At high latitudes the bombardment is so intense that the atmosphere is made to glow and produce the Aurora and disturb the normal layers of ionization in the atmosphere so violently as to disrupt radio communications. The exact origin of the electrons is unknown but they are thought to be connected in some way with the particles in the Van Allen belts surrounding the Earth.

The specific questions to be answered by the R.S.R.S. experiments are: in what numbers do the electrons arrive; how fast are they moving when they enter the atmosphere; and by how much is the normal layer of ionization changed? Geiger counters are used to count the number of electrons with various speeds and penetrating powers (up to 40 keV). A newer and more sensitive detector, effective for less than 10 keV, the channel multiplier, is also used. The effect of the incoming electrons on the atmosphere is determined from the electric current drawn from the disturbed atmosphere by a spherical probe carried at the top of the rocket's payload.

Measurement of Ionospheric Electric Fields by Gun Launched Space Probes

A joint British-Canadian space research project is being carried out by the University of Southampton Space Physics Group, the University of Sussex Plasma Physics Group, and the Space Research Institute of Montreal as part of their project HARP (High Altitude Research Programmes) activities.

The near-vertically pointing 16-inch extended naval gun near Bridgetown on the Barbados coast will be used to launch flight vehicles which will release a number of barium ion clouds at altitudes of about 100–110 miles. The motion of the ion clouds, tracked photographically from several ground stations, yields information on electric fields in the ionosphere. Synoptic measurements of these electric fields are needed for better understanding of ionospheric behaviour; this should eventually lead to improved ionosphere prediction services for radio communications.

† 'Space Research at University College London', *The Radio and Electronic Engineer*, **34**, No. 1, p. 15, July 1967.

U.D.C. 621.372.57

An Investigation of the Effect of the Divisor Polynomial on the Responses of R-C Active Networks Designed by the Yanagisawa Procedure

By

A. G. J. HOLT,
Ph.D., C.Eng., M.I.E.E., M.I.E.R.E.†

AND

F. W. STEPHENSON,
B.Sc., Ph.D. (*Graduate*)†

Summary: The paper outlines the R-C active synthesis procedure due to Yanagisawa and shows how it may be applied to the design of networks, the responses of which are described by simple all-pole functions. Expressions are given for the voltage transfer ratios of these networks in terms of the element values, whilst curves show the effects of component and converter error on the network response.

The possibility of reducing the number of passive elements by varying the choice of divisor polynomial is considered. The effect of such choice upon the error due to k-variation is studied in some detail. Curves are given showing the error in the response of all-pole networks designed by the Linvill procedure and are compared with the Yanagisawa configurations.

Finally, it is demonstrated that the error for the networks considered is approximately linear for element changes of up to 10%.

List of Symbols

$N(p)$	numerator polynomial of response function
$D(p)$	denominator polynomial of response function
k	conversion factor of negative impedance converter (n.i.c.)
p	complex frequency variable
$F(p) = \prod_{i=1}^{n-1}(p-\sigma_i)$	= arbitrary divisor polynomial in Yanagisawa synthesis, where σ_i are $(n-1)$ points on the negative real-axis
Y_a, Y_b, y_a, y_b	admittances of elements of the L-networks in Yanagisawa synthesis
x	coefficient of p' in second-order response
a, a_1, a_2, a_3	coefficients of the p^0 term in the various divisor polynomials, $F(p)$

1. Introduction

In this paper the use of the R-C active synthesis procedure due to Yanagisawa is briefly explained and is illustrated by its application to second-order all-pole functions.

In this, as in some other R-C active synthesis methods, it is necessary to introduce an arbitrary polynomial, the choice of which affects the sensitivity of the final network.

† Department of Electrical Engineering, The University of Newcastle-upon-Tyne.

The above problem is investigated for a second-order all-pole network of specified numerator constant and the error due to variation in k is shown to depend upon the choice of divisor polynomial, as also is the number of passive elements in the network. It is shown in the paper that the number of elements may be reduced from six to four by suitable choice of the arbitrary polynomial $F(p)$. Thus, it is possible to exchange sensitivity for element economy in appropriate situations. It is obviously important to know the effects of error on the responses of the circuits since this knowledge will allow the designer to decide whether the available economy is worth the accompanying increase in sensitivity.

When k and the passive elements are equal to their nominal values the numerators of the expressions for (E_1/E_2), the voltage transfer function of the filter, are constants. This is as one would expect for all-pole structures. If these nominal values are departed from, then the numerator expressions become frequency dependent. Expressions in terms of k and the element values for both four- and six-element structures are given in later sections of the paper for the voltage transfer functions of second-order Butterworth and Chebyshev filters. From these expressions it can be shown that equal errors in certain elements have equal effects on the response; this would appear to offer a possible method of cancelling out the effects of error. Curves are given which show the error in response produced by small changes in k and the passive elements for the Butterworth and Chebyshev filters. The investigation has been restricted to second-order

sections, since these are the basic sections for higher-order filters.

It is of interest to compare different procedures applied to the synthesis of networks having the same response. To enable a comparison to be made, curves similar to the above are obtained for the second-order Butterworth and Chebyshev filters designed using the Horowitz optimization (which takes account of the effect of numerator constant, as well as divisor polynomial, on network sensitivity), for both Yanagisawa and Linvill techniques.[4,5]

2. Synthesis Procedure

The method used to synthesize the networks considered in the following sections was first reported by Yanagisawa[1] and has been described in another paper by the authors.[2]

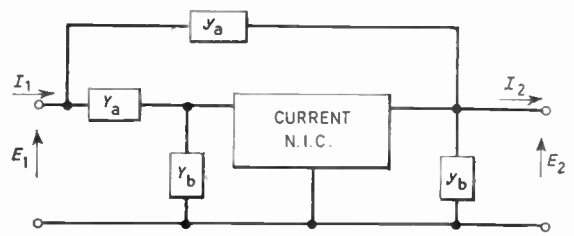

Fig. 1. Yanagisawa-circuit using L networks.

The resultant network in this synthesis technique is shown in Fig. 1, the transfer function of which is given by:

$$\frac{E_2}{E_1} = \frac{(y_a - Y_a)}{(y_a + y_b) - (Y_a + Y_b)} = \frac{N(p)}{D(p)} \qquad \text{.....(1)}$$

It is necessary to select $(n-1)$ points σ_i on the negative real axis of the p-plane, where n is the highest order of the numerator or denominator polynomial in eqn. (1) above.

Let the arbitrary polynomial be formed:

$$F(p) = \prod_{i=1}^{n-1} (p - \sigma_i) \qquad \text{.....(2)}$$

Both numerator and denominator of eqn. (1) are divided by $F(p)$ and it follows, from a partial fraction expansion of $N(p)/F(p)$, that y_a and Y_a can be determined, while y_b and Y_b will result from a partial fraction expansion of $[D(p) - N(p)]/F(p)$.

3. N.I.C. Conversion Factor

Consider the conversion factor of the current n.i.c. as being related to the input and output signals by the expression

$$\begin{vmatrix} E_1 \\ I_1 \end{vmatrix} = \begin{vmatrix} 1 & 0 \\ 0 & -k \end{vmatrix} \begin{vmatrix} E_2 \\ I_2 \end{vmatrix} \qquad \text{.....(3)}$$

Equation (1) above assumed the existence of an ideal converter, with $k = 1$. If non-ideal converters are used then the overall expression becomes:

$$\frac{E_2}{E_1} = \frac{(ky_a - Y_a)}{k(y_a + y_b) - (Y_a + Y_b)} \qquad \text{.....(4)}$$

4. Second-order Synthesis

Let us consider the Yanagisawa method as applied to a second-order all-pole function given by:

$$\frac{E_2}{E_1} = \frac{N(p)}{D(p)} = \frac{H}{p^2 + xp + V} \qquad \text{.....(5)}$$

Select $F(p) = (p+a)$ then,

$$\frac{y_a - Y_a}{p} = \frac{N(p)}{pF(p)} = \frac{H}{p(p+a)} = \frac{H}{pa} - \frac{H}{a(p+a)}$$

and

$$y_a - Y_a = \frac{H}{a} - \frac{Hp}{a(p+a)}$$

Assigning the positive residue to y_a and the negative residue to Y_a, we obtain:

$$y_a = H/a \qquad \text{.....(6a)}$$

$$Y_a = \frac{Hp}{(p+a)a} \qquad \text{.....(6b)}$$

Similarly,

$$y_b - Y_b = p + \frac{p(x-a) + (V-H)}{(p+a)}$$

If we consider only functions for which $V = H$, then

$$y_b - Y_b = p + \frac{p(x-a)}{(p+a)} \qquad \text{.....(7)}$$

It will thus be seen that the form of y_b and Y_b will depend upon the relative values of x and a. There are three cases to be considered:

Case 1:

$$x > a$$

$$y_b = p + \frac{p(x-a)}{(p+a)} \qquad \text{.....(8a)}$$

$$Y_b = 0 \qquad \text{.....(8b)}$$

The resultant network is shown in Fig. 2(a) and its analysis yields

$$A_1 = \frac{E_2}{E_1} = \frac{H\left\{\frac{p(k-1)}{ak} + 1\right\}}{p^2 + p\left\{\frac{H(k-1)}{ak} + x\right\} + H} \qquad \text{.....(9)}$$

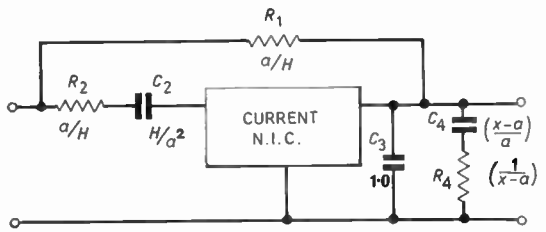

(a) $x > a[A_1]$

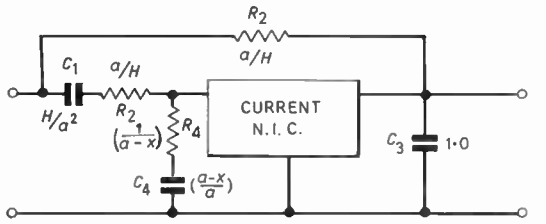

(b) $x < a[A_2]$

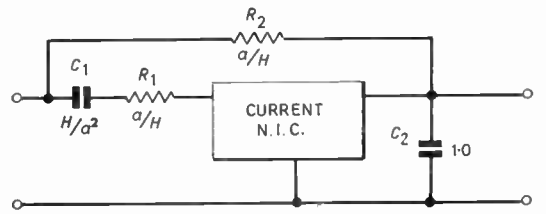

(c) $x = a[A_3]$

Fig. 2. Second-order Yanagisawa network.

Case 2:

$$x < a$$

$$y_b = p \qquad \text{.....(10a)}$$

$$Y_b = \frac{(a-x)p}{(p+a)} \qquad \text{.....(10b)}$$

The resultant network is shown in Fig. 2(b) and its analysis yields

$$A_2 = \frac{E_2}{E_1} = \frac{H\left\{\dfrac{p(k-1)}{ak}+1\right\}}{p^2+p\left\{\dfrac{(k-1)}{ak}[H+a^2]+\dfrac{x}{k}\right\}+H} \qquad \text{.....(11)}$$

Case 3:

$$x = a$$

$$y_b = p \qquad \text{.....(12a)}$$

$$Y_b = 0 \qquad \text{.....(12b)}$$

The resultant network is shown in Fig. 2(c), analysis of which yields

$$A_3 = \frac{E_2}{E_1} = \frac{H\left\{\dfrac{p(k-1)}{ak}+1\right\}}{p^2+p\left\{\dfrac{H(k-1)}{ak}+a\right\}+H} \qquad \text{.....(13)}$$

5. Sensitivity Considerations

Given a particular function to synthesize, the designer thus has the choice of a four-element network or one of two six-element structures.

Before selecting a particular network, some knowledge of the resultant change in response due to variation in k will be needed.

In order to avoid confusion in comparing the three networks, the following symbols will be used for the coefficient of the divisor polynomial, $F(p)$:

Case 1:

$$a = a_1 \quad (a_1 < x)$$

Case 2:

$$a = a_2 \quad (a_2 > x)$$

Case 3:

$$a = a_3 \quad (a_3 = x)$$

The magnitudes of the various response functions will now be considered.

Case 1: From eqn. (9) it follows that

$$|A_1| = \frac{H\sqrt{\dfrac{(k-1)^2\omega^2}{a_1^2k^2}+1}}{\sqrt{(H-\omega^2)^2+\left[\dfrac{H(k-1)}{a_1k}+x\right]^2\omega^2}} \qquad \text{.....(14)}$$

Let $k = 1+\Delta$, where $|\Delta| \ll 1$ and consider

$$|A_1|_{\omega=\sqrt{H}} = |A_1'|,$$

$$|A_1'| = \frac{\sqrt{H}\sqrt{1+\dfrac{\Delta^2H}{a_1^2(1+\Delta)^2}}}{\left(\dfrac{H\Delta}{a_1(1+\Delta)}+x\right)}$$

which, since $\Delta^2H \simeq 0$, simplifies to

$$|A_1'| \simeq \frac{\sqrt{H}}{x}\left(1-\frac{\Delta H}{a_1x}\right) \qquad \text{.....(15)}$$

Case 2: From eqn. (11) it follows that

$$|A_2| = \frac{H\sqrt{\dfrac{\omega^2(k-1)^2}{a_2^2k^2}+1}}{\sqrt{(H-\omega^2)^2+\left\{\dfrac{(k-1)}{a_2k}[H+a_2^2]+\dfrac{x}{k}\right\}^2\omega^2}} \qquad \text{.....(16)}$$

As above, let $k = 1+\Delta$ and consider

$$|A_2|_{\omega=\sqrt{H}} = |A_2'|$$

It can be shown that

$$|A_2'| \simeq \frac{\sqrt{H}}{x}\left\{1-\Delta\left[\frac{H+a_2^2}{a_2 x}-1\right]\right\} \quad \ldots\ldots(17)$$

Case 3: From eqn. (13) it follows that

$$|A_3| = \frac{H\sqrt{\dfrac{\omega^2(k-1)^2}{x^2k^2}+1}}{\sqrt{(H-\omega^2)^2+\left\{\dfrac{H(k-1)}{kx}+x\right\}\omega^2}} \quad \ldots\ldots(18)$$

As above, let $k = 1+\Delta$ and consider

$$|A_3|_{\omega=\sqrt{H}} = |A_3'|$$

It can be shown that

$$|A_3'| \simeq \frac{\sqrt{H}}{x}\left[1-\frac{\Delta H}{x^2}\right] \quad \ldots\ldots(19)$$

From eqns. (15), (17) and (19) the terms causing error are:

Case 1:

$$|A_1''| = \frac{H}{a_1 x} \quad \ldots\ldots(20)$$

Case 2:

$$|A_2''| = \frac{(H+a_2^2)}{a_2 x} - 1 \quad \ldots\ldots(21)$$

Case 3:

$$|A_3''| = \frac{H}{x^2} \quad \ldots\ldots(22)$$

For a given function, H and x will be constant. Thus, the choice of network for least variation due to k can be selected by a study of eqns. (20–22).

It will be immediately apparent that

$$|A_1''| > |A_3''|$$

and thus Case 1 (in which $a_1 < x$) produces a network which is more sensitive to k-variation than Case 3 (in which $a_3 = x$).

The relative merits of Cases 2 and 3 will depend upon the function to be synthesized. Let us consider the ratio $\dfrac{|A_2''|}{|A_3''|}$. When this ratio is less than unity, A_2 will be the most suitable choice and, when the ratio is greater than unity, A_3 will be the best choice. The condition

$$\frac{|A_2''|}{|A_3''|} < 1$$

means that

$$\frac{x^2\left\{\dfrac{H+a_2^2}{a_2 x}-1\right\}}{H} < 1$$

which leads to

$$a_2^2 - a_2\left(\frac{x^2+H}{x}\right) + H < 0 \quad \ldots\ldots(23)$$

Thus, the range of values over which the inequality holds is given by

$$a_2 = \frac{\left(\dfrac{x^2+H}{x}\right) \pm \sqrt{\left(\dfrac{x^2+H}{x}\right)^2 - 4H}}{2} \quad \ldots\ldots(24)$$

It should be noted that values of a_2 are only permissible for which $a_2 > x$ (initial definition of a_2).

If a legitimate range of a_2 does not exist, then A_3 is the most suitable network.

If a legitimate range for a_2 does exist, then the optimum (minimum) value can be found as shown below.

From eqn. (21)

$$\frac{\mathrm{d}|A_2''|}{\mathrm{d}a_2} = \frac{\mathrm{d}}{\mathrm{d}a_2}\left\{\frac{H+a_2^2-a_2 x}{a_2 x}\right\} = 0$$

which yields

$$a_2 = \sqrt{H} \quad \ldots\ldots(25)$$

6. Filter Designs

6.1 *Second-order Butterworth*

The transfer function is given by

$$\frac{E_2}{E_1} = \frac{N(p)}{D(p)} = \frac{1}{p^2+\sqrt{2}p+1} \quad \ldots\ldots(26)$$

This is equivalent to eqn. (5) with

$$H = V = 1 \quad \text{and} \quad x = \sqrt{2}$$

From eqn. (24)

$$a = \sqrt{2} \quad \text{or} \quad 1/\sqrt{2}$$

Since legitimate values of a_2 lie outside this range, the synthesis must be performed such as to produce the A_3 network ($a_3 = x$) as shown in Fig. 3(a).

Thus $F(p) = (p+\sqrt{2})$.

It should be noted at this point that the investigation has been restricted to functions in which $H = V$. If the Horowitz optimization (which guarantees minimum sensitivity) is used, this restriction is removed and a different network may result.

In the synthesis of the Butterworth function, Horowitz yields a five-element network with

$$F(p) = (p+1) \quad \text{and} \quad H = (2-\sqrt{2}).$$

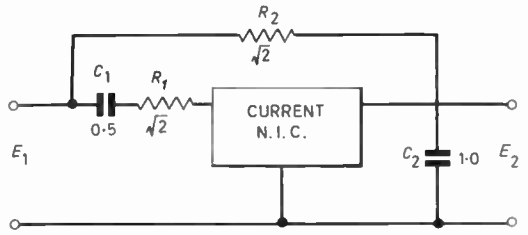

(a) 4-element Yanagisawa [A_3]

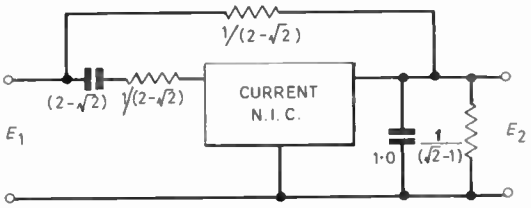

(b) 5-element Yanagisawa (Horowitz optimized) [A_H]

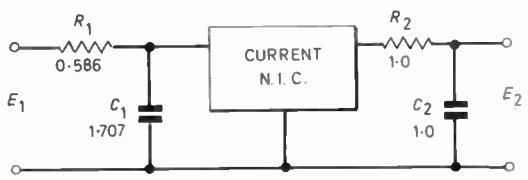

(c) Linvill network [L_2]

Fig. 3. Networks providing second-order Butterworth response.

The network (A_H) is shown in Fig. 3(b) and the error due to +2% variation in k is shown in Fig. 7.

6.2 *Second-order Chebyshev Response* (3dB *ripple*)

The transfer function is given by

$$\frac{E_2}{E_1} = \frac{1}{p^2+0{\cdot}6449p+0{\cdot}70795} \qquad \text{.....(27)}$$

This is equivalent to eqn. (14) with

$$H = V = 0{\cdot}70795 \quad \text{and} \quad x = 0{\cdot}6449.$$

From eqn. (24),

$$a_2 = 1{\cdot}0982 \quad \text{or} \quad 0{\cdot}6449.$$

From eqn. (25), the minimum value of a_2 is equal to 0·8414. Since this value lies within the range over which $|A_2| < |A_3|$ and is also greater than x, the synthesis should be performed such as to yield the A_2 structure, as in Fig. 4(a).

Thus,

$$F(p) = (p+0{\cdot}8414).$$

This network is identical to that produced by the Horowitz optimization.

7. Errors due to Element Variations

The change in response due to change in element value as well as converter characteristic (k), can be investigated by changing the active and passive elements by small known percentages and calculating the resulting variations in network response.

In this section, the effect of element variation in second-order functions is investigated.

7.1 *Second-order Butterworth*

The network is shown in Fig. 3(a) and can be analysed to give:

$$\frac{E_2}{E_1} = \frac{p(kC_1R_1 - C_1R_2)+k}{p^2(C_1R_1C_2R_2k)+p[k(C_1R_1+C_2R_2)-C_1R_2]+k} \qquad \text{.....(28)}$$

The expression reduces to the Butterworth second-order response function when $k = 1$ and the elements have the values shown in Fig. 3(a). It can be shown that, as far as the shape of the response is concerned, variation in the value of R_1 causes the same effect as variation in the value of R_2. This result is not general and only applies to certain functions, Butterworth being one of them.

A selection of the results obtained due to component variation is given in Figs. 5(a), (b) and (c).

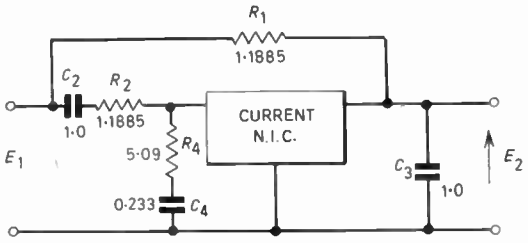

(a) 6-element Yanagisawa [A_2]

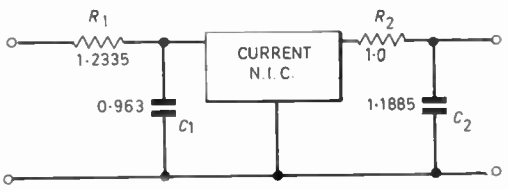

(b) Linvill network [L_2]

Fig. 4. Networks producing second-order Chebyshev response.

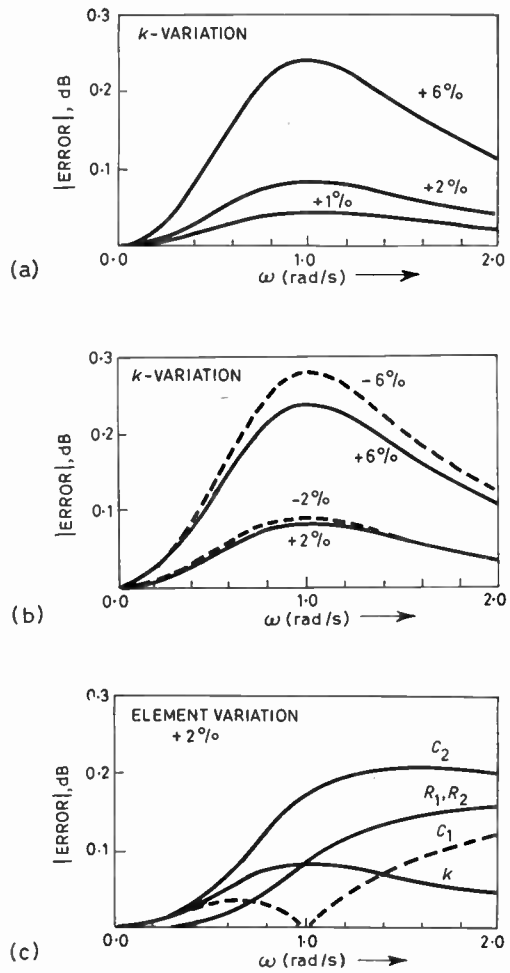

Fig. 5. 4-element Butterworth responses.

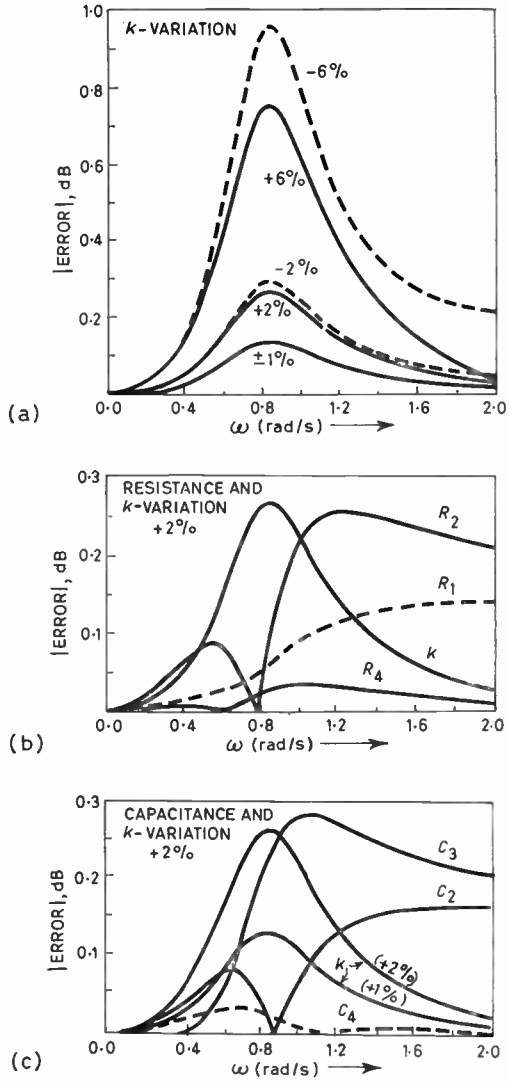

Fig. 6. 6-element Chebyshev filter responses.

7.2 *Second-order Chebyshev*

The network is shown in Fig. 4(a) and can be analysed to give:

$$\frac{E_2}{E_1} = \frac{Ap^2+Bp+k}{Dp^3+Ep^2+Fp+k} \qquad \text{.....(29)}$$

where

$$A = (kT_2 - T_{21})T_4$$
$$B = k(T_2+T_4) - T_{21}$$
$$D = kT_2T_4T_{31}$$
$$E = k(T_2T_4 + T_{31}T_4 + T_{31}T_2) - (T_4T_{21} + T_2T_{41})$$
$$F = k(T_2+T_4+T_{31}) - (T_{41}+T_{21})$$

and

$$C_xR_y = T_{xy} \quad \text{and} \quad C_xR_x = T_x \qquad \text{.....(30)}$$

A selection of the results obtained from the network is shown in Figs. 6(a), (b) and (c).

8. Comparison of Linvill and Yanagisawa Networks

The Butterworth and Chebyshev responses described in the previous section can also be obtained by means of the Linvill synthesis procedures.[3] This section compares the error due to k-variation in both Linvill and Yanagisawa networks.

8.1 *Butterworth Response*

The three networks producing a second-orde Butterworth response are shown in Fig. 3(a), (b) and (c). For convenience, these will be referred to as follows:

L_2—Horowitz-optimized Linvill network

A_3—four-element Yanagisawa network

A_H—Horowitz-optimized Yanagisawa network.

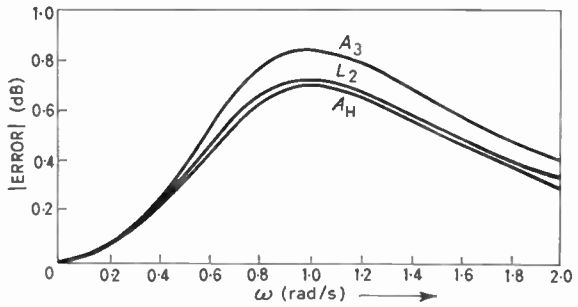

Fig. 7. Comparison of error in Butterworth networks. (k-variation +2%).

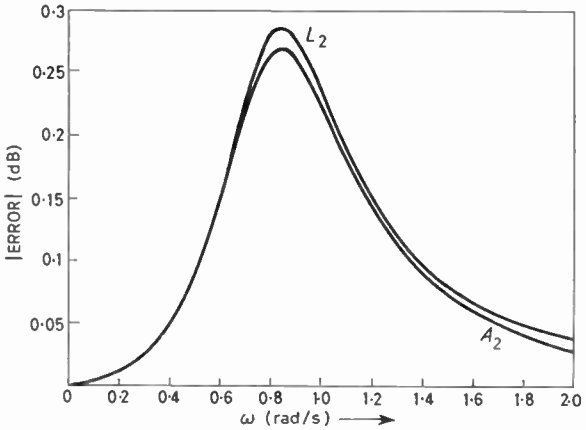

Fig. 8. Comparison of error in Chebyshev networks. (k-variation +2%).

The error in response curve due to +2% variation in k is shown for the three networks in Fig. 7.

It will be seen that the Linvill circuit is less sensitive than A_3, but slightly more sensitive than A_H.

The error in the response curve due to +2% variation in k is shown for the two networks in Fig. 8.

It will be seen that A_2 produces slightly more error than L_2.

8.2 *Chebyshev Response*

The two circuits used to produce a second-order Chebyshev response are shown in Figs. 4(a) and (b). They will be referred to as follows:

L_2—Horowitz-optimized Linvill network

A_2—Horowitz-optimized Yanagisawa network.

9. Linearity of Error

The curves shown in Figs. 9, 10 and 11 illustrate error in response against component variation. From a study of such curves, the following observations may be made:

(*a*) Increase in a component value causes an error unequal, and in the opposite sense to, that produced by an equal decrease in the same component.

(*b*) Component variation in a given sense (i.e. either an increase or a decrease) is proportional, to a first approximation, to the resulting error in the response curve.

The above statements apply to the circuits described in this paper.

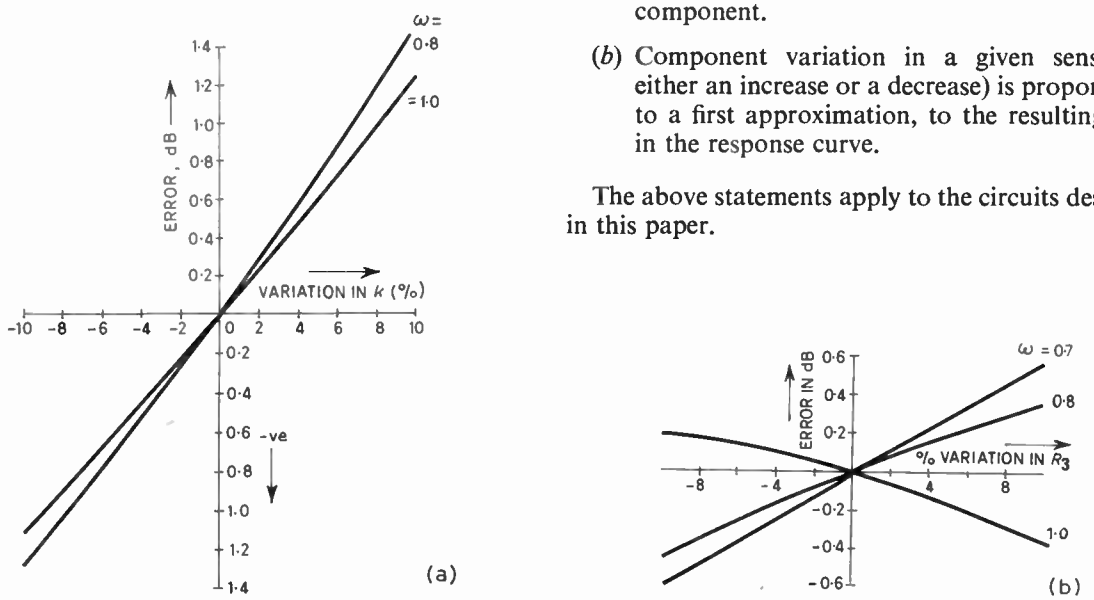

Fig. 9. Linearity of error in second-order Chebyshev filter (Linvill).

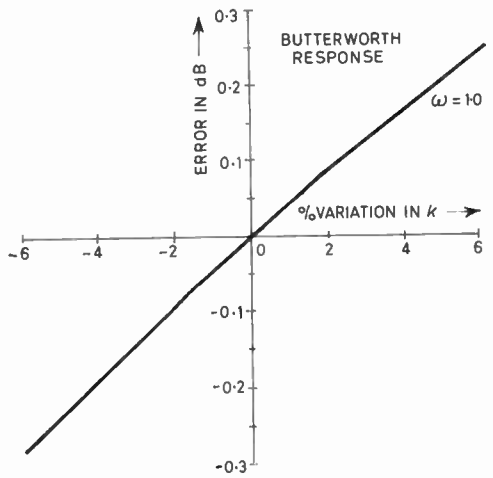

Fig. 10. Linearity of error in 4-element Yanagisawa network.

10. Conclusions

The paper has illustrated the effect of the divisor polynomial on the error due to k-variation in a second-order network. A procedure to select the least sensitive network has been derived.

Whilst the Horowitz networks represent the optimum which can be achieved, there may be cases when the designer will be prepared to sacrifice an amount of sensitivity in favour of a saving in network elements.

11. References

1. T. Yanagisawa, 'RC active networks using current inversion type negative impedance converters', *Trans. Inst. Radio Engrs on Circuit Theory*, **CT-4**, p. 140, January 1957.
2. A. G. J. Holt and F. W. Stephenson, 'Design tables for active filters having 2nd- and 4th-order Chebyshev responses in pass and stop bands', *Proc. Instn Elect. Engrs*, **111**, No. 11, pp. 1807–20, November 1964. (I.E.E. Paper No. 4560E.)
3. J. G. Linvill, 'RC active filters', *Proc. I.R.E.*, **42**, pp. 555–64, March 1954.
4. I. M. Horowitz, 'Optimization of negative impedance conversion methods of active RC synthesis', *Trans. I.R.E.*, **CT-6**, pp. 296–303, September 1959.
5. D. A. Calahan, 'Notes on the Horowitz optimization procedure', *Trans. I.R.E.*, **CT-7**, pp. 352–4, September 1960.

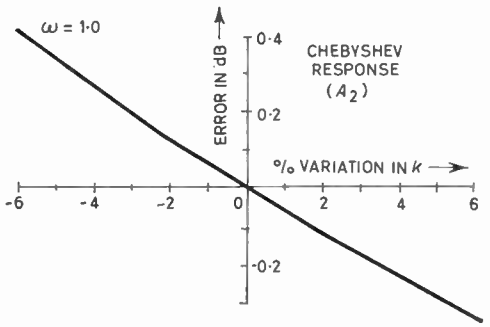

(a) 6-element Yanagisawa network.

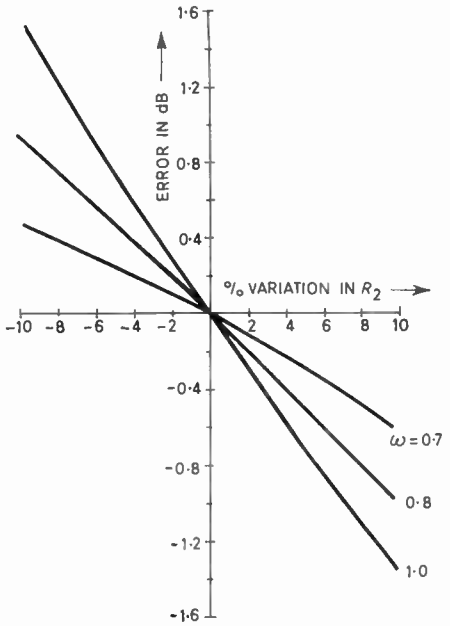

(b) Second-order Chebyshev filter (Linvill).

Fig. 11. Linearity of error.

Manuscript first received by the Institution on 24th March 1966, in revised form on 28th July 1967 and in final form on 31st January 1968. (Paper No. 1176/CC1.)

U.D.C. 621.385.62/3

Noise Spectra of Beam-type Microwave Oscillators

By

B. V. RAO, M.Sc., Ph.D.†

AND

Professor W. A. GAMBLING, B.Sc., Ph.D., C.Eng., F.I.E.R.E.‡

Summary: The paper describes measurements of amplitude modulation, frequency modulation and total noise spectra for several types of klystrons and backward-wave oscillators. Computations of the noise to be expected have also been carried out and the theoretical and experimental results are compared.

List of Symbols

A_0	constant
B	bandwidth of noise
c	velocity of light
D_0	frequency deviation constant for f.m. noise
e	electron charge
g_e	electronic conductance
I_b	d.c. component of beam-current
I_{st}	starting current
I_1	noise component of beam-current
ΔI	small change in current
J_n	Bessel function of nth order
k	Boltzmann's constant
k_c	coupling factor for noise
k_r	ratio of reflected current to cathode current
K	pushing figure
L	length of fingers of ladder line
m	electron mass
M	transit-time factor in resonator gap
N	length of slow-wave circuit in wavelengths
P	power output
P_n	noise power
$2p$	pitch of ladder line
Q	loaded Q-factor of the resonator
$R(t)$	correlation function
T	temperature
t'	electron transit-time
u_0	d.c. component of beam velocity
Δu	fluctuation in beam velocity
V_a	a.c. component of resonator voltage
V_0	d.c. component of resonator voltage
ΔV_N	fluctuation in voltage due to noise
$W(\omega)$	noise power spectrum
$W_m(f)$	noise power spectrum of modulating voltage
$W_{fm}(f)$	f.m. output noise spectrum
X	bunching parameter
α	$\theta M/2V_0$
η_e	electronic efficiency
η_0	output efficiency
θ_e	drift angle in repeller space of klystron
θ	drift angle through repeller space and resonator
ω	angular frequency
ω_0	angular frequency of carrier

1. Introduction

The problem of noise in microwave beam-type amplifiers has been extensively studied both theoretically and experimentally and the general principles are well known although not completely understood. On the other hand, the topic of noise in microwave oscillators has received far less attention and is less-well understood. Oscillator noise can have a deleterious effect in many types of microwave systems, for example, where the oscillator is used as a Doppler transmitter, as a pump source for masers or parametric amplifiers, as a source for a microwave spectrometer, or as a local oscillator in a receiver. Some knowledge of the noise properties of microwave oscillators is therefore desirable. This paper describes a theoretical and experimental investigation of the noise spectra, for sideband frequencies in the range 1 to 100 MHz, of several types of klystrons and backward-wave oscillators.

† Formerly at the Department of Electronics, University of Southampton; now Assistant Professor at the Department of Electrical Engineering, Indian Institute of Technology, Bombay, India.

‡ Department of Electronics, University of Southampton.

The various types of oscillator noise spectra, and suitable measuring techniques, have been discussed elsewhere.[1,2] Basically it is possible to measure a.m. sideband plus background noise spectra and f.m. sideband plus background noise spectra using direct-detection methods, or total (a.m. plus f.m. plus background) noise spectra using a superheterodyne receiver. For further details the reader should refer to the existing literature. In all of the measurements reported here the noise calibration, and the measurement of carrier power, are referred to the microwave mixer input. Noise levels are therefore quoted both in dB above thermal noise at the mixer input and as a carrier/noise ratio where appropriate.

2. Results of Measurements

Most of the measurements reported here represent the average of a number of separate measurements. The overall accuracy is thought to be about 1 dB.

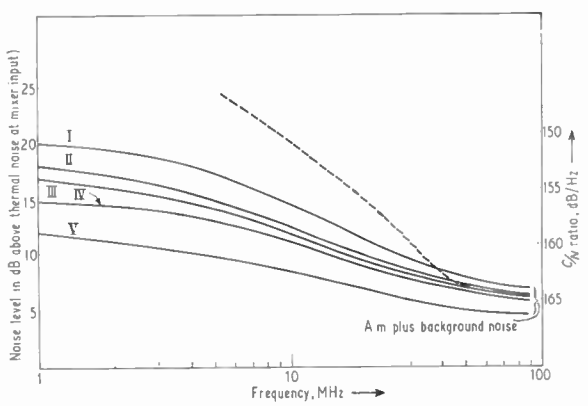

Fig. 1. A.m. plus background noise (solid curves) in reflex klystrons as follows: I—723 A/B; II—E.M.I. R9525 (serial number 305); III—E.M.I. R9525 (serial number 324); IV—E.M.I. R9525 (serial number 25); V—Varian V55. The dotted curve indicates f.m. plus background noise corresponding to curve III.

Table 1

Comparison of measurement of C/N ratio by different methods

Frequency (MHz)	C/N ratio (dB/Hz)		
	Balanced mixer (corrected)	Cavity filter	Suppressed and re-inserted carrier
20	161	159·8	158·4
30	162	161·0	160·5
40	162·8	163·2	161·4
60	164·2	165·0	163·5
80	164·8	165·6	165·2

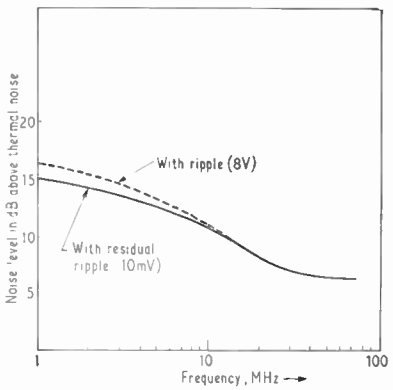

Fig. 2. Effect of ripple in reflector supply on a.m. plus background noise of klystron E.M.I. R9525 (serial number 25). The solid curve is for a ripple voltage of 10 mV and the dashed curve for a ripple voltage of 8 V.

2.1 *A.M. plus Background Noise in Reflex Klystrons*

The carrier/noise (C/N) ratios of a.m. plus background noise for several reflex klystrons are shown in Fig. 1. The measurements were conducted mainly with the cavity-filter and balanced-mixer methods.[1] For one of the E.M.I. klystrons the suppressed-and-reinserted carrier method was used as a check (Table 1) and it is seen that there is excellent agreement between the three types of measurement. This indicates that there is little, if any, conversion of f.m. to a.m. noise with the carrier suppression filter used. It would appear from these and other[3] measurements that klystrons operating with higher operating voltages have lower noise, although this is apparently not always the case.[4]

2.1.1 Effect of ripple

The effect of superimposing a 50 Hz voltage on the d.c. resonator voltage of a reflex klystron to simulate the effect of power supply ripple was studied. No change in the a.m. plus background noise spectrum for the E.M.I. R9525 klystron was found over the range of superimposed voltage from the initial residual value of 1·5 mV peak-to-peak up to 2% of the resonator voltage of 350 V. In addition there appeared to be no appreciable change in the a.m. plus background noise spectrum when a ripple voltage was introduced into the heater supply voltage. The situation was unchanged even when the heater voltage was derived fully from an a.c. supply. A similar procedure for the reflector voltage resulted in the behaviour shown in Fig. 2. In all the measurements the cathode was strapped to one terminal of the heater supply to prevent stray cathode modulation effects.

The increase in noise due to ripple in the reflector voltage is unexpected since the klystrons were nor-

mally operated at the mode centre. However, the ripple voltage was relatively large and the effect was probably due to the peaked nature of the mode pattern. Detuning from the mode centre certainly caused a much larger increase in noise.

2.2 *F.M. plus Background Noise in a Reflex Klystron*

A typical f.m. plus background noise spectrum for an E.M.I. klystron is shown in Fig. 1 and may be compared with the a.m. plus background noise spectrum. According to theoretical treatments of f.m. noise in oscillators (see reference 5 and Section 3.2) a 6 dB per octave slope is predicted, at least over the i.f. range pertinent to the present investigation. The measurements give a value of 5·6 dB/octave and confirm an earlier result[2] with other klystrons that f.m. noise predominates up to about 50 MHz.

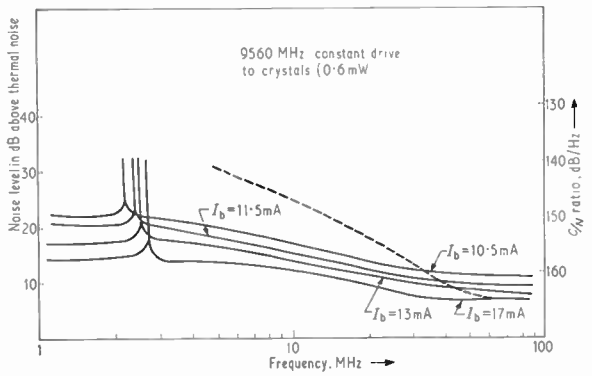

Fig. 3. A.m. plus background noise for various beam currents in backward-wave oscillator type CO43. The dashed curve indicates f.m. plus background noise.

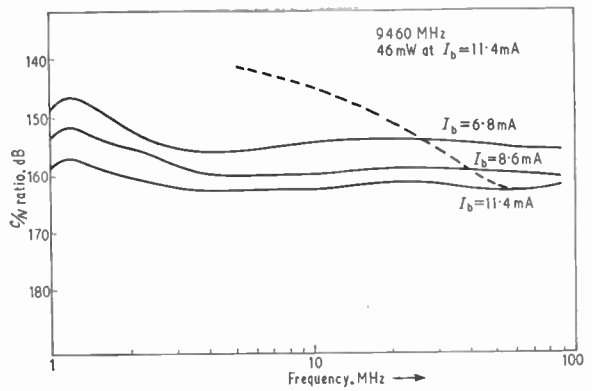

Fig. 4. A.m. plus background noise in backward-wave oscillator type BA9–20 for various beam currents. The dashed curve indicates f.m. plus background noise.

No change was observed in the f.m. plus background noise spectrum over the i.f. range of the measurements when up to 2% ripple was introduced on the reflector or cathode. This could be explained by the fact that the change in carrier frequency deviation was not large enough to affect the 6 dB/octave slope. This was confirmed by taking carrier-frequency deviation measurements.[3] A carrier-frequency deviation of 1·3 kHz was measured. This increased to nearly 1·5 kHz when the ripple voltage was applied to the reflector only. No change was noticed when the ripple was applied to the cathode.

Table 2

Variation of relative noise level with beam-current for different tubes

(i) Ophitron No. 173: f = 9520 MHz

Line current (mA)	Relative noise level (dB) (experiment)
6·3	0
5·8	+1·5
5·5	+1·3
4·8	+2·3
4·15	+3·9
3·5	+5·0

(ii) BA9–20: f = 9460 MHz

Beam current (mA)	Relative noise level (dB) (experiment)
10·2	0
9·0	+0·2
8·0	+1·2
7·0	+2·3
6·0	+3·9
5·0	+5·7
4·0	+8·4

(iii) CO43: f = 9560 MHz

Beam current (mA)	Relative noise level (dB) (experiment)
16·5	0
12·9	+3·0
11·0	+4·3
9·8	+5·2
8·2	+6·6
6·6	+9·6

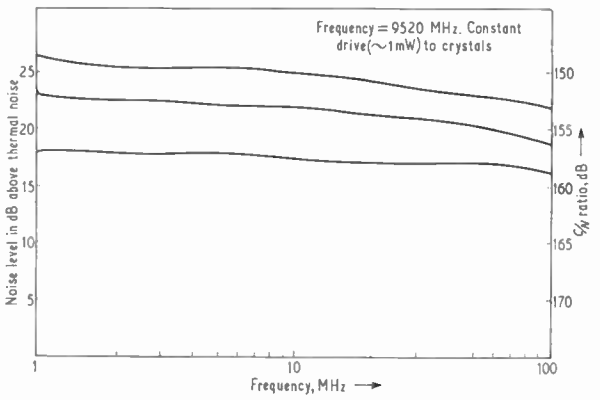

Fig. 5. A.m. plus background noise in Ophitron No. 27.

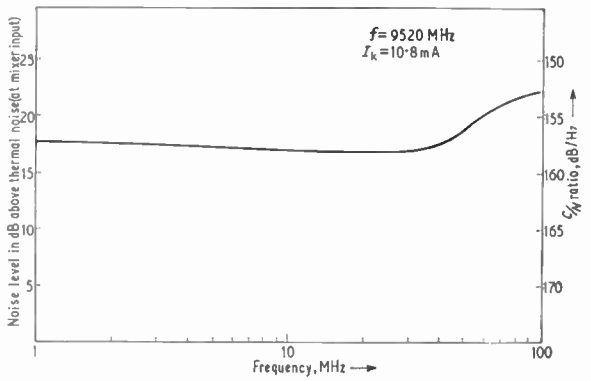

Fig. 7. A.m. plus background noise in Ophitron No. 173 after modification.

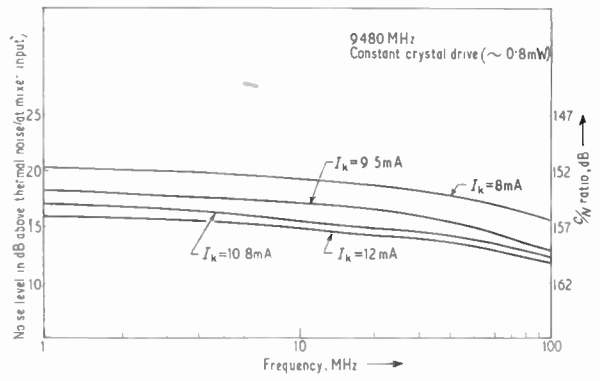

Fig. 6. A.m. plus background noise in Ophitron No. 173.

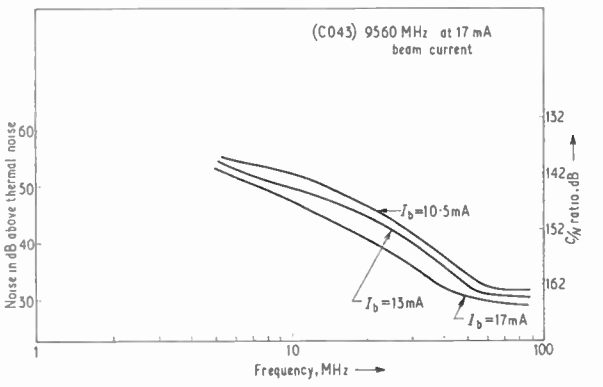

Fig. 8. F.m. plus background noise for backward-wave oscillator type CO43 as a function of beam current.

2.3 *A.M. plus Background Noise in Backward-wave Oscillators*

The a.m. plus background noise spectra of a backward-wave oscillator (b.w.o.) with permanent magnet focusing (CO43) are shown in Fig. 3. In the sideband range up to a few megahertz noise peaks and discrete oscillations alternated randomly during the measurements. From about 5 MHz the noise spectra were observed to be nearly flat.

It should be pointed out that the magnetically-focused oscillators were not of the most recent manufacture, for the effect of ions can now be prevented. The frequencies of the ion oscillations and noise peaks observed in the experimental tubes are in accordance with those predicted from a study of plasma ion oscillations.[3,6]

The a.m. plus background noise spectra for the b.w.o. type BA 9–20 are shown in Fig. 4 and are similar to those for the CO43. The variation of a.m. plus background noise with beam-current at an intermediate frequency of 20 MHz is shown in Table 2, which gives the relative change in noise output after correcting for the change in power output with beam-current.

Measurement of a.m. plus background noise on two ophitrons[7] shows that the tubes are free from ion oscillation noise or discrete spurious oscillations (Figs. 5, 6). In one of the two ophitrons investigated (No. 173) the separation between the focusing plates and the slow-wave structure was increased with the expectation that the noise output would be reduced if partition noise made an appreciable contribution to the overall noise content. The measurements did not reveal much change at lower intermediate frequencies in the C/N ratio as may be noticed from Figs. 5 and 6. The increase in the a.m. plus background noise output at the higher frequencies which occurred after some time had elapsed in the case of the modified tube could be due to an enhanced gain at a spurious oscillation peak (Fig. 7).

2.3.1 Effect of ripple

As in the case of the reflex klystron no change was observed in the a.m. plus background noise spectrum when a ripple voltage of up to 1% was applied, first to the line voltage and then to one of the anode voltages, of each b.w.o. Thus the contribution of ripple voltages to the non-linear mixing of noise with noise is apparently negligible.

2.4 *F.M. plus Background Noise in Backward-wave Oscillators*

F.m. plus background noise measurements were carried out on the BA9–20 and the CO43 (Figs. 3, 4). The curves obtained show a slope of 5·7 and 5·8 dB/octave for the CO43 and BA9–20 respectively. This confirms, in addition to the result for the reflex klystron, the general theory of f.m. noise in oscillators. The effect on f.m. plus background noise of varying the beam current was studied in the case of the CO43 (Fig. 8). The slope of the curve was unaffected while the C/N ratio increased with increasing beam-current.

No change was observed when a ripple voltage of up to 1% of the line voltage was introduced on the line electrode of the BA9–20.

2.5 *Total Noise Measurements on Backward-wave Oscillators*

Total noise was measured in all of the backward-wave oscillators both while oscillating and below start of oscillation (Figs. 9–12). In the case of one ophitron (modified tube), a spurious oscillation peak appeared over the lower sideband. This affected the a.m. plus background noise spectrum, as mentioned in Sect. 2.3.1.

The curves of total or background noise below start of oscillation all seem to have the same general shape. Theoretical analysis[18] shows that in each case this shape is similar to that of the gain/frequency characteristic of the tube acting as a backward-wave amplifier (b.w.a.). The peaks of noise power output below start of oscillation may be observed to flatten as the beam current is decreased.

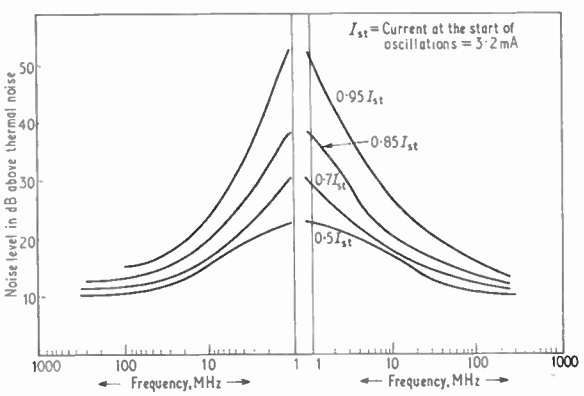

Fig. 9. Noise below start of oscillation for backward-wave oscillator type CO43.

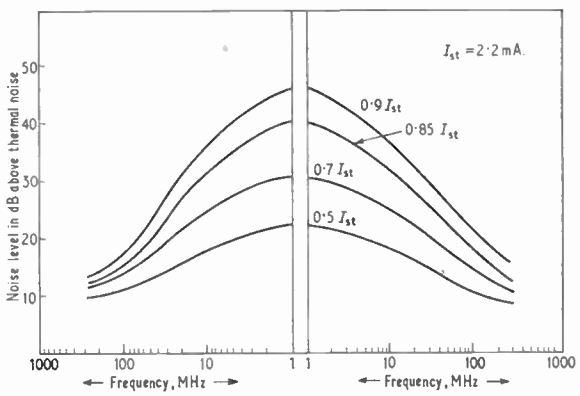

Fig. 10. Noise below start of oscillation in backward-wave oscillator type BA9–20.

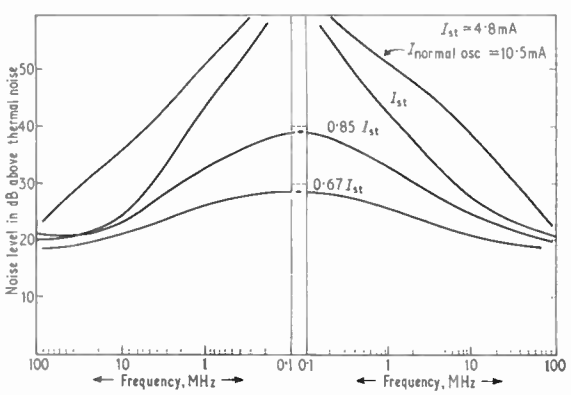

Fig. 11. Total noise in Ophitron No. 27.

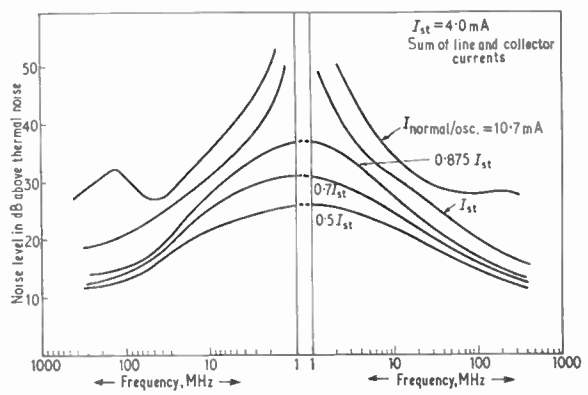

Fig. 12. Total noise in Ophitron No. 173.

3. Theoretical Study

In addition to the measurements described above some calculations of the noise to be expected in the tubes under investigation have been made. In most cases the only source of noise is taken to be unsmoothed shot noise and velocity fluctuations in the beam. The calculations, which make the usual assumptions of one-dimensional single-velocity flow and a large longitudinal magnetic field, are rather involved and have been carried out with a digital computer.

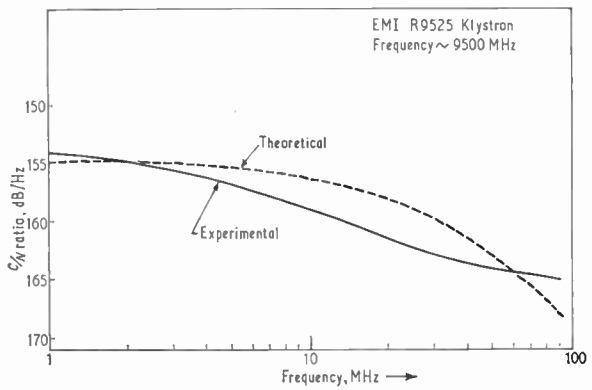

Fig. 13. Comparison of measured and calculated a.m. plus background noise in reflex klystron, type E.M.I. R9525.

3.1 *A.M. plus Background Noise Spectrum of Reflex Klystrons*

The calculation of the a.m. plus background noise spectrum of reflex klystrons is based on the treatment by Knipp[8] as simplified by Häggblom.[9] The noise power output at a frequency $\Delta\omega$ away from the carrier is given by (notation mainly as in Häggblom's paper):

$$P_n = \frac{M^2\overline{|I_1|^2}V_0 X J_1(X)}{kI_b\theta\left[\{XJ_2(X)\}^2 + \frac{8Q^2}{\omega_0^2}\{J_1(X)M(\Delta\omega)\}^2\right]} \quad \ldots\ldots(1)$$

where M = transit-time factor in resonator gap,
I_1 = noise current,
V_0, I_b = mean beam voltage and current,
X = bunching parameter,
k_r = fraction of cathode current returning through resonator gap,
θ = drift angle in repeller space and resonator,
Q = loaded resonator Q-factor,
ω_0 = carrier angular frequency,
$J_1(\ )$ = Bessel function.

To determine the carrier/noise ratio it is necessary to know the output efficiency of the klystron. The electronic efficiency [10] is expressed by

$$\eta_e = \frac{g_e V_a^2}{2k_r I_b V_0} = \frac{g_e V_a}{k_r I_b}\left(\frac{X}{\theta}\right)$$

where g_e = electronic conductance,
V_a = alternating component of resonator voltage.

Now

$$\left(\frac{g_e V_a}{k_r I_b}\right)_{max} \simeq \frac{1}{2}$$

Assuming $X = 2$ and $\theta = 2\pi \times 4\frac{3}{4}$ for the E.M.I. R9525 klystron and a circuit efficiency of 30%, the output efficiency $\eta_0 \simeq 1\%$. The calculated carrier/noise ratio of the E.M.I. R9525 klystron has been plotted for sideband frequencies of 1 to 100 MHz in Fig. 13. The experimental curve is also shown for comparison.

3.1.1 Variation of a.m. plus background noise with resonator voltage

Additional information on the behaviour of a.m. and background noise may be obtained by investigating how noise perturbs the electronic conductance g_e of the resonant circuit coupled to the beam.[11]

The instantaneous power output for a fixed load impedance is $P = V_a^2 g_e$. When signal and additive noise are considered the output is given by

$$P' = V_a'^2 g_e' = (V_a + \Delta V_n)^2 g_e(V_a + \Delta V_n, I_b + \Delta I_n)$$

where ΔV_n and ΔI_n are the fluctuations in voltage and beam current.

The noise power output is therefore obtained as

$$\begin{aligned} P_n &= P' - P \\ &= \Delta V_n^2\left[g_e + 2V_a\left(\frac{\partial g_e}{\partial V_a}\right)I_b + V_a^2\left(\frac{\partial^2 g_e}{\partial V_a^2}\right)I_b\right] + \\ &\quad + \Delta V_n \Delta I_n\left[2V_a\left(\frac{\partial g_e}{\partial I_b}\right)V_a + 2V_a^2\left(\frac{\partial^2 g_e}{\partial V_a \partial I_b}\right)\right] + \\ &\quad + \Delta I_n^2\left(\frac{\partial^2 g_e}{\partial I_b^2}\right)V_a \quad \ldots\ldots(2) \end{aligned}$$

Now expressing ΔI_n in terms of voltage fluctuations by the relation

$$\Delta I_n = \left(\frac{\partial I_b}{\partial V_e}\right) g_e \Delta V_n$$

the following relation for ΔP_n is obtained:

$$\begin{aligned} \Delta P_n = \Delta V_n^2 &\left[g_e + 2V_a\left(\frac{\partial g_e}{\partial V_a}\right)I_b + V_a^2\left(\frac{\partial^2 g_e}{\partial V_a^2}\right)\right] + \\ &+ \frac{\partial I}{\partial V_a}\left[2V_a\left(\frac{\partial g_e}{\partial I_b}\right)V_a + 2V_a^2\left(\frac{\partial^2 g_e}{\partial V_a \partial I_b}\right) + \right. \\ &\left. + \left(\frac{\partial I}{\partial V_a}\right)^2 g_e\left(\frac{\partial^2 g_e}{\partial I_b^2}\right)V_a\right] \quad \ldots\ldots(3) \end{aligned}$$

The electronic conductance[10]

$$g_e = -2Mk_r I_b \frac{J_1(\alpha V_a)}{V_a}$$

where

$$\alpha = \frac{\theta_e M}{2V_0}$$

A coupling factor for noise which relates the noise voltage to fluctuations in output power is defined by

$$k_c^2 = \frac{P_n}{g_e |\overline{\Delta V_n}|^2 V_a^2}$$

Therefore,

$$k_c^2 = \frac{1}{V_a^2} - \frac{2}{V_a^2 J_1(x)}[x^2 J_1''(x) + x J_1'(x)] \quad \text{.....(4)}$$

The coupling factor, k_c, has the significance of a modulation factor for noise modulating the carrier. On substituting the values of x, $J_1(x)$, $J_1''(x)$ and $J_1'(x)$ for $x = 2$, it is seen that

$$k_c^2 = A/V_a^2 \quad \text{.....(5)}$$

where A is a numeric.

Thus it may be inferred from this result that the larger the cavity resonator voltage the less the a.m. plus background noise. As mentioned in Section 2.1 this is in agreement with the experimental results and the work of Sutton and Watt,[12] but not with the work of Smith.[4]

3.2 *F.M. Noise in Reflex Klystrons*

For a theoretical study of f.m. noise in reflex klystrons it is necessary to determine the behaviour of the various perturbing influences, such as velocity and/or current fluctuations, on the carrier frequency. In particular the r.m.s. carrier-frequency deviation due to noise and the f.m. noise power spectrum are required.

3.2.1 Carrier-frequency deviation

An estimate of the r.m.s. carrier-frequency deviation has been made by assuming that in a reflex klystron it is due to pushing, i.e. frequency changes due to beam-current fluctuations, and that the microscopic and macroscopic pushing effects are identical.[13] The r.m.s. carrier-frequency deviation is then obtained from the relation

$$\Delta f = \frac{KI_b}{(QI_b/\omega e)^{\frac{1}{2}}} \quad \text{.....(6)}$$

where K is the pushing figure expressed in MHz/mA, Q as before is the loaded-Q of the resonator and e is the electron charge. For the E.M.I. R9525 klystron the deviation was found to be 1·4 kHz.

3.2.2 F.M. noise spectrum

The f.m. noise power spectrum $W_{fm}(f)$ may be obtained by calculating the deviation constant for noise, D_0, which is the ratio of the phase change (in radians) of the carrier per unit noise voltage. The deviation constant is then used in the following formula[14]

$$W_{fm}(f) = \frac{A_0}{2}\int_0^\infty \cos \Delta\omega t \times \times \left[\exp\left\{-D_0^2 \int_0^\infty \frac{W_m(f)}{\omega^2}(1-\cos\omega t)\,d\omega\right\}\right] dt \quad \text{.....(7)}$$

where A_0 = output term (constant part),

$W_m(f)$ = noise power spectrum of modulating voltage.

If a normalized rectangular power spectrum is assumed for the modulating voltage such that

$$W_m(f) = B^{-1} \quad \text{for } 0 < f < B$$
$$= 0 \quad \text{for } f > B$$

where B is the (normalized) modulating voltage spectral bandwidth, then the f.m. noise power spectrum may be calculated from the above formula to have the form[14]

$$W_{fm}(f) = \frac{\text{constant}}{(\pi D_0^2/B)^2 + (\Delta\omega)^2} \quad \text{.....(8)}$$

Since in the range of intermediate frequencies of interest for local-oscillator applications $D_0^2/B \ll \Delta\omega$ the noise power spectrum is seen to have a slope of 6 dB/octave. This is in reasonable agreement with the experimental value of 5·6 dB/octave over the intermediate frequency range 10 to 50 MHz.

3.3 *A.M. Noise in Backward-wave Oscillators*

As indicated above the calculated values for noise in reflex klystrons is in reasonably good agreement with experiment. However, with backward-wave oscillators the agreement is rather less satisfactory. For example, noise spectra for beam currents below the starting value have been calculated assuming that beam noise at the collector end is amplified by the tube acting as a backward-wave amplifier. Using accepted expressions[16–18] for the effective gain and noise figure under these conditions gives calculated noise powers that are much higher than those measured.[18] On the other hand, for beam-currents greater than the starting value computations of carrier/noise ratio are in fair agreement with experiment. This situation is rather unusual since better agreement is to be expected for the simpler, i.e. non-oscillating, case. Further investigation thus seems to be necessary and is underway.

3.4 *F.M. Noise in Backward-wave Oscillators*

3.4.1 R.m.s. carrier-frequency deviation

The analysis described here for evaluating the r.m.s. carrier-frequency deviation is confined to beam/circuit interaction for a particular type of slow-wave circuit, namely, the ladder line. The total frequency fluctuation is obtained from the frequency versus beam velocity characteristic of a b.w.o. and from the pushing figure. The total frequency deviation is assumed to be due to the uncorrelated action of the random current and velocity fluctuations in the electron beam.

The frequency is given in terms of the beam velocity u_0 by

$$f_0 = \frac{u_0}{2p + 2(L+p)\dfrac{u_0}{c}}$$

where $2p$ = pitch of the ladder line

and $2L$ = twice the length of the fingers of the ladder line.

Since the r.m.s. fluctuation in beam velocity $(\overline{|\Delta u|^2})^{\frac{1}{2}}$ is small the denominator may be assumed constant for small changes in u_0. Thus we may put

$$f_0 = \frac{u_0}{2p'}$$

where

$$p' = p + (L+p)\frac{u_0}{c}$$

The calculation of Δf_0 corresponding to $(\overline{|\Delta u|^2})^{\frac{1}{2}}$ is described below.

The noise bandwidth $W_m(f)$ of the equivalent low-pass modulator (cf. eqn. (7)) responsible for the f.m. noise contribution due to velocity fluctuations must first be calculated. A method proposed by Stewart[19] is used. Let t' be the electron transit time from cathode to anode; the correlation function $R(t)$ is zero at $t = t'$. For a simple estimate of $R(t)$ assume that

$$R(t) = \begin{cases} 1 - \dfrac{t}{t'} & \dfrac{t}{t'} < 1 \\ 0 & \dfrac{t}{t'} > 1 \end{cases}$$

The power spectrum corresponding to this $R(t)$ is then

$$W(\omega) = 4\int_0^\infty R(t)\cos\omega t\,\mathrm{d}t = t'\left(\frac{\sin(\omega t'/2)}{\omega t'/2}\right)^2$$

The frequency difference corresponding to the half-power points of $W(\omega)$ is the radian bandwidth

$$B = \frac{2{\cdot}74}{t'}$$

Now t' can be calculated from the active length N in electron wavelengths of the ladder line, since C and $(CN)_{start}$ are known. In this manner, the bandwidth B was determined for an accelerating voltage of 800 V and was found to be approximately 50 MHz. Using the modified Rack formula[20] for velocity fluctuations,

$$\overline{|\Delta u|^2} = \frac{e}{m}\cdot\frac{4kTB}{I_b}f(\alpha)$$

where

$$f(\alpha) = 0{\cdot}215$$

Therefore,

$$\Delta f = \frac{[\overline{|\Delta u|^2}]^{\frac{1}{2}}}{2p'}$$

$$= 2{\cdot}26\ \text{kHz}$$

where

$$2p' = 0{\cdot}58 + \frac{2{\cdot}58}{16}$$

$$= 0{\cdot}74\ \text{mm for the CO43}$$

Frequency deviation due to pushing is estimated with a method proposed by Cicchetti and Munushian[13] according to which (see also eqn. (6)),

$$(\Delta f)_p = \frac{KI_b}{\sqrt{t'I_b/e}}$$

$$= 2{\cdot}6\ \text{kHz}$$

for the t' assumed above and for $K = 5$ MHz/mA. If current and velocity fluctuations are uncorrelated then the overall frequency deviation is 4·86 kHz.

3.4.2 F.m. noise power spectrum

Applying eqn. (7), the continuous portion of the required noise spectrum is obtained as[21]

$$W_{fm}(f) = \frac{\text{constant} \times \pi D_0^2 t'}{\left(\dfrac{D_0^2 t'}{8}\right)^2 + (\Delta\omega)^2}$$

provided $t > t'$ in the integral.

The noise power spectrum is therefore decided by the intermediate frequency since $D_0^2 t'$ is, in practice, always numerically much smaller than $\Delta\omega$. Thus the f.m. noise power spectrum has a slope of 6 dB/octave. This result which is not restricted to microwave oscillators, agrees essentially with that obtained by Edson.[5] An extensive analysis of the problem of f.m. noise and its power spectrum by Middleton, especially for the case of finite bandwidth of modulation, has resulted in an identical conclusion. In the analysis indicated here the bandwidth limitation has been achieved by the condition that the variable of integration t should always be greater than t'.

4. Conclusions

The experimental and calculated a.m. plus background noise spectra of a reflex klystron agree reasonably well. The experimental a.m. plus background noise spectra of several reflex klystrons show that the noise is lower in the case of tubes which operate with higher resonator voltages. A theoretical result obtained by application of a theory of models confirms the above observation. Ripple voltage applied to the resonator or heater supply did not affect the a.m. plus background noise spectra of any of the reflex klystrons examined. A slight increase in the noise, especially at the lower intermediate frequencies, was noticed when a ripple voltage was applied to the reflector. The f.m. noise of the reflex klystron was found to have a slope in good agreement with the theoretical value.

The a.m. plus background noise spectra of three types of b.w.o. were measured. Ion oscillations or noise peaks were noticed except in the case of the electrostatically-focused tube (ophitron). The a.m. plus background noise spectrum of the b.w.o. was found to vary roughly inversely as the square of the line current. Ripple voltages of up to 1% of the line voltage did not affect either the f.m. or the a.m. plus background noise spectrum. The f.m. noise spectrum of the b.w.o. was found to have a slope which agreed well with the theoretical value.

5. Acknowledgments

The authors gratefully acknowledge the help received from Dr. D. M. Kitching in obtaining the suppression characteristics of the carrier suppression filter using the measuring system developed by him. One of the authors (B.V.R.) wishes to thank the Commonwealth Scholarship Commission (U.K.) and the British Council for the award of a scholarship.

6. References

1. B. G. Bosch and W. A. Gambling, 'Techniques of microwave noise measurement', *J. Brit. Instn Radio Engrs*, **21**, pp. 503–15, June 1961.
2. B. G. Bosch and W. A. Gambling, 'A microwave panoramic noise spectrum analyser', *Proc. Instn Elect. Engrs*, **109B**, Supplement No. 23, pp. 658–64, 1962. (I.E.E. Paper No. 3706E, May 1962.)
3. B. G. Bosch and W. A. Gambling, 'Noise in reflex klystrons and backward-wave oscillators', *J. Brit. I.R.E.*, **24**, pp. 389–403, November 1962.
4. N. W. W. Smith, 'Noise in backward-wave oscillators', *Proc. Instn Elect. Engrs*, **105B**, pp. 800–4, September 1958.
5. W. A. Edson, 'Noise in oscillators', *Proc. Inst. Radio Engrs*, **48**, pp. 1454–66, August 1960.
   D. Middleton, 'Introduction to Statistical Communication Theory' (McGraw-Hill, New York, 1962).
6. I. Langmuir and L. Tonks, 'Ion oscillations in a warm plasma', *Phys. Rev.*, **33**, p. 195, 1929.
7. R. B. Dyott, H. A. C. Hogg, M. A. Hulley and E. Kettlewell, 'The ophitron—an electrostatically-focused backward-wave oscillator', *Nachrichtentech. Fachberichte*, **22**, pp. 114–16, 1960.
8. J. K. Knipp, 'Theory of Noise from the Reflex Oscillator', M.I.T. Radiation Laboratory Report, N-873, January 1946.
9. H. Häggblom, 'Spectral density of a.m. noise in klystrons', *Proc. Instn Elect. Engrs*, **106B**, pp. 497–500, February 1959.
10. D. R. Hamilton, J. K. Knipp and J. B. H. Kuper, 'Klystrons and Microwave Triodes' (McGraw-Hill, New York, 1948).
11. D. Middleton, 'Theory of phenomenological models and measurements of the fluctuating output of c.w. magnetrons', *Trans. I.R.E. on Electron Devices*, **ED-1**, pp. 56–90, December 1954.
12. A. J. Sutton and K. H. Watt, 'A Survey of the Noise Performance of some Low-power X-band Valves for use as Low-noise Oscillators, or as High-level Noise Generators', A.S.W.E. Technical Note, November 1961.
13. J. B. Cicchetti and J. Munushian, 'Noise characteristics of a backward-wave oscillator', *Inst. Radio Engrs Nat. Conv. Rec.*, **6**, pp. 84–93, 1958
14. J. L. Stewart, 'The power spectrum of a carrier frequency-modulated by Gaussian noise', *Proc. Inst. Radio Engrs*, **42**, pp. 1539–42, October 1954.
15. F. W. Ballou, 'Linear Theory of Signal-to-Noise Ratio in Backward Oscillators', Cornell University School of Electrical Engineering, No. 511, 1961.
16. T. E. Everhart, 'Concerning the noise figure of a backward-wave amplifier', *Proc. Inst. Radio Engrs*, **43**, pp. 444–9, April 1955.
17. R. G. E. Hutter, 'Beam and Wave Electronics' (Van Nostrand, New York, 1960).
18. B. V. Rao, 'Noise in Microwave Oscillators', Ph.D. Thesis, University of Southampton, July 1965.
19. J. L. Stewart, 'Theory of frequency modulation noise in tubes employing phase focusing', *J. Appl. Phys.*, **26**, pp. 409–13, April 1955.
20. F. N. H. Robinson, 'Space-charge smoothing of microwave shot noise in electron beams', *Phil. Mag.*, **43**, pp. 51–62, 1952.
21. Bierens de Haan, 'Tables of Integrals', Table No. 157. (Stechert, New York, 1939).

Manuscript first received by the Institution on 28th September 1966 and in revised form on 31st August 1967. (Paper No. 1177)

Radio Engineering Overseas . . .

The following abstracts are taken from Commonwealth, European and Asian journals received by the Institution's Library. Abstracts of papers published in American journals are not included because they are available in many other publications. Members who wish to consult any of the papers quoted should apply to the Librarian giving full bibliographical details, i.e. title, author, journal and date, of the paper required. All papers are in the language of the country of origin of the journal unless otherwise stated. Translations cannot be supplied.

INTERMITTENT RADIO COMMUNICATIONS

A typical feature of most radio channels is the presence of considerable random variations of the signal received, that is, fading. Among the effective methods of combating fading available to the communication engineer, a well-known method is diversity reception, which consists in using several, possibly independent, channels. The channels are subsequently combined or the one ensuring the best output signal is selected.

Another reception method adapted to the case of deep fading is intermittent communication. In an intermittent-communication system the receiver analyses continuously the state of a communication channel in terms of some parameter of the signal received (as a rule, the signal amplitude or the signal/noise ratio). At the same time, control signals are generated and are transmitted over the return channel, enabling information to be transmitted only under favourable reception conditions. As a result, transmission occurs during separate periods; the duration of these periods and of the intervals between them will depend on the statistical properties of the signal parameter.

By the use of intermittent-communication techniques, for a given error probability, one can either substantially increase the mean transmission rate or reduce the required transmitter power. At the same time, intermittent-communication systems suffer from specific drawbacks. Thus, the transmitter power is utilized for information transmission only during a fraction of its total operating time when favourable reception conditions exist. The transmitter utilization is better the longer this useful fraction of time (the so-called channel-utilization factor or duty ratio). Because there are intervals between individual operation periods, intermittent communication gives rise to delays, characterized by the average waiting time for the transmission of a message of specified length.

The use of diversity reception in intermittent-communication systems, with a view to improving their main characteristics, namely, the false-reception probability, channel-utilization factor and waiting time, is considered in a Soviet paper. The characteristics of diversity-reception systems for intermittent radio telegraphy, without any restrictions as to the type of signal or the statistical properties of the fading channel are discussed, and the relative improvement in error probability and channel-time utilization factor, which occurs when intermittent radio-telegraphy channels are combined, is analysed as a function of the utilization factor of the individual channels.

'Diversity reception in intermittent radio communication', B. P. Shcherbakov, *Telecommunications and Radio Engineering* (English language edition of *Elektrosvyaz* and *Radiotekhnika*), No. 6, pp. 111–114, June 1967.

PRE-EMPHASIS TECHNIQUE FOR FACSIMILE TRANSMISSIONS

A standard method of improving signal noise immunity is pre-emphasis at the transmitter and subsequent restoration of the signal shape at the receiver. Since the bandwidth of a standard telephone channel is sufficient for the transmission of facsimile or low-definition television signals, optimization of the signal/noise ratio in the low-frequency route of a single telephone channel by introducing pre-emphasis is considered in a Soviet paper.

The advantages of pre-emphasis in a standard frequency-multiplexed f.m. link telephone channel are discussed. The improvement in output signal/noise ratio is obtained in terms of the pre-emphasis and restoration circuit responses for a facsimile signal pre-emphasized at the carrier frequency.

'Estimating the effectiveness of pre-emphasis when facsimile signals are transmitted over radio link telephone channels', V. K. Marigodov and G. S. Panteleyev, *Telecommunications and Radio Engineering* (English language edition of *Elektrosvyaz* and *Radiotekhnika*), No. 7, pp. 17–21, July 1967.

LIGHT BEAM WAVEGUIDE

Since the advent of lasers, the possibility of high-capacity optical communication has received considerable attention. Before the broadband optical communication system is put into practical use, a stable and low-loss transmission line for the light beam over a long distance has to be realized.

A beam waveguide consisting of a periodic sequence of lenses to transmit the light beam by converging it is regarded as one of the most promising transmission lines for the light beam, because it can transmit the beam without deviation from the transmission axis, keeping the same form as that of the incident beam. It also can have low loss and small distortion in the frequency range of the optical spectrum.

The stability problem of the beam waveguide can be divided into three classes: (i) the stability of the light path; (ii) the stability of the beam spot size; and (iii) the stability of the mode.

A Japanese paper lays emphasis on problems associated with the stability of a light beam at the bends and discusses, in detail, the beam matching between a laser and a beam waveguide or between beam waveguides of different parameters. Variation of the light path due to the matching system is also considered.

'On the stability of a light beam at the bends of a beam waveguide', *Electronics and Communications in Japan* (English language edition of *Denki Tsushin Gakkai Zasshi*), 49, No. 12, pp. 56–54, December 1966.

U.D.C. 621.372.54

A C.W. Comparator for Precision R.F. Attenuators

By

R. W. A. SIDDLE,
C.Eng., M.I.E.R.E.†

AND

I. A. HARRIS,
C.Eng., M.I.E.E., M.I.E.R.E.†

Reprinted from the Proceedings of the Joint I.E.R.E.-I.E.E. Conference on 'R.F. Measurements and Standards', held at the National Physical Laboratory, Teddington, on 14th–16th November 1967.

Summary: The most accurate piston attenuators work at frequencies below 100 MHz and standard piston attenuators are usually operated at a fixed frequency such as 30 MHz or 60 MHz. In designing a comparator in which attenuators operating at any frequency up to, say, 3 GHz can be compared with a standard over a wide range of attenuation up to 100 dB, a number of problems had to be solved. Chief among these was the need to keep the noise sufficiently below the signal level at −107 dBm and the need to design frequency changers which are linear to much better than 0·01 dB over the range of levels −7 dBm to −107 dBm. The paper describes how these problems were solved in the design of a comparator which would function with a c.w. source of any frequency between 0·18 GHz and 1 GHz with an uncertainty of comparison well within ±0·01 dB.

1. Introduction

Following the pioneering work[1] at the National Physical Laboratory on methods for calibrating standard-signal generators and radio-frequency attenuators, a number of different types of apparatus for comparing attenuators with standard piston attenuators have been developed. Most of these employ the parallel i.f. substitution method with square-wave modulation of the source and the oscillator for the standard i.f. attenuator.[2–6] Recently, the series i.f. substitution method has been applied experimentally to the measurement of the wide range of attenuation (100 dB) which hitherto could be measured only by the parallel method, by using a system of noise compensation.[7]

Apart from the need to modulate any source which may be the subject of calibration, such as a standard-signal generator, one disadvantage of using square-wave modulation is that it is difficult with the usual null detector employed to ascertain whether the source is completely switched off every half cycle. Also, it is difficult to examine the constancy of level of the subject of calibration and the standard attenuator separately.

With the series method, it is necessary to have a first i.f. amplifier of at least 30 dB gain preceding the standard attenuator to compensate for the minimum loss in the piston attenuator. With this, it is necessary to have a precisely linear response over the working range of levels in the first i.f. amplifier which is more difficult to obtain for the higher signal levels than in the frequency changer (mixer). At the detector, the noise contribution from the mixer and the first i.f. amplifier varies with the setting of standard piston attenuator, while the noise contribution from the first stage of the second i.f. amplifier which follows the standard attenuator will remain constant. When measuring large values of attenuation this gives rise to error, unless noise can be injected at the inlet of the second i.f. amplifier and be varied to keep the noise at the detector constant. Such compensation can increase the complexity of a measurement. The parallel i.f. substitution method with square-wave modulation applied in opposite phase to each source is probably the most convenient for rapid calibration work of moderate accuracy. For standards work, on the other hand, a different approach is preferred in which all likely sources of error are minimized over a wide range of attenuation of at least 100 dB. The attenuator comparator described here is of this latter type and uses the parallel i.f. substitution method with manual switching between the standard and unknown attenuators with their sources. To achieve the required degree of accuracy in comparison (i.e. less than 0·01 dB in uncertainty over 100 dB) a number of problems had to be solved and these form the greater part of the subject of this paper.

2. Requirements and General Arrangement

The use of manual switching between the comparator and the outputs of the standard and unknown attenuators demands a very high degree of stability

† Electrical Inspection Directorate, Ministry of Technology, Harefield, Middlesex.

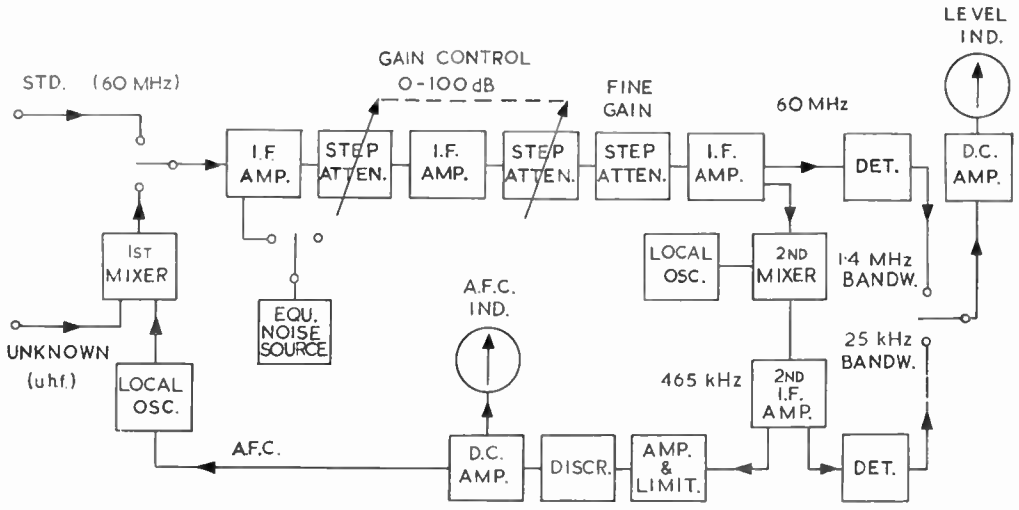

Fig. 1. Block diagram of level comparator.

with time of the gain of the i.f. amplifier. The precise comparison of attenuators over a range up to 100 dB with an uncertainty of comparison within 0·01 dB requires the detection of c.w. levels of about 1 μV across 50 ohms at the inlet with a discrimination of 0·005 dB. To achieve this, special steps have to be taken to minimize the effects of noise. The means used to achieve these two broad requirements and a number of consequential requirements can best be described in outline by reference to the block schematic diagram in Fig. 1.

To achieve the required gain stability in the i.f. amplifier approaching ±0·001 dB for ½ minute, it was found necessary to use thermionic valves which are run under steady bias conditions with large d.c. (but not r.f.) cathode feedback in each stage and, of course, with stabilized h.t. and heater supplies. Gain control is achieved by inserting variable ladder attenuators in the i.f. channel, one near the entrance stage and another near the outlet stage. The controls are coupled in such a way that for steps of attenuation up to 50 dB the attenuator near the outlet is inserted, while for attenuation from 50 to 100 dB the attenuator near the inlet is then inserted. An attenuator with 1 dB and 0·1 dB steps is also included near the outlet, together with a fine control. An attempt to use the more conventional method of gain control by varying the bias voltages resulted in a slow drift of about 0·05 dB in gain for a period up to 2 minutes. The amount of this drift would be too small to be noticeable in conventional applications of amplifiers, but it would be unacceptable in the present application.

The means adopted to minimize the effects of noise were chosen after experiments had been made with various types of coherent detection and double heterodyne detection to determine the performance and stability with time. For low-noise operation, a second frequency changer (mixer) was adopted, changing the 60 MHz to 465 kHz to enable narrower bandwidths to be obtained. Amplitude detectors are provided directly from the 60 MHz first i.f. with its −3 dB bandwidth of 1·4 MHz, and from the 465 kHz second i.f. with the choice of two −3 dB bandwidths of 160 kHz and 25 kHz. With the 25 kHz bandwidth, the noise at the output is reduced sufficiently below the smallest c.w. signal level to enable a sensitivity of better than 0·01 dB to be obtained at the level.

In using double heterodyne detection with a narrow bandwidth after the second mixer, it is necessary to stabilize the local oscillators of the two mixers so that both i.f. signals are maintained precisely at the peaks of their respective response curves. For the second mixer, the frequencies are fixed and the local oscillator is quartz controlled. The local oscillator for the first mixer is controlled in frequency so that the frequency-changed incoming c.w. is precisely 60 MHz in the first i.f. amplifier. In order to ensure that the automatic frequency control (a.f.c.) of the first (u.h.f.) local oscillator is adequate for the narrow-band condition, the a.f.c. discriminator is fed from the 465 kHz amplifier. It is necessary for the a.f.c. system to function properly when the c.w. signal is near or even below the noise level at the discriminator.

The 'standard' and the 'unknown' attenuators are fed by stable sources of appropriate frequency and the output from each is sampled in turn by the comparator. Selection is made by a specially designed coaxial switch which has a low insertion loss

and leakage smaller than −100 dB. This switches the 60 MHz c.w., the output from the 'unknown' attenuator having been changed in frequency by the first mixer. This mixer inevitably affects the accuracy of reproducing at 60 MHz the level-ratios of the 'unknown' attenuator, so it is of the utmost importance that the first mixer is linear, i.e. the output level is directly proportional to the input level with a high degree of precision over the full range of levels needed. This performance should be within 0·005 dB for the range of input c.w. signals −7 dBm to −107 dBm, i.e. from 100 mV (r.m.s.) down to 1 μV (r.m.s.) across 50 ohms.

When comparing the two c.w. outputs at the lowest levels, the output level indicator is actuated by noise as well as c.w., and it is necessary to equalize the noise in the 'standard' and 'unknown' positions of the coaxial switch. This is done simply by switching off the c.w. sources, increasing the gain (by switching a stage in the 465 kHz amplifier) to bring the noise level at the indicator up to the standard level and adding noise from an adjustable noise generator at the first i.f. inlet when the coaxial switch is connected to the source with the lower noise.

The foregoing broad description of the requirements and the means adopted to satisfy them is followed by a more detailed description of the design of the various units and their performance.

3. Design of the Frequency Changers

The primary requirement of the frequency changer of mixer is to achieve direct proportion between the input voltage at radio frequency (v.h.f. or u.h.f.) and the output voltage at i.f. Assuming a linear characteristic for positive applied voltage and zero current for negative voltage in the mixer device, a theoretical analysis based on the assumption that the i.f. voltage follows the envelope of the resultant higher frequency curve[8,3] leads to the following relation between the local oscillator voltage V_o, signal voltage V_s across the mixer and the resultant voltage V:

$$V = V_o(1+r^2)^{\frac{1}{4}}(1-0{\cdot}0625k^2-0{\cdot}0146k^4\ldots)+ \\ +\frac{V_s\cos\omega t}{(1+r^2)^{\frac{1}{4}}}(1+0{\cdot}0938k^2+0{\cdot}0341k^4\ldots)+ \\ +\text{higher harmonics,} \quad \ldots(1)$$

where $k = 2r/(1+r^2)$, $r = V_s/V_o$ and ω is the angular frequency of the i.f., the difference between the angular frequencies of the local oscillator and the signal. The term in V_o gives the d.c. component, which shows that if r and therefore k are not small, increase in the level of the signal will increase the bias voltage if auto-bias powered by the local oscillator output is used. The term in V_s gives the i.f. component, which will depart from linearity if r and therefore k are not small. Approximate relations for small r are:

$$V_{d.c.} \simeq V_o(1+\tfrac{1}{4}r^2) \quad \ldots(2)$$

$$V_{i.f.} \simeq V_s(1-\tfrac{1}{8}r^2) \quad \ldots(3)$$

The relations (1), (2) and (3) give the limiting values of non-linearity when the mixer characteristic is ideal. Non-linearity of the positive characteristic of the mixer[9] will undoubtedly increase the departure from linearity between $V_{i.f.}$ and V_s. It is known that this effect is a minimum with a diode mixer. Nevertheless, these equations show that the ratio $r = V_s/V_o$ must be very small with the largest signal level encountered if the departure from linearity is to be negligible. Also, unless the non-linearity is to be made worse by a small increase in bias when the signal is increased to its maximum, self bias using a resistor should be avoided, a fixed bias of low effective source resistance being preferred.

The requirement is for a departure from linearity of less than 0·005 dB at 100 mV across 50 ohms input (about 0·4 volt across the diode), which requires a local oscillator voltage of the order of 10 V across the diode. This rules out the possibility of using a silicon semiconductor diode, for which the typical departure from linearity is about 0·01 dB for 20 mV across 50 ohms at the input, increasing to about 1 dB for 220 mV across the input. A thermionic diode is therefore used. Actually a small disk-seal microwave triode with the grid strapped to the anode by a very low impedance conductor is employed (type 7077) and this, with its close inter-electrode spacing and high conductance, gives very satisfactory results at frequencies below and well above 1 GHz. It has the advantage that, provided the heater voltage is stabilized, it is extremely steady in operation and the linearity and conversion loss are substantially independent of ambient conditions and are unaffected by accidental overload from large signals.

The general form of the mixer circuit is shown in Fig. 2. The use of a pre-tuned pi-circuit for 'matching' to the coaxial switch and the i.f. amplifier is essential in order to achieve optimum performance in accordance with established theory.[9]

The use of a resonant circuit, tuned to the signal, at the inlet ensures that the image frequency 'source' impedance is substantially independent of the impedance of the 'unknown' attenuator, and is capacitive or inductive according to whether the oscillator frequency is above or below the signal frequency.[5,10] The thermionic diode mixer has a slightly worse noise performance than a semiconductor diode and the source impedance presented to the image frequency may not necessarily improve the noise performance. Nevertheless, the increased dynamic range

resulting from the improvement in linearity achieved by using a thermionic diode is greater than that resulting from the improvement in noise that could be obtained by using a semiconductor diode, especially in view of the precautions taken to deal with noise in other parts of the comparator.

For the reasons given in connection with eqn. (1), +9 V fixed bias is applied to the cathode of the diode and the local oscillator amplitude is adjusted to obtain a steady component of current of 0·5 mA. The bias supply is held at a constant 9 V by means of a Zener diode (Fig. 2). To show the effect of self-bias on linearity, an interesting experiment was carried out using a number of bias resistor values. The results were as follows for a signal level at the input of 0·1 V (r.m.s.):

10 kΩ – 0·06 dB error
5 kΩ – 0·03 dB „
2 kΩ – 0·01 dB „

With the fixed bias and the same current of 0·5 mA, the error with 0·1 V (r.m.s.) input was less than 0·005 dB and with 0·22 V (r.m.s.) input (0 dBm) the error was not more than 0·01 dB.

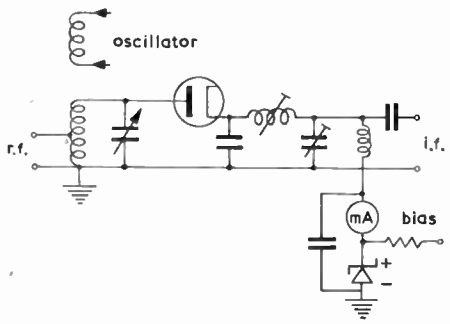

Fig. 2. Circuit of mixer, showing the i.f. pi-section matching network and low-impedance d.c. bias supply.

A low resistance, iron-cored inductor is inserted in the bias circuit to enable 1 kHz modulation to be applied when initially tuning the frequency-changer unit to the 'unknown' attenuator output. In conjunction with a miniature loud-speaker which is switched to the output of the comparator, this simple facility makes initial tuning easy. The facility is switched out of circuit when using the comparator.

To cover the range from 180 MHz to 1050 MHz, four frequency-changer units are employed: 180–300 MHz, 300–420 MHz, 400–650 MHz and 650–1050 MHz. The general form of a typical mixer and local oscillator is shown in Fig. 3. Each unit is housed in a small rectangular metal box and in each

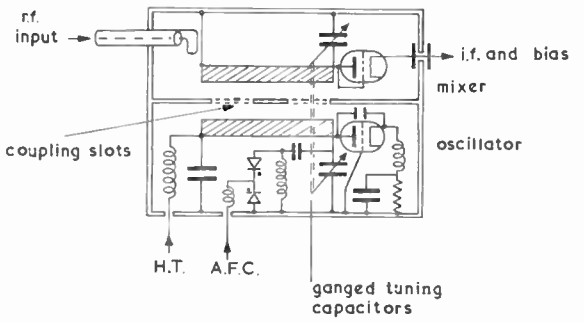

Fig. 3. Arrangement of typical frequency-changer, showing coupling between oscillator and mixer, and a.f.c. variable capacitance diodes.

case the inductance of the main resonant circuit is formed by a conducting strip which, together with the box forms a short transmission line. The variable tuning capacitors are shunted by padding capacitors (not shown) and are ganged to provide single-knob tuning. Coupling between the oscillator and mixer circuits is by slots in the common wall of the two adjacent boxes. By this method, adequate coupling is achieved over the whole frequency band to give a local oscillator voltage of about 9 V across the mixer diode. Across the oscillator tuning capacitor, two variable capacitance diodes are shunted. The bias voltage across these diodes is derived from the a.f.c. amplifier and the frequency control is achieved by the small variation of diode capacitance with applied bias.

4. The I.F. Amplifiers, the A.F.C. Circuits and the Output Level Indicator

It has already been stated that the most important requirement for the i.f. amplifier is constancy of gain to about ±0·001 dB for at least ½ minute. Other requirements, such as a low noise factor of about 1·5 : 1 and quick recovery from accidental overloading are not unusual. On account of these requirements, it was decided at an early stage in the development that the problems would be solved more readily by using thermionic valves instead of transistors, especially for the 60 MHz amplifier. Also, the need to run the amplifier valves at a steady mean current with full amplification and to control the gain by switched ladder attenuators has already been described in Section 2. The stages of the first (60 MHz) i.f. amplifier are as follows: cascode, 5 × 10 dB switched steps of attenuation; cascode and 2 pentode stages, 5 × 10 dB switched steps of attenuation; 13 × 1 dB switched steps of attenuation, 3 pentode stages; diode detector, 10 × 0·1 dB attenuator and 0 to 0·1 dB continuously variable attenuator. The bias arrangements

for a typical pentode stage are shown in Fig. 4. Pre-set controls are provided in the first two pentode stages to adjust the unattenuated gain to the required value. The total amplification without attenuation is about 10^7 (140 dB).

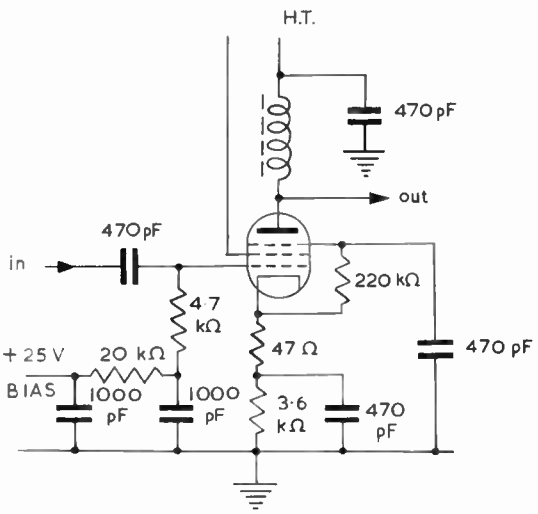

Fig. 4. Typical i.f. amplifier stage, showing d.c. bias and feedback arrangement to ensure constancy of operation.

The second frequency changer, which is fed from the last 60 MHz amplifier stage, employs a diode mixer and a local oscillator with a quartz crystal to control the frequency to 59·535 MHz, in the conventional manner. This is followed by a 465 kHz pentode amplifier with two switched resonant circuits, one for 160 kHz bandwidth and the other for 25 kHz bandwidth. A triode cathode-follower stage precedes the diode detector. This cathode-follower stage also feeds a limiter stage followed by a Foster-Seeley discriminator, the d.c. output from which is amplified and is fed, via a change-over switch, to the a.f.c. line and a centre-zero instrument to show the condition of the a.f.c. adjustment. The discriminator and the stage preceding it have an unusual feature to enable the a.f.c. system to function when the c.w. signal is below the r.m.s. noise level. When the discriminator is set so that its indicating instrument is at the centre zero for 60 MHz input to the comparator (corresponding to the crossover point in Fig. 5(a)), and the u.h.f. input is then switched through the first mixer to the i.f. inlet, the first local oscillator is tuned to bring the a.f.c. indicator to a point between the peaks. The a.f.c. voltage is then switched to the variable capacitance diodes in the local oscillator which will then be 'locked' to give 60 MHz first i.f. and 465 kHz second i.f., while the a.f.c. indicator will read zero. If, now, the u.h.f. signal is attenuated until the output signal is comparable with the noise, the a.f.c. meter indication will be found to shift away from zero, and with further reduction of the signal to a value well below the r.m.s. noise, the indication may shift beyond one of the peaks (Fig. 5(a)) after which the first local oscillator will not be controlled by the a.f.c. without further adjustment. To prevent this effect, a small variable capacitance diode is coupled to the tuned circuit preceding the discriminator so that the tuning of this circuit can be varied slightly. When the i.f. gain is increased to give appreciable noise, this variable capacitance is adjusted (by a simple voltage control) until the a.f.c. indication, with noise alone, is zero. Then when the first local oscillator is adjusted for a.f.c. zero indication and is 'locked in', reduction of the signal below the noise level no longer prevents the a.f.c. system from working. The reason for this can be seen by reference to Fig. 5. When the noise is appreciable, noise of all frequencies conditioned by curve b enters the discriminator, and if the respective

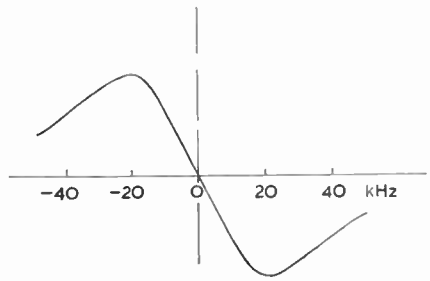

(a) Characteristic of discriminator.

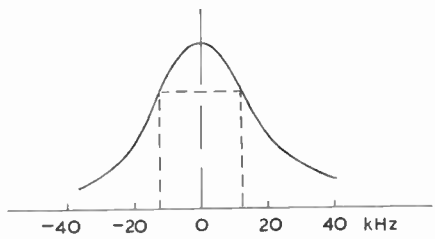

(b) Response curve of 2nd i.f. amplifier.

Fig. 5.

curves, including parts well away from the resonant point, are not both symmetrical about the resonant point, the discriminator will produce an a.f.c. voltage which will be shown on the indicator and which will shift the first local oscillator frequency. If the symmetry for noise is restored by varying the tuning of the circuit preceding the discriminator, however, the noise will produce no a.f.c. voltage and the c.w. signal,

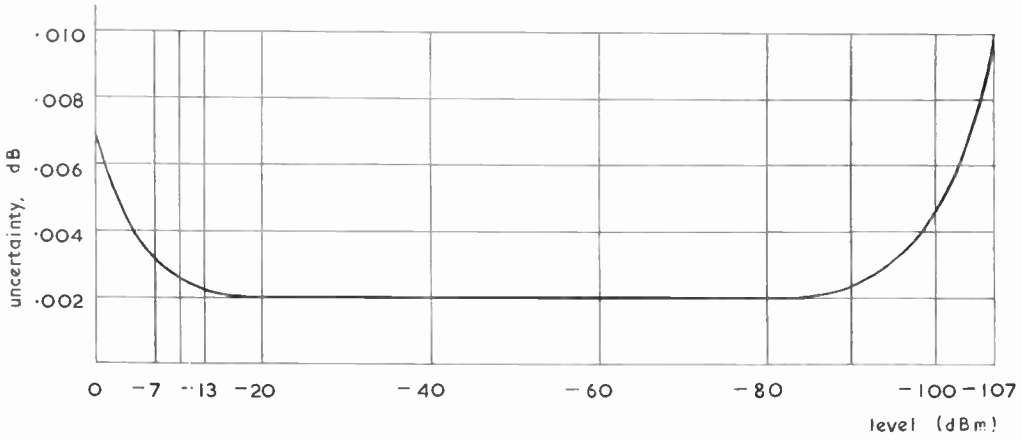

Fig. 6. Uncertainty in comparison of levels as a function of level.

although small, will be effective in maintaining frequency control.

The level output indicator is a moving coil instrument fed from a balanced d.c. amplifier. A choice of three time-constants is provided to vary the compromise between rapid response, which is preferred when working entirely with signals above −87 dBm, and heavy damping to minimize pointer fluctuations due to noise, which is preferred when working with small signals between −87 dBm and −107 dBm. The sensitivity of the indicator over the lower two thirds of its scale is about 0·002 dB per small division (1/50 of full scale) so that a change of 0·001 dB can be detected when the sensitivity of the system is at maximum. The level indicator can also be switched to any of three reduced sensitivities, 0·006 dB, 0·014 dB and 0·28 dB per small division of the meter scale, which are useful when making initial adjustments or when making measurements on apparatus for which the highest precision is not meaningful. A limiter is included to protect the meter from overload, however excessive.

5. Overall Performance and Conclusions

The uncertainty in the comparison of an attenuator at, say, 400 MHz with a standard attenuator at 60 MHz depends on the stabilities of the two sources as well as on the comparator. The comparator merely enables one to make judgments of equality, greater than or lesser than between the values of two radio-frequency c.w. voltages one at any frequency between 180 and 1050 MHz and the other at 60 MHz. The accuracy of the comparator is determined first by the short-term stability of the gain (±0·001 dB) and the sensitivity of the amplifier (±0·001 dB), which gives ±0·002 dB. For larger signals, non-linearity of the mixer introduces an error (in one direction) of about 0·01 dB at 0 dBm and 0·002 dB at −7 dBm u.h.f. input level. The direction of the error is such that the measured u.h.f. level is lower than the true value by the stated ratio. For very small signals, which are not large compared with the noise level, the sensitivity is reduced slightly and the output level indication fluctuates slightly by an amount that depends on the time constant used. Experiments have shown that with a signal at the 'unknown' inlet of about 1 μV across 50 ohm, the uncertainty is within ±0·01 dB.

The resultant uncertainty in determining the equality of two signal levels is shown in Fig. 6 in which it is assumed that a correction is applied for the effect of mixer non-linearity, and the resultant uncertainty is taken to equal half the measured departure from linearity.

In conclusion, it should be noted that the comparison of an attenuator operated at any frequency in the range 180 to 1050 MHz with a standard attenuator operated at 60 MHz involves two comparisons of level, one at each end of the attenuation range measured. Thus a measurement in the range −7 dBm to −87 dBm has a total uncertainty of comparison of ±0·005 dB, while a measurement in the range −7 dBm to −107 dBm has a total uncertainty of comparison of ±0·015 dB. A measurement of attenuation in the restricted range of levels −13 dBm to −87 dBm has a comparison uncertainty of ±0·004 dB. To this must be added the short-term stability ratios of the two sources and the uncertainty of the standard attenuator in order to obtain the overall uncertainty in measured attenuation.

The comparator has been designed for the comparison of precision piston attenuators or the com-

parison of any attenuator with a standard piston attenuator in the v.h.f. and u.h.f. ranges of frequency. The present range of 180 to 1050 MHz is to be extended upwards to at least 3 GHz and downwards to as low a frequency that is practicable with a 60 MHz standard, probably 5 MHz.

6. References

1. G. F. Gainsborough, 'A method of calibrating standard signal generators and radio-frequency attenuators', *J. Instn Elect. Engrs*, **94**, Pt. III, pp. 203–10, 1947.
2. B. O. Weinschel, G. U. Sorger and S. J. Raff, 'Calibration of signal generator output voltage in the range 100 to 1000 Mc/s', *Trans. Inst. Radio Engrs on Instrumentation*, **I-7**, pp. 275–8, 1958.
3. B. O. Weinschel, G. U. Sorger and A. L. Hedrich, 'Relative voltmeter for v.h.f./u.h.f. signal generator attenuator calibration', *Trans. I.R.E.*, **I-8**, pp. 22–31, 1959.
4. R. F. Clarke and B. J. Dean, 'A precision attenuator standard for X-band', *Trans. I.R.E.*, **I-11**, pp. 291–3, 1962.
5. R. J. Turner, 'Equipment for the measurement of the insertion loss of waveguide networks in the range 3·8–4·2 Gc/s', *Proc. I.E.E.*, **109**, Pt. B, Supplement 23, pp. 775–82, 1962.
6. D. L. Hollway and F. P. Kelly, 'A standard attenuator and the precise measurement of attenuation', *Trans. Inst. Elect. Electronics Engrs on Instrumentation*, **IM-13**, pp. 33–44, 1964.
7. H. L. Kaylie, 'A new technique for accurate r.f. attenuation measurements', *Trans. I.E.E.E.*, **IM-15**, pp. 325–32, 1966.
8. F. E. Terman, 'Radio Engineering', pp. 307–8. (McGraw-Hill, New York, 1932.)
9. E. G. James and J. E. Houldin, 'Diode frequency changers', *Wireless Engineer*, **20**, pp. 15–27, 1943.
10. H. J. O'Neill, 'Image frequency effects in a microwave crystal mixer', *Proc. I.E.E.*, **112**, pp. 2019–24, 1965.

Manuscript received by the Institution on 29th August 1967. (Paper No. 1178.)

STANDARD FREQUENCY TRANSMISSIONS

(Communication from the National Physical Laboratory)

Deviations, in parts in 10^{10}, from nominal frequency for February 1968

February 1968	24-hour mean centred on 0300 U.T.			February 1968	24-hour mean centred on 0300 U.T.		
	GBR 16 kHz	MSF 60 kHz	Droitwich 200 kHz		GBR 16 kHz	MSF 60 kHz	Droitwich 200 kHz
1	− 300·1	− 0·1	0	16	− 300·0	0	+ 0·1
2	− 300·0	+ 0·1	0	17	− 300·0	0	0
3	− 299·9	+ 0·1	0	18	− 300·0	0	+ 0·1
4	− 300·0	0	0	19	− 300·1	0	0
5	− 300·0	0	0	20	—	0	0
6	− 300·1	− 0·2	− 0·1	21	—	+ 0·1	− 0·1
7	− 300·1	− 0·1	− 0·1	22	− 300·0	0	− 0·1
8	− 300·0	− 0·1	− 0·1	23	− 300·0	0	0
9	− 300·0	+ 0·1	0	24	− 300·0	+ 0·1	0
10	− 300·0	− 0·1	0	25	− 299·9	+ 0·1	0
11	− 300·0	0	0	26	− 300·1	0	+ 0·1
12	− 299·9	0	0	27	− 299·9	+ 0·1	0
13	− 300·1	0	0	28	− 299·9	+ 0·1	0
14	− 300·0	0	0	29	− 300·0	− 0·1	0
15	− 300·0	− 0·1	0				

Nominal frequency corresponds to a value of 9 192 631 770·0 Hz for the caesium F,m (4,0)–F,m (3,0) transition at zero field.

Notes: (1) All measurements were made in terms of H.P. Caesium Standard No. 134 which agrees with the NPL Caesium Standard to 1 part in 10^{11}.
(2) The offset value for 1968 will be −300 parts in 10^{10} from nominal frequency.
(3) From March 29, 1968 at 0600 U.T. until April 1, 1968 at 2000 U.T. the GBR and MSF transmitters will cease emissions for urgent repairs to the aerial system.

U.D.C. 629.19

Attitude Determination of the *Ariel III* Satellite

By R. B. BENT, B.Sc., Ph.D.†

A formal discussion contribution at the Symposium on 'The Ariel III Satellite' held in London on 13th October 1967.

The three radio experiments on the *Ariel III* satellite require a knowledge of spin-axis direction in order to deduce the fields measured by their loop aerials. The solar aspect sensors provide the angle between the direction of the spin-axis and the Sun, which defines a conical surface containing the spin-axis. Some other frame of reference is required in order to find the exact position of the spin-axis on this cone and a method was therefore proposed similar to that used on *Telstar*.[1] Six echelon mirrors were placed on the satellite from which glints of solar reflections could be monitored by visual, photographic or photoelectric techniques on the ground. At the instant when glints are received the position of the satellite is known in relation to the observer and to the direction of the Sun, as also is the angle of the mirror to the spin-axis of the satellite; a second cone is therefore determined on which the spin-axis lies. From the intersections of these two cones the final attitude of the spacecraft is calculated. Any one observation yields two possible directions, but successive observations enable the true direction to be determined.

Ariel III was launched with a spin rate of 30 rev/min; thus when the spin-axis is correctly related to the directions of the Sun and the observer there are three reflections per second from the mirrors. Similarly the body solar cells reflect glints at a rate of six per second with the appropriate directions to the spin-axis and the double-sided boom solar cells at a rate of two per second. As an example, with the Sun's direction normal to that of the spin-axis there are glints at angles of 25, 60, 90 and 155 degrees to the spin-axis direction. The mirrors were intentionally made flat to only 1° thereby giving a 2½° dispersion of the Sun's image. This allows the observer to see about ten 7 ms glints of 1st magnitude over a period of about 4 seconds. The solar cell panels have greater dispersion leading to 1st magnitude glints of 25 ms duration observed over a period of about 15 seconds.

Excellent results have been obtained and the spin-axis direction has been monitored to an accuracy of better than 2°. Results from a photo-electric camera in Ohio have enabled the coning angle, or angle between dynamic and geometric axes, to be determined to better than 0·1°. Furthermore, because the spin-axis direction changes only slowly, a series of observations of the glints is sufficient to measure these angles without the use of solar aspect sensors, particularly when more than one set of glints can be observed during a single pass. By these means the use of telemetry channels for transmitting solar aspect data is avoided.

The initial results have been published in Reference 2.

† Science Research Council, Radio and Space Research Station, Ditton Park, Slough, Bucks.

References

1. J. S. Courtney-Pratt, J. H. Hett and J. W. McLaughlin, 'Optical Measurements on *Telstar*', Bell Telephone System Monograph 4575, 1963.
2. R. B. Bent, 'Attitude determination of the *Ariel III* satellite,' *Nature*, **216**, No. 5110, pp. 45–7, 7th October 1967.

Discussion on the *Ariel III* Satellite

Under the chairmanship of
Mr. L. H. Bedford, C.B.E., C.Eng., F.I.E.E., F.I.E.R.E., and Dr. J. A. Saxton, C.Eng., F.I.E.E.

Mr. J. H. Howard: Would Messrs. Campbell and Ladd‡ like to comment on what significant changes they would like to see in both the technical and organization sides if an identical contract were placed today?

‡ F. P. Campbell and A. C. Ladd, 'The *Ariel III* project', *The Radio and Electronic Engineer*, 35, No. 1, pp. 17–32, January 1968.

Mr. A. C. Ladd (*in reply*): The organization of any future project of a similar nature would probably be somewhat simplified from that evolved for *Ariel III* which had to cope with many new tasks in the U.K. for the first time.

Like any large project, with many interface problems, final success is ultimately dependent on the personal competence and mutual co-operation of technical staff at all

levels. One feature to be borne in mind on any future project is that with a time-scale of several years it can be anticipated that many of the individuals in senior project appointments will change during the project. This was certainly the experience on the *Ariel III* project both in the U.K. and the U.S.A.

Mr. J. G. Fielding: I was interested when Mr. Ladd said that after the launch everyone concerned with the construction of the satellite could go home, as only the collection of data remained.

Who is in charge of any panic measures which have to be taken if, for instance, a battery gets hot or something like that?

Mr. Ladd (*in reply*): *Ariel III* is a relatively simple scientific satellite compared with many of those now in orbit and, as you have heard, it only accepts two radio commands—the tape recorder replay command and the telemetry transmitters changeover command. This limitation in command facilities naturally seriously limits any remedial action that can be taken from the ground. The particular point you mention of the battery getting too hot is partly taken care of in the design of the satellite power system which reduces the battery charging level should the battery temperature exceed 40°C.

Each day since launch the housekeeping data received from the satellite during one pass recorded at Winkfield have been examined by staff at G.E.C. and the temperatures and performance of the various systems have been notified to the Space Research Management Unit.

Mr. R. W. Young: The solar array voltage–current output curves in Mr. Treble's paper‡ are given for two temperature conditions of the satellite (Figs. 3 and 4). The curve for the higher temperature condition shows a distinct kink which is not apparent on the lower temperature curve. Would Mr. Treble comment on this?

Mr. F. C. Treble (*in reply*): The voltage-current curves of the load and battery arrays are constructed from the instantaneous output characteristics of a number of illuminated body and boom panels connected in parallel. In the design attitude, the boom panels run cooler than those on the body and do not attain such a low angle of incidence. Therefore they produce lower short-circuit currents and higher open-circuit voltages than the body panels. This causes the kinks in the curves marked 'Array Output (Hot)'. In the cold condition, however (i.e. when the satellite is emerging from the Earth's shadow), the temperatures of all the panels are much the same and, as the differences of illumination do not greatly affect the high voltage end of the curve, the kinks are less apparent.

Mr. R. W. Young: With the stated signal/noise ratio margins of about 20dB for both the telemetry and command links at maximum slant range, the accurate measurement of the satellite radiation pattern is probably not essential.

In view of the problems in making full scale radiation patterns measurements at 136 MHz, could Mr. Hildersley§ give an estimate of the probable error in the measurements made at Lasham?

Mr. R. S. Hildersley (*in reply*): It is true that many difficulties are encountered in measuring the satellite radiation pattern at 136 MHz, and of course it is essential to minimize ground reflections and other spurious signals so that the results will forecast accurately the true free-space pattern. Because of the practical difficulties encountered in handling the spacecraft, scale models or full size prototype satellites have been used for the tests in preference to flight equipment. Minor variations in the physical position of solar cell paddles, experimenters' probes, and loop aerials have a noticeable effect on the radiation pattern, and therefore each spacecraft has its own radiation pattern 'signature'. However, the main objective of this work is to predict the communications saftey factor when the satellite is in orbit, and to allow for the effect of possible faults such as the failure of an aerial to erect during the launch phase. Experience with *Ariel III* since launch has tended to

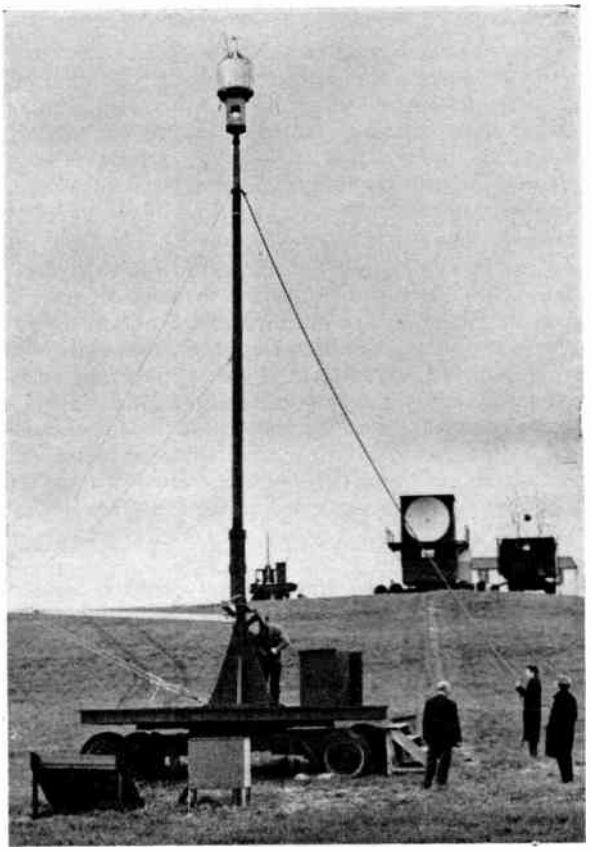

The D2 model of *Ariel III* undergoing radiation pattern tests at Lasham, Hants.

[*Photograph by R. S. Hildersley, F.R.P.S.*

‡ F. C. Treble, R. C. Cook and P. G. Garratt, 'The *Ariel III* power system,' pp. 135–141, March 1968.

§ R. S. Hildersley, 'Some design aspects of the *Ariel III* v.h.f. communications systems', pp. 149–155, March 1968.

emphasize the importance of radiation pattern work. Mr. R. W. Hogg of R.A.E. Space Department has been directly involved in these measurements and can add further information on the details.

Mr. R. W. Hogg: Initially, measurements on radiation patterns were made at the Lasham Test Site of the Radio Department of R.A.E. using a one-third-scale model of *Ariel III*. At these frequencies, ground reflections were eliminated using high-gain circularly-polarized receiving aerials and the resulting patterns were satisfactory.

In due course, the radiation patterns of the *Ariel III* prototype and flight models were checked in the equatorial plane by mounting the satellite on a small turntable in a flat field at B.A.C., Stevenage. Measurements were made with receiving aerials horizontally polarized and also vertically polarized. The resulting radiation patterns were disappointing—four lobes with nulls in between as high as 10dB.

It was therefore decided to do a thorough radiation pattern check at Lasham on a full-scale model. The D2 development satellite was seconded for this purpose, after first checking that its radiation pattern at B.A.C. displayed the same quadrantal symmetry. Horizontally and vertically polarized receiving aerials were available and it was shown on the sloping site at Lasham that the contribution from ground reflections did not seriously affect the measurements.

Equatorial plane measurements were made, and also a number of patterns with satellite spin-axis horizontal were determined. From the latter, conical cuts were produced with the equatorial plane measurement providing a check on the diagram for a cone angle of 90°. Agreement was to within 2dB, which is the approximate order of accuracy claimed for this work.

Over a cone of semi-angle 20° from the nose aspect, the polarization emanating from the satellite was circular to within 1dB; at 40° it was 2dB, and in the satellite equatorial region the radiation was plane polarized. To avoid nulls in the reception of a satellite pass due to cross polarization, circularly polarized telementry ground receiving arrays were specified for use at Winkfield and other N.A.S.A. STADAN stations. Even so, nulls somewhat in excess of the 7dB limit below isotropic predicted have been experienced—a matter which is being investigated further. The signal strength of data received at Winkfield has however always been excellent.

Dr. W. F. Hilton: The University of Sheffield measurements† indicate a concentration of 16 kHz radiation from Rugby at the conjugate point. Does this mean that their curvature matches that of the Earth under appropriate electromagnetic conditions?

Dr. K. Bullough (*in reply*)*:* The 16 kHz radiation leaks through the atmosphere/ionosphere interface above Rugby and is then loosely guided along the geomagnetic field line from Rugby to the conjugate zone. Yabroff has shown by ray-tracing that, for a station at the latitude of Rugby, there is a focusing effect whereby radiation leaking into the ionosphere to the south of Rugby will deviate from the local field line so as to terminate at a higher latitude in the conjugate zone (see Ref. 9 in our paper). The addition of many such rays transmitted into the ionosphere along the magnetic meridian in the northern hemisphere gives rise to a well-defined peak in the wavefield centered on the conjugate point to Rugby.

Mr. R. Dalziel: The coupling between the Birmingham and the Jodrell Bank experiments that has just been reported was of course not discovered before launch, because there was no environmental test that called for operation of all experiments in an ionized atmosphere. I have heard of two other space research vehicles in which coupling via the ionosphere has adversely affected, if not spoiled, the performance of scientific experiments. There are no doubt technological difficulties in providing a suitable ground test facility but one wonders whether it would not be worthwhile for providing a ground test. Has the possibility been examined? Can any of the authors please comment?

Mr. J. H. Wager‡ (*in reply*)*:* There are two ways in which coupling between experiments could be investigated in an ionized atmosphere.

One is to produce a simulated ionospheric plasma in a relatively small volume and to use a working scaled-model of the space vehicle. In this case the plasma simulation is not necessarily difficult to achieve but the practical implications of such a scaled model are formidable and the interpretation of the results, especially when radio frequency aerials are involved, must needs be open to doubt with no guarantee that the behaviour of a full-size space vehicle would be identical.

The second approach would be to use a full-size working space vehicle in a large vacuum chamber and attempt to produce a simulated ionosphere in a large volume. Such an approach, whilst not impossible, would be more difficult and costly as provision for many extra facilities on the vacuum tank would have to be met. In order that a loop aerial as used on *Ariel III* did not have its working Q altered appreciably, the diameter of the vacuum chamber, would have to be many times that of the loop.

Generally speaking, the first approach would be the more feasible, especially from the financial standpoint, but the doubts outlined would still remain.

On *Ariel III*, an attempt was made to investigate possible coupling between the telemetry transmitter and one of the propagation experiments. The results however, whilst indicating that such coupling was absent, were inconclusive due to the limited size of the vacuum chamber available and unwanted noise being generated in the simulated plasma.

† K. Bullough, A. R. W. Hughes, and J. R. Kaiser, 'V.l.f. observations on *Ariel III*: a preliminary report', pp. 103–108, February 1968.

‡ J. H. Wager, 'The University of Birmingham electron density and temperature experiments on the *Ariel III* satellite', pp. 55–63, January 1968.